Republic of Iraq
Ministry of Higher Education
and Scientific Research
University of Babylon
College of Education for Pure Sciences
Department of Physics

Prepation and Charactrization Study of Polymeric Blend:Bi_2O_3 Nanomaterial

A thesis

submitted to the council of the college of education for pure sciences , university of Babylon in partial fulfillment of the requirements for the degree of master in education / physics

by

Hiba Ahmed Makki badr

(University of Kufa - 2010)

Supervised by

Prof. Dr. Ali Razzaq Abdulridha

2022 A.D. **1444 A.H.**

بِسْمِ اللَّهِ الرَّحْمَنِ الرَّحِيمِ

{ يَرْفَعِ اللَّهُ الَّذِينَ آمَنُوا مِنْكُمْ وَالَّذِينَ أُوتُوا الْعِلْمَ دَرَجَاتٍ وَاللَّهُ بِمَا تَعْمَلُونَ خَبِيرٌ }

سورة المجادلة اية 11

Dedication

To my family “ My parents ,

brothers and sisters ,

to my son Karrar the sunshine of my life “

Hiba

Acknowledgements

Praise be to Allah, His Majesty for His uncountable blessings and best prayers and peace be to his best messenger Mohammed, his pure descendant and his noble companions.

I wish to express my deepest gratitude and appreciation to my supervisor Prof. Dr. Ali Razzaq Abdalridha for his guidance, suggestions, support, and encouragement through the research work.

Thanks to the deanship of the College of education for Pure SciencesBabylon university and the Department of Physics for offering me the opportunity to complete my research. I also would like to express grahtude to all teachers, instructors and students of department of physics for their assistance and supports

Finally, I am very grateful to every person who is related for this work to be done.

Hiba

Summary

In this work, (PVA-PVP/Bi_2O_3) and (PVA-CMC/Bi_2O_3) nanocomposites were prepared by casting method with different weight concentrations of Bismuth oxide (0,1,3 and 5)wt% with the average particle size between 20-30 nm. As well as a study of the effect of concentrations of Bi_2O_3 nanoparticles on the structural, optical, and electrical properties of the (PVA-PVP) and (PVA-CMC) blend.

The results of the optical microscope images showed the Bismuth oxide nanoparticles distributed uniformly homogeneous and regular within the polymeric mixture of (PVA-PVP) and (PVA-CMC). The Fourier Transition Infrared Spectroscpy (FTIR), absorptions spectrum showed a change in the intensity, shape, and displacement of the peak's sites compared to the pure films of the (PVA-PVP / Bi_2O_3) and (PVA-CMC /Bi_2O_3) nanocomposites ,which refers to the corresponding vibrations of the two polymers and the Bi_2O_3 nanoparticles.

The results of the optical properties of (PVA-PVP/Bi_2O_3) and (PVA-CMC/Bi_2O_3) nanocomposites such as extinction coefficient ,absorption, absorption coefficient, refractive index, optical conduction and the real and imaginary isolation constant were increased with the increasing the concentrations of Bismuth oxide, while the transmittance values and the energy gaps permeability decreased.

The results of the A.C. electrical properties of (PVA-PVP/Bi_2O_3) and (PVA-CMC/Bi_2O_3) nanocomposites showed the dielectric loss and dielectric constant decreased with increasing the frequency the concentrations of Bismuth oxide nanoparticles, electrical conductivity of A.C was increased with increasing both the frequency and concentrations of Bismuth oxide nanoparticles .

The results of application for nanocomposites showed that the attenuation coefficient for gamma radiation increased with increasing in Bi_2O_3 nanoparticles .

List of Contents

List of Tables

List of Figures

List of Symbols

Symbols	Physical Meanings
$\sigma_{A.C}$	A.C electrical conductivity
I_A	Absorbed intensity of light
A	Absorbance
α	Absorption coefficient
E_{act}	Activation energy
W	Angular frequency
C	Capacitance
I_q	Capacitance current
ε	Complex dielectric constant
N	Complex refractive index
I_p	Conduction current
C.B	Conductive band
ε'	Dielectric constant
ε''	Dielectric loss
Tanδ	Dielectric loss tangent
K	Extinction coefficient
ε_2	Imaginary dielectric constant
Z	Impedance
I_o	Incident intensity of light
I_T	Intensity of transmittance
V_m	Maximum voltage
No.	Number of transmitted particle

Symbols	Physical Meanings
Eg^{opt}	Optical energy gap
Ω	Ohm
R_P	Parallel resistance
E_{ph}	Phonon energy
C_p	Parallel capacitance
V	Potential exerted
ε_1	Real dielectric constant
n	Refractive index
d	thickness of the matter
T_r	Transmittance
UV	Ultraviolet spectrum
C_o	Vacuum capacitor
ε_o	Vacuum permittivity
V.B	Valens band
c	Velocity of light
K	Wave vector

List of Abbreviations

Symbol	Physical Meanings
A.C	Alternating current
Bi_2O_3	Bismuth Oxide
CMC	Carboxymethyl Cellulose
FT-IR	Fourier Transition Infrared Spectroscpy
OM	Optical Microscope
PVA	Polyvinyl Alcohol
PVP	Polyvinyl Pyrrolidone
UV	Ultraviolet

.

Chapter One

Introduction and Literature Review

1.1. Introduction

As we cannot imagine our planet without the atmosphere layer ,we also cannot ideate our daily life without polymers, specially the synthetic ones Polymers are all around us and could be responsible for the life itself, we may find them in food, water, clothes, buildings, cars and even in our bodies[1]. The term polymer is usually used to describe a wide range of materials from synthetic materials like plastic, fibers, nylon, …etc , to the natural polymers such as cellulose , silks, hair, DNA and RNA …etc [2]. So we can say that polymers are the tiny basis of every materials around us, living or not living , organic or inorganic bodies[3].

There is an immemorial history for us to observe polymers starting with the theory saying that the world consist of four elements .i.e. water, air, fire and earth reaching to the Maxwell's theory of atom's motion (Boltzmann1872)[2].We can consider polymers is the fifth element , in addition we already know that mankind lived in several ages, like stone age, ice age, bronze age, …etc , at the present time we could numerate this age by polymer age [4],the full understanding of polymers was in the middle of 20th century where the clear nature of polymeric materials had been came with the creation of plastic, so the developments are continuous since ever. However ,with all this evolution and magnificence of industry we still severity need man- made polymeric materials[2].

In every field of science there is an investigation methods to be responsible for the materials properties and their applications and results , generally polymers, polymers blends, polymers composites and filled polymers represent the principle basis of polymer materials science[4]. For several millennia, mankind had been exploited matter in technology through the ages and the materials which engineered for useful applications based on a good understanding of molecular properties .The 19th century

was the age of iron and steel which are known as the "Hard" materials , the 20th century witnessed the invention of new types of engineered materials notably polymers , which in plastics form interline in many applications overtake a lot of the traditional hard materials and this leads to the birth of new and important class of inorganic and semiconductors materials which became the basis of the second industrial revolution recently known as "Soft" materials [5],polymers had replaced natural materials in many fields and applications and it is seem for some daily objects so difficult to imagine them not made of polymers, plants and animals use natural polymers to assume an assortment of knotted tasks, for example silk worms when they produce silk or the spiders to build their webs they produce a polymer fibers with a wide range of mechanical and structural properties[6].

1.2. Polymers

Polymers are built up by linking together monomers in large numbers. Monomers are molecules with functional groups or elements which react with each other to form large molecules. The degree of polymerization determines the size of a polymer. The polymer size is the total number of structural units which includes the end groups and is also related to both chain length and molecular weight[14]. Polymers are macromolecules which are constructed by the covalent linking of simple molecular repeated units. The structure is implied in the phrase “poly,” meaning many, and “mer,” designating the nature of the repeating unit [2–4]. Polymers are modified to provide specific compatibility, durability or properties dictated by their expected use in industry and there has been expanded use of polymer blends and composites in industrial applications. Polymers from synthetic resources are mainly non-biodegradable materials[15]. Polymers, the molecules of plastic, are predominantly derived from fossil-based feedstocks. They are remarkably lightweight, durable, protective,

conductive, and self-healing, which are just a few of their many attributes.Polymers play a vital role in human activities by contributing to the sophistication and comfort of society. They are insoluble materials whose properties are modified by using fillers and fibers to suit the highstrength/high modulus requirements[16].

1.3 Polymer Structure

Polymers are categorized as thermoplastics and thermosets. The category is based on the characteristics of the recycling nature of the end products. Polymers have attracted attention because their physical properties differ from the starting monomer material. Polymers can be linear (polystyrene, polypropylene), branched (polyethylene) or cross-linked (epoxy) [11].

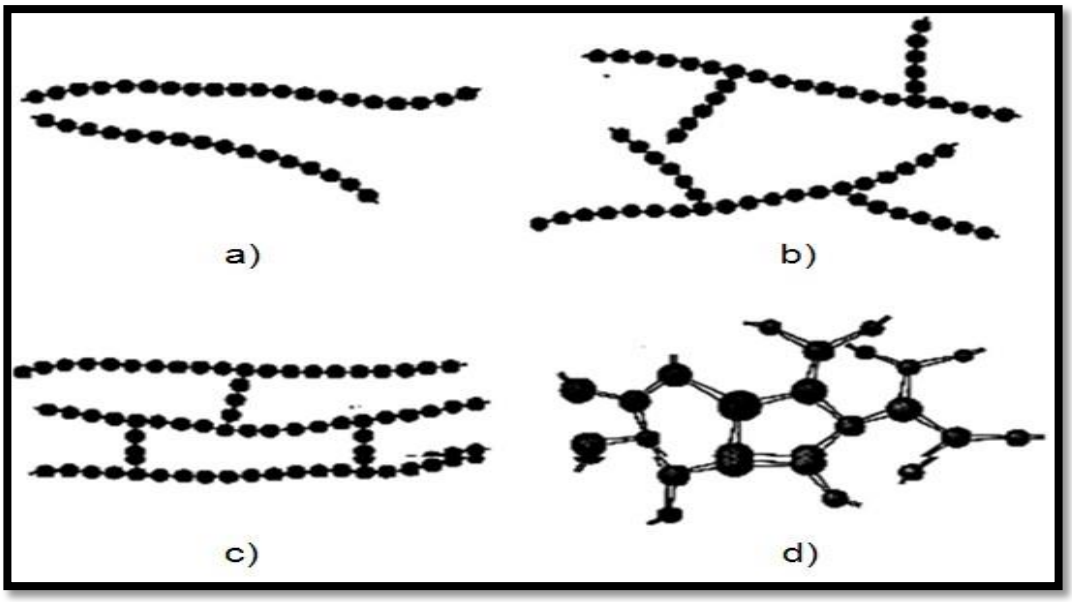

Figure 1.1: These four types of polymers illustrated .

Thermoplastics are lengthy polymer chains that have a high molecular weight. These chains can be crystalline or amorphous, depending on the thermoplastic. The high molecular weights of polymers are what give them their useful features, including as superior mechanical capabilities and the capacity to be molded into a wide variety of different kinds of parts (injection molded, extruded, etc). Thermoplastics can have no crystallinity,

making them amorphous. This causes the lengthy chains to become entangled with one another, giving the impression that the material is "like a bowl full of spaghetti." Since the polymer chains are going through random Brownian motion and slithering past one another, the late Professor Garth Wilkes from Virginia Polytechnic Institute used to compare molten polymers (like linear amorphous) to a bowl full of snakes. [6] He was referring to the fact that molten polymers are like linear amorphous.

Thermosets are a type of polymer that start out as small molecules (monomers and oligomers), but through the process of a chemical reaction, they are able to polymerize into a network structure. In the fully cured and final condition, the crosslinks bind the chains together, which provides both strong mechanical qualities and dimensional stability, but thermosets will not flow (and are not dimensionally stable) above their T_g [7].

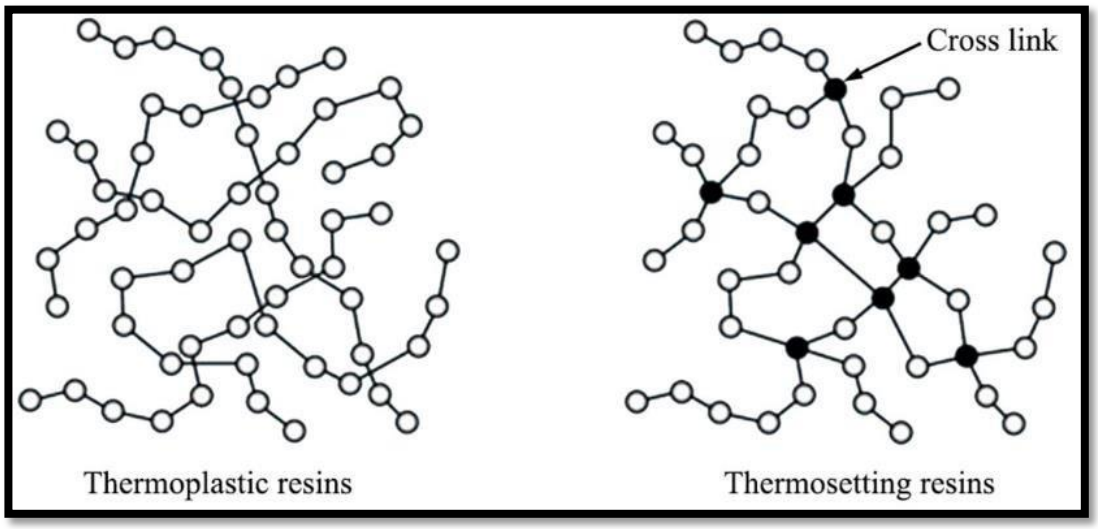

Figure (1.2): Difference between thermoplastic and thermoset polymers[7].

1.4. Polymer Blends

Polymer blends are a class of materials which share similarity with metal alloys, as at least two polymers are mixed to form a single mixture with differing physical characteristics [8]. The destiny of polymer blends is extracted from miscibility of their blend's components. Many scientific experiments have been conducted using solvent casting, but most industrial polymer mixtures are prepared by melting, using extruders with a twin screw. Because of the one of a kind interaction between the polymer chains, the two types of polymer can mix together without any problems. In the following equation, which represents the second law of thermodynamics, the laborer of entropy may be used to explain this phenomenon:

$$\Delta G_{Mix} = \Delta H_{Mix} - T \Delta S_{Mix} \quad \text{..... (1.1)}$$

where, ΔG = change in free energy, ΔH = change in enthalpy, ΔS = change in entropy, T= absolute temperature.

The free mixing energy of Gibbs must have a negative value in order for there to be a homogenous miscible mixture. When it comes to polymer combinations with a larger molecular weight, the increase in entropy is not detectable at all. Therefore, in order for the free mixing energy to be negative, the mixing heat also needs to be negative. This indicates that the combination must be exothermic, which typically includes precise interactions between the components that are being blended [9]. In general, there are three types of polymer blends: compatible, miscible, and immiscible polymer blends [10]. Compatible polymer blends are those that may be mixed with other compatible polymers.

Forming polymer blends is a typical way of producing modern products with improved properties. Unfortunately, due to the broad enthalpy and poor mechanical properties, most polymer mixtures prefer to

separate phases. The regulation of phase behavior and morphology is therefore a key factor in deciding upon the efficiency of polymer blends, which mainly depend on the interface between the polymer components [17].

1.5 Nanomaterials and Nanocomposites

Nano is a prefix for any unit, such as a second or a meter, that comes from the Greek word for dwarf or abnormally small human. Nanomaterials are materials with individual particles in the range of 1-100 nm, in one dimension or more, and are described as a billionth $(10)^{-9}$ of that unit. One nanometer is equal to ten hydrogen atoms or five silicon atoms aligned in a straight line. [18].

Nano composite materials encompass a vast range of systems, including one-dimensional, two-dimensional, three-dimensional, and amorphous materials, many of which are made up of dissimilar elements that are combined at the nanometer scale. [19].

A nanocomposite is a composite substance of which one or both of the elements has a nanoscale in one dimension, and a composite is a mixture of two or more different materials combined in an effort to combine the best properties of each at least. There are three basic types of materials, metal, ceramic and polymer, each one of them have a specific properties, metals are strong, ductle and conductive. Ceramics are strong, chemically resistant, insulating and brittle. Where polymers are usually impact resistant, insulating and ductle[20].

Polymers are outshined over metals and ciramics due to their low density, high stiffness, high strength and facility to fabricate of complex part over a large scale by using traditional injection molding, however, polymers have low electrical conductivity, poor mechanical properties, and low thermal conductivity, so all these properties can be enhanced by adding

appropriate volume fraction of fillers like fibers or particulates into the polymer matrix, which called nano composites. A composite is a mixture of two or more of these material types. A nano composites is also a mixture of two different materials. The composite itself doesn't determine all the properties of the material, every material have a structure that may contribute to these properties to be considered[21].

1.6. The Materials Used in The Study

1.6.1 Polyvinyl Alcohol (PVA)

Polyvinyl Alcohol is Water-soluble synthetic polymers produced by humans will normally be absorbed, scattered, and swollen in nature. It is a non-toxic and odorless polymer with strong chemical resistance and mechanical properties. Its drawbacks include a high price tag and minimal barrier and thermal properties[22].

PVA comes in a variety of shapes, including powder, film, and fiber. PVA is semi crystalline polymer composed of mainly amorphous phases with little pet of crystallinity. The majority of the properties of PVA are determined by its molecular weight as well as the degree of hydrolysis with the molecular weight; the molecular weight of PVA ranges between (10,000-400,000) g/mol, which is based on the length of vinyl acetate that was used to produce PVA, and the range of hydrolysis is typically between 80 and 99 percent, such as in the cases of: Increases in molecular weight and degree of hydrolysis are accompanied by decreases in water sensitivity, stability, and solubility. However, increases in tensile strength, solvent resistance, and water block all occur simultaneously. PVA is one of the most significant hydrophilic polymers; it has a high sensitivity to moisture, which enables it to be employed in the composites and blends used in the production of packaging materials. [23].

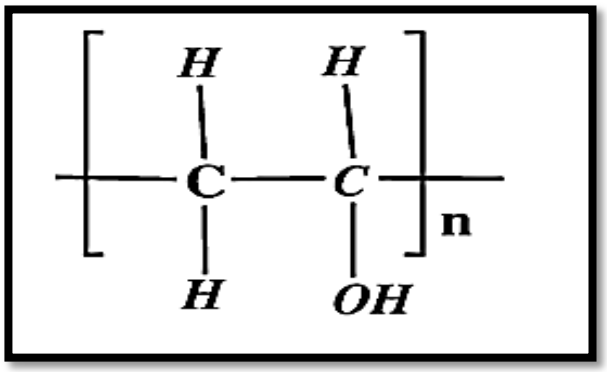

Figure (1.3): Chemical structure of PVA[23].

1.6.2.Carboxymethyl Cellulose (CMC)

Carboxymethyl cellulose is an ionic linear polymer that is employed in a wider variety of applications all over the world than any other water-soluble polymer that is currently known. CMC is a cellulose derivative that has carboxy methyl groups bonded to some of the hydroxyl groups of the glucopyranose monomers that make up the cellulose backbone [24].

These hydroxyl groups are found in the cellulose backbone. In the 1930s, Germany was the first country in the world to synthesize carboxymethyl cellulose. Since 1947, it has been produced in the United States of America. It was put to use in the manufacturing of a synthetic version of laundry detergent. In the meantime, CMC was beginning to find use in a wide variety of other industries. In most cases, CMC is made by reacting alkali cellulose with monochloroacetate or the sodium salt of monochloroacetate in an organic medium. [25].

Today, CMC is used to improve surface or barrier qualities, increase viscosity, manage the rheology of a solution, prevent the separation of water from a suspension, and prevent the separation of water from a suspension. The purified form of CMC is a powder that ranges in color from white to cream and is odorless, tasteless, and free flowing [26].

Additionally, CMC is utilized as a component in oil drilling fluids, where it serves the dual purpose of regulating the viscosity and preventing the evaporation of water. Ion-exchange chromatography is used to purify proteins, and a cation exchange resin made of insoluble microgranulated carboxymethyl cellulose is one of the components utilized in this process. CMC can also be used in cooling inserts, which makes it possible to create a eutectic mixture, lowers the temperature at which melting occurs, and provides superior cooling in contrast to traditional ice. CMC can be dissolved in water to create aqueous solutions that can be used to disseminate carbon nanotubes [27].

In the food business, carboxymethyl cellulose sees widespread application. CMC has the ability to improve the taste as well as the consistency of dairy drinks and spices. In addition, carboxymethyl cellulose is utilized in the production of ice cream, bread, cake, biscuits, instant noodles, and rapid paste foods for the purposes of product molding, the enhancement of flavor, and the strengthening of tenacity. The items that have an extremely high viscosity also have a strong capacity for thickening. Drying is the next step in processing for the majority of the CMC, which originally had a moisture content of forty percent [28].CMC structure is shown in Figure (1.4)

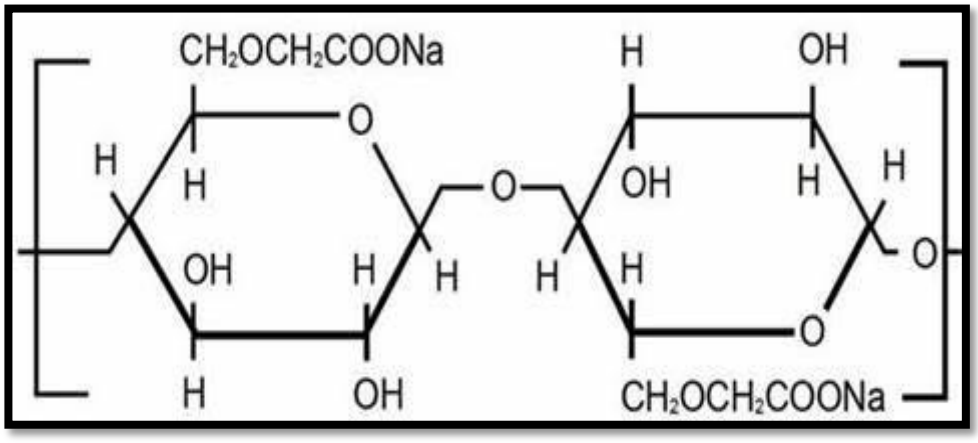

Figure (1.4): Structure of Carboxymethyl cellulose[28].

1.6.3.Polyvinyl Pyrrolidone (PVP)

Polyvinyl Pyrrolidone was introduced by Germans in world war II as a replacement for blood plasma [29]. A water-soluble polymer whose most valuable property is its ability to shape loose addition compounds with a wide range of substances. PVP is a biocompatible and hydrophilic material that has take advantage of the pharma industries, in addition, it has some eminent applications in wound healing[30].

From the commercial mental view, PVP has the major advantages of uses due to its relative ease and low cost[31]. Povidone is one of PVP common applications, as its used as a carrier of iodine [32]. The preparation of the monomer from acetylene, formaldehyde and ammonia, PVP may be sold in this form or spray dried to give a fine powder after polymerization in a watery solution produces a solution containing 30% polymer. The molecular weights produced are between 10,000 and 100,000 g/mol (k values 20-100) .

Because of its affinity for dyestuffs, polyvinyl pyrrolidone is used extensively in the garment industry, in the process of dye-leveling, the elimination of identity tints, and the formulation of sizes and finishes, as well as for the purpose of providing assistance in these procedures. Because of its unique ability to form loose addition compounds with both skin and hair, PVP is also utilized in the field of cosmetics[33].

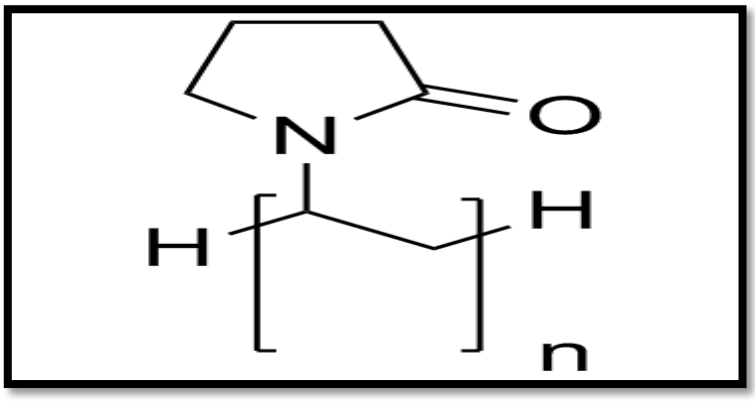

Figure (1.5): Chemical structure of Polyvinyl Pyrrolidone[33].

Table 1.1: Physical and Chemical Properties of Polyvinyl Alcohol (PVA), carboxymethyl cellulose (CMC) and polyvinylpyrrolidone (PVP) [34-36].

Parameter	PVA	CMC	PVP
Chemical formula	$(C_2H_4O)n$	$C_8H_{16}O_8$	$(C_6H_9NO)n$
Molar mass	86.09 g/mol	250000 g/mol	2,500–2,500,000 g/mol
Molecular weight	12.000-18.000	1.7×10^4	40000
Melting point	230 °C	274 °C	150 °C Increases as molecular weight increases
Glass transition	85°C	135°C	-180°C
Density	1.19-1.31 g/cm^3	1.6 g/cm^3	1.2 g/cm^3
solubility	Soluble in water, ethanol	Soluble in water,	Soluble in water and in ethanol. Insoluble in ether

1.6.4 Bismuth(III) oxide (Bi_2O_3)

Bismuth oxide (Bi_2O_3) nanoparticles with particle size between (20-30)nm, purities 99.8% , and yellow solid powder.It's an important functional material, and is widely used as excellent organic synthesis ,ceramic coloring agents, flame retardant plastics, pharmaceutical astringents, glass additives, high refractive index glass , glass manufacturing nuclear engineering and nuclear reactor fuel [37].

Nanometer Bi_2O_3 with the properties of the general size and due to the finer granularity, Bi_2O_3 nanoparticles can be used to inorganic pigments,optical materials, electronic materials superconducting materials, special functional ceramic material, acathode ray tube wall paint and so on [38].

Bi_2O_3 nanoparticles when combined with a specific polymeric mixture are a good candidate for use as patient radiation shielding in high-dose medical procedures [39].

Also the Bi-based composite oxide is a good photocatalyst which uses solar energy to eliminate pollutants.To protect the environment , maintain ecological balance , to achieve sustainable development contributes a lot. Bi-based composite oxide due to its unique physical properties can be used as an ion conductor, sound and light materials, light conductors, gas sensors, and photocatelysts [40].

Table 1.2: The most Important Properties of Bismuth(III) oxide [37].

Bismuth(III) oxide	
chemical formula	**Bi_2O_3**
Appearance	**Yellow crystals or powder**
Crystal structure	**Monoclinic**
Molar mass	**465.96 g/mol**
The Density	**8.9 g/cm^3 (solid)**
Melting point	**817 °C**

1.7 Litreture Review

M. A. Habeeb,**In 2013** [41] studied the A.C electrical and thermal properties for (PVA-PVP/Ag) nanocomposites. He found that the thermal conductivity increase with the increasing of the concentration of nanosilver and temperature, and the dielectric constant, dielectric loss and the A.C electrical condu-ctivity increases with the increasey of the concentration of nanosilver, the dielectric constant and dielectric loss decreases with the increasey in frequency, where the A.C electrical conductivity of nanocomposites is increasing with increasing of the frequency.

S. Asath Bahadur *et al.* in (2014)[42] studied polymer blend electrolyte based on PVA/PVP with proton salt, which prepared by solution

casting technique, The amorphous nature of the polymer electrolyte was shown by XRD, FTIR indicated the development of a complex between the polymer and the salt, whereas DSC revealed a drop in Tg when salt concentration was increased.

K. Hemalatha *et al.* in (2015)[43] studied the micro-structure, A.C conductivity and spectroscopic studies of copper sulphate doped PVA-PVP polymer composites, which prepared by casting technique, The amount of $CuSO_4$ in polymer composites increased the amorphousness of the matrix, according to XRD measurements, UV-Vis spectra revealed the presence of an optical energy gap in the films, while FTIR measurements revealed stretching and bending in the absorption bands in the films. A.C conductivity shown how the conductivity of these samples depending on the amount of $CuSo_4$ present.

A. M. El Sayed *et al.* in (2015)[44] Studied the manipulation of the physical characteristics of functional materials. Nanoparticles of copper oxide (CuO) with a monoclinic phase and an average crystallite size of 35 nm. For the preparation of (CMC),(PVA-CMC) and copper oxide/polyvinylalcohol (CMC) nanocomposite films, by a solution casting. Following the inclusion of PVA, the transparency of the CMC film rised by 87 percent; however, this transparency diminished after the integration of CuO nanoparticles. Mixing CMC with PVA and doping it with CuO nanoparticles allows for precise manipulation of the material's insulating characteristics, as well as its refractive index and optical constants. After being mixed with PVA, the optical transmittance (T percent) of CMC improved from 87 to 89 percent, but it dropped to 77 percent after being doped with 0.5 weight percent CuONPs. The inclusion of PVA caused a drop in the refractive index of CMC, which decreased from 1.645 to 1.576. The index then rise to 1.852 when CuO were doped into the

PVA/CMC mixture. PVA and CuO nanoparticles were also shown to have an effect on the optical constants of CMC film.

Z. A. Al-Ramadhan *et al.* in (2016)[45] studied the optical and morphological properties of (PVA-PVP-Ag) nanocomposites, which prepared by casting method,UV-Vis spectroscopy at a wavelength of (200-900)nm was used to evaluate the optical characteristics, By increasing nanoparticle concentration and refractive index, the energy gap of indirect transition (allowed and forbidden) decreased from (4.8-3.9 allowed) to (4.7-3.8 forbidden) as the amount of Ag was increased, the AFM and OM data revealed a homogeneous distribution, a very smooth surface, and minimal roughness.

Sk. Shahenoor Bash *et al*. in (2017)[46] studied the synthesis and spectrum characterisation of PVA-PVP/GO based mix polymer electrolytes, which were made using the casting method. As a result of the amorphous nature of the host polymer, SEM analysis revealed that GO was completely diffused throughout the polymer blend. Furthermore, a determination made using DSC showed that Tg decreased as GO wt percent increased up to 0.3 wt percent.

A. M. Ismail,*et al*.in (2018)[47] studied the optical properties of Lithium ions-doped polyvinyl alcohol/polyvinyl pyrrolidone(PVA-PVP) films.The results indicated that absorbance A and absorption index (α) are increased,. The optical band gap Eopt g of the composites showed significant decrease from 2.98 to 2.196 eV by adding Li_2SO_4 . The dependence of read dielectric constant Ɛ1, imaginary dielectric constant $Ɛ_2$ and optical conductivity (σ_{op}) opt on photon energy hυ were also studied. The indirect optical gap of the doped blend refers to the existence of charge transfers complexes in the host polymer by the addition of small amounts of Li ions.

S. Choudhary *et al.* in (2018)[48] examined the Polymer nanocomposite (PNC) films based on the blend matrix of poly(vinyl alcohol)(PVA)–poly(vinyl pyrrolidone) (PVP) (50/50wt%) included zinc oxide (ZnO)nanoparticles (i.e., (PVA–PVP)–x wt percent ZnO; x = 0, 1, 3, and 5). These films were made using the solution- The concentration of, direct and indirect optical energy band gap, refractive index, electrical conductivity, and activation energy are all impacted by ZnO's presence. It was found that the dispersion of just one weight percent of ZnO nanoparticles in the matrix of the PVA–PVP blend had a significant impact on a number of the characteristics of the PNC film. When the concentration of ZnO is increased up to 5 weight percent, both the dielectric permittivity and the electrical conductivity rise. The observed values of their structural, morphological, thermal, optical, dielectric, and electrical parameters have confirmed that the optical band gap of the PVA–PVP blend is slightly higher than 5 eV and decreases non-linearly while the refractive index increases with the increase of ZnO contents in the PNC films. These results have been confirmed by the observed values of their structural, morphological, thermal, optical, dielectric, and electrical parameters.

K. Rajesh et al. in (2019) [49] studied the structural, optical, mechanical, and dielectric properties of titanium dioxide doped PVA/PVP nanocomposite by solvent casting approach. TiO_2 nanoparticles bring about a narrowing of the optical energy gap when they are introduced. According to the dielectric plot, the dielectric constant rises up to the point where there is a doping concentration of 12wt %TiO_2. After that point, an increase in the doping concentration results in a decrease in the dielectric constant.

F.M.Ali *et al.* (2019)[50] explored the Structural and optical characterization of PVA-PVP-Cu^{2+} composite films containing high quality semiconducting polymers of copper ions doped poly(vinyl alcohol) (PVA): poly(vinyl pyrrolidone (PVP). poly(vinyl pyrrolidone) with a

weight ratio of 50:50 PVA-PVP with x wt% copper+ . The standard method of solution casting was used, and it was successful in producing composite films with x values of 0, 3, 5, 15, and 20 wt% .

The incorporation of Cu2+ ions into the (PVA-PVP) blend chains has a significant impact on the optical energy gaps as well as the high frequency refractive indices. The optical gap was reduced from 4.68 eV for pure (PVA-PVP) polymer blend to 2.95 eV for PVA-PVP -20 wt % Cu^{2+} and the high frequency refractive index was raised from 2.42 to 2.78. According to the data that was gathered, the copper ions doped (PVA:PVP) polymer blend composite films have the potential to be a useful, innovative and easy to work with material for the construction of UV filters, semiconducting polymer devices, planar polymer waveguides and polymer solar cells.

H. S. Rasheed *et al.* in (2020)[51] utilizing the casting method, investigated the effect of adding ZrC nanoparticles to a (PVP-PVA) blend and how it affected the optical characteristics of the mixture for a humidity sensor application. The optical properties showed a decrease in absorbance with increasing concentration of ZrC nanoparticles, The energy gap gets larger as the amount of ZrC nanoparticles in the sample's weight increases. The coefficient of extinction (k), as well as both the real and imaginary constants, were found to be increased with increasing in the concentration of ZrC nanoparticles.

A. A. Abid *et al.* in (2020) [52] studied the Structural and Electrical Properties of (PVA-PVP-Carbon black (C.B)) Nanocomposites . The nanocomposites (PVA-PVP-C.B) were prepared by casting process. The optical microscope, infrared spectroscopy, and electrical properties have also been investigated .With increasing the value of frequency, the dielectric constant with the dielectric loss of the samples was decreased.

During the operation of an electric field, an increase in A.C electrical conductivity was observed as the frequency value increased. With increasing carbon black concentrations, the electrical conductivity (A.C), dielectric loss, and constant of all the samples increased.

A. Hashim1. in (2020)[53] studied the Structural, Optical, and electronic properties of In_2O_3 and Cr_2O_3 nanoparticles doped polymer blend for flexible electronics and potential applications. The results of structural, optical, electronic and electrical characteristics indicated to the PVA-PVP-In_2O_3 and PVA –PVP-Cr_2O_3 nanocomposites can be used in sensors, transistors, photovoltaic, solar cells, electronics gates and other fields with excellent properties which include flexible, high corrosion resistance, low weight. The results showed that the both nanocomposites have good optical properties with energy band gap range (2.8–1.1) eV which make it suitable for various optoelectronics industries. Also, the results indicated to the PVA-PVP-In_2O_3 and PVA-PVP-Cr_2O_3 nanocomposites have excellent electronic and electrical conductivity which can be used for different photonics and electronics applications.

Mohammed Irfan *et al.* in (2021) [54] studied the Solid polymer electrolyte films of (PVA)/ (PVP) doped with sodium fluoride (NaF) of different weight ratios (2, 4, 6, 8, and 10 wt%) have been prepared by using solution casting method, The result showed that the X-ray diffraction (XRD) spectra show a characteristic PVA peak signifying its semi-crystalline nature. As NaF salt is incorporated into the polymer blend, the peak intensity decreases gradually, implying a decrease in the degree of crystallinity of the samples. The FTIR study confirmed the complexation, functional group occurred, and interaction between the different components in the polymer blend electrolyte, which suggests the micro-structural variations, takes place in polymer blended films by addition of

NaF salt. The dielectric constant was found to decrease with increase in frequency and increased with temperature increase.

V.Siva *et al.* in (2021) [55] studied the simple solution casting approach was used to manufacture a hybrid kind of polymer nanocomposites based on(PVA-PVP-SnO) nanocomposites. These nanocomposites were fabricated using PVA and PVP. According to the findings of the FTIR study, the presence of hydrogen bonding interaction between SnO and the PVA-PVP mix matrix was indicated.

Doaa E. Al- Kateb *et al.* in (2021)[56] studied the Structural and optical properties of (PVA-PVP-Sn2NO3) nanocomposites, which were prepare by casting technique with varying concentrations of Sr_2No_3.In this study, the optical properties obtained by a UV-Vis spectrometer, an OM spectrometer, and an FTIR spectrometer were revealed. The absorbance increased with increasing concentrations of Sn_2NO_3 nanoparticles, while the energy-gap transitions (both allowed and forbidden) decreased with increasing concentrations of nanoparticles.

H. A. H. Alzahrani, in(2022) [57] studied Morphological, Optical, Thermal, Dielectric, and Electrical Characteristics of Copper dioxide (CuO) nanoparticles and Multiwall carbon nanotubes (MWCNTs) filled poly(vinyl alcohol) (PVA) and poly(vinyl pyrrolidone) (PVP) blend matrix (50/50 wt%) based polymer nanocomposites (PNCs) (i.e., PVA/PVP:(15-x)CuO(x)MWCNTs for x = 0,1,5,7.5, 10,14, and 15wt%) have been prepared to employ the solution-cast method. The FTIR, SEM, and AFM measurements of PNCs were used to investigate the development of the miscible mix, polymer-polymer and polymer–nanoparticle interactions, and the influence of CuO and MWCNTs nanofillers on the morphology aspects on the main chain of PVA/PVP blend. It found that optical energy gap decrease with an increase in the nanoparticles The DC conductivity values

augment with the upsurge in nanofiller level for maximum x = 14 wt%, The rise in applied frequency reduces dielectric permittivity and impedance values and enhances ac electrical conductivity.

1.9. The Aims of the Work

The aim of this work can be summarized in the following points:

1. Studying the structural, optical, and A.C electrical properties of (PVA-PVP-Bi_2O_3) and (PVA-CMC/ Bi_2O_3) nanocomposites.
2. Studying the absorbance of gamma rays of (PVA-PVP/Bi_2O_3) and (PVA-CMC-Bi_2O_3) nanocomposites.

Chapter Two

Theoretical Part

2.1. Introduction

In this chapter, we will focus on the theoretical part of this study, which include the physical concepts, relationships, devices and laws that deal with the study.

2.2 The Structural Properties

The structural properties involve two aspects: the optical microscope and the FTIR.

2.2.1 Optical Microscope

One of the first techniques used to study the topography of a surface is noptical microscopy, also called light microscopy, is a type of microscope that uses visible light and a system of lenses to magnify images of small samples.

Optical microscopes are the oldest design of microscope and were possibly designed in their present compound form in the 17th century. An optical microscope usually has a single eyepiece which can often be fitted with a camera for photography[58].

Traditional optical microscopes have a resolution restricted by the size of submicron particles approaching the wavelength of visible light (400–700 nm)include:

1- Transmission: beam of light passes through the sample.

2- Reflection: beam of light reflected off the sample surface.

An example is the polarizing or petrographic microscope for which the samples are usually fine powder or thin slices (transparent). Another example is the metallurgical or reflected light microscope which is used for the surfaces of materials, especially opaque ones[59].

The image from an optical microscope can be captured by normal light sensitive cameras to produce a micrograph. Typically, images were captured by photographic film but modern developments in supplementary metal oxide semiconductor and charge-coupled device (CCD) cameras permit the capture of digital images. Simply, digital microscopes are now available that use a CCD camera to examine a sample, showing the resulting image directly on a computer screen without the need for eyepieces[60].

2.2.2 Fourier Transforms Infrared (FT-IR) Spectroscopy

The Fourier Transform Infrared (FTIR) Spectroscopy is a non-destructive chemical characterization method. This spectral region is classified into three regions far-infrared, near-infrared and, mid-infrared which are between (4~400 cm^{-1}), between (400~4,000cm^{-1}) and lastly, between (4,000~14,000 cm^{-1}), respectively. FTIR spectroscopy is a vibrational spectroscopic method that can be used for the optical study of molecular shifts. The allowable existence of this technology relies on the identification of vibration in the sample by the chemical functional group. Wherever an interaction takes place between infrared light and matter, the chemical bonds will stretch. Infrared radiation is absorbed by the chemical functional group at a specific wavenumber frequency, independent of the rest of the molecule composition [61].

The FTIR spectroscopy form is advantageous in several advanced areas, such as microanalysis (whereby higher sensitivity is needed), in the dark, solid state samples or analysis of aqueous solutions that involve the focus on quantitative assessment, and in studies whereby study time is a limiting factor, such as in quality control measurements or processing [62]. Various spectroscopic techniques are applied in studying the different samples. However, FT-IR spectrometers are becoming increasingly

common because they deliver, speed precision and sensitivity which were previously difficult to obtain through dispersive spectrometer wavelengths. This technicality enables micro samples to be analyzed rapidly to reach for nano-gram levels. Given that FT-IR is a crucial tool for solving issues within various fields of study, it still needs more research, as its concepts vary from those dispersive spectroscopy techniques which use interferometers within spectrometers [63].

2.3 The Optical Properties

The optical absorption spectra research offers a very efficient instrument to the study of electronic transitions that have an optical induction. They also present a perspective on the energy gap and band structure of crystalline and amorphous materials. The theory behind such an approach is that photons that have an energy level over the band gap energy are captured by the absorption and transition of ultra-violet and visible energy [64,65].

In recent years, the search for optical properties has increased due to their use in integrated optics, such as optical data storage and optical information [66,67]. Research on the optical and electrical properties of polymers has also received a great deal of interest in the light of their application in similar apparatus. Electrical conduction in polymers was examined with a view to understanding the characteristic features of the load transport prevailing in these materials, whereas optical properties are developed to enhance reflective and anti-reflective interference and polarization properties [68].

2.3.1 Absorbance(A)

Absorbance is defined as the intensity of the absorbed light (I_A) by the materials to the incident intensity of light (I_o) as a ratio, and which are given in the following equation [69]:

$$A = \frac{I_A}{I_o} \qquad \ldots\ldots(2.1)$$

2.3.2 Transmittance (T)

The intensity of transmitted rays from the film (I_T) over the intensity of incident rays on the film (Io) is called the transmittance (T), and can be obtained as follows [70]:

$$T = I_T / I_o \qquad \ldots\ldots (2.2)$$

2.3.3 Absorption Coefficient (α)

Absorption coefficient (α) can be described as the decrement rate of incident radiation proportional to the unit length within the direction of wave propagation through the medium [71]. It depends on the photon energy (hυ) Photon energy produced by Planck's relationship [72]:

$$E = h\upsilon = hc / \lambda \qquad \ldots\ldots(2.3)$$

Where (c) represents the speed of light, and (λ) represents the wavelength of light.

The transmittance of the absorbing medium of thickness d is indicated by [73]:

$$T = (1 - R)^2 e^{-\alpha d} \qquad \ldots\ldots(2.4)$$

Where (**T**) is the transmittance, and **(R**) is the reflectance.

When the light of intensity (I_o) occurs on the film of thickness (d), the transmitted intensity (I_T) can be given as follows [74]:

$\alpha d = 2.303 \log (I_o / I_T)$ ..... (2.5)

where the quantity of log I/Io represents the absorbance (A). The absorption coefficient can be calculated as below[68]:

$\alpha = (2.303 \times A) / d$ ..... (2.6)

2.3.4. Fundamental absorption edge

Fundamental absorption edge could be described as the fast increase in absorbency whenever the absorbed energy radiation nearly equals the energy band gap. As a result, the fundamental absorption edge reflects lesser energy difference from the peaks in the valance band (V.B) to the bottom point in the conduction band (C.B). The absorption regions can be divided into three regions, as seen in Figure (2.1) [75].

A) High absorption region

The value of (α) in part A is greater than or equals $10^4 cm^{-1}$. The size of the prohibited optical band gap (Eg_{opt}) could be added from this region.

B) Exponential region

As for part B, the value of (α) should be in the range 1 $cm^{-1} < \alpha < 10^4 cm^{-1}$. It indicates the transition from the extended level at the top of the valence band towards the localized level at the conductive band and vice versa, from the local level at towards the extended level at the bottom from conductive band[76].

C) Low absorption region

Part C involves a relatively smaller value of (α), being about $\alpha < 1 cm^{-1.}$ The transition occurs in this region as a result of the state of density within space motion due to structural faults [76].

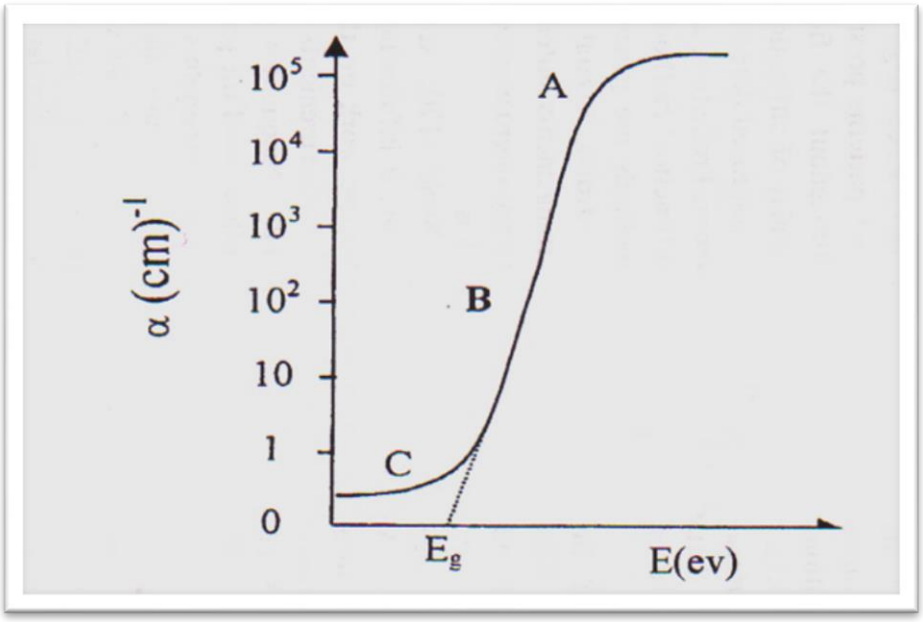

Figure (2.1): The absorption regions [76].

2.3.5. The Electronic Transitions

There are two basic forms of electronic transition: direct and indirect transition.

2.3.5.1. Direct Transitions

This kind of transitions occurs in semi-conductors, where the bottom of the conduction is precisely above the top of the valance band, thus implying that they share similar wave vector values i.e. ($\Delta K=0$). In such a case, the absorption would occur at ($h\upsilon = E_{gopt}$). Therefore, the phonons do not take part in direct transition since the phonon's wave vector (K) is much greater than that of the photons. This transition type requires the laws of conservation in momentum and energy**.** The direct photon transition to the energy of the minimum gap reaches no satisfaction of the demand for conserving the wave vector, as the photon wave vectors could be neglected in the given energy range [77]. There are two kinds of direct transitions [78].

A) Direct Allowed Transition

It occurs from the top points of the valance band and the bottom point of the conduction transition and, as see in figure (2.2-a).

B) Direct Forbidden Transitions

It takes place between the close top points of the valance band and the bottom points of the conductive band, as presented in figure (2.2-b). Its absorption coefficient is presented in [79]:

$$\alpha h\upsilon = B\,(h\upsilon - Eg^{opt})^{r} \qquad \ldots\ldots(2.\ 7)$$

Where (Eg^{opt}) is the energy gap between direct transition

(B) is the constant (according to the type of material)

(r) is the exponential constant (according to the type of transition).

The value of (r) is (1/2) and (3/2) for the allowed and forbidden direct transition.

2.3.5.2. Indirect Transitions

As for the electronic optical indirect transition, the bottom of conduction band and the top of valance band are in various regions of space (k). This type of transformation happens with the aid of the phonon to maintain the motion arising from variation in the electron wave vector. Two types of indirect transition exist, namely whenever the transition is between the top point of valance band and the lower point of the conduction band, which is located in the various regions of the space (k) called allowed indirect transition as shown in Figure(2.2c)and when these transitions happen between near points in the top of valance band and near points in the bottom of conductive band called forbidden indirect transitions , as shown in Figure(2.2d). As seen in Figure (2.2), the

absorption coefficient for transition with a phonon absorption can be obtained through the following equation[80]:

$$\alpha h\upsilon = B\left(h\upsilon - Eg^{opt} \pm E_{ph}\right)r \quad \ldots\ldots (2.8)$$

Where (E_{ph}) is the energy of phonon. Its value is (-) when the phonon is absorbed, whereas it is (+) in case the phonon is emitted. The value of (r) is (2) and (3) for the allowed and forbidden indirect transitions, respectively.

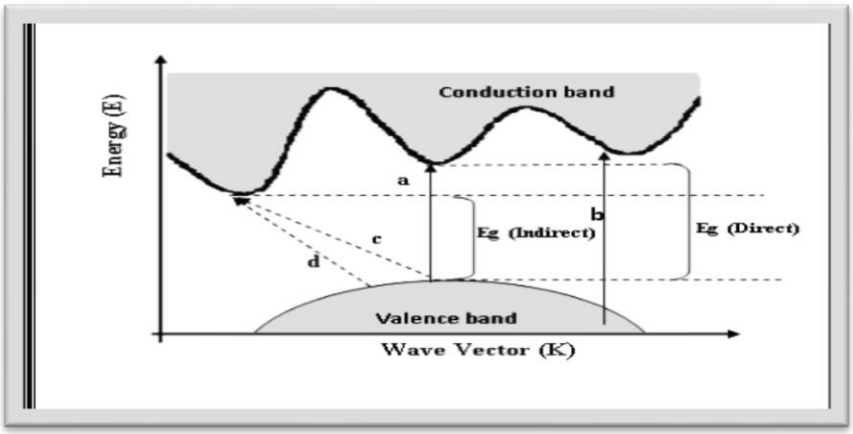

Figure (2.2): The Electronic Transitions Types of (a) Allowed direct, (b) Forbidden Direct Transition, (c) Allowed Indirect and d) Forbidden Indirect Transitions [81].

2.3.6. The Refractive Index (n)

A material's coefficient of refraction represents the rate of speed of light within vacuum to the speed of light within the samples [82]:

$$n = \frac{c}{v} \quad \ldots\ldots(2.9)$$

Where (c) and (v) are the speed of light in vacuum and in the samples, respectively [74]. The reflectance (R) was calculated from the transmission (T) and absorbance (A) values through the following equation[82]:

$$R+T+A=1 \quad \ldots\ldots (2.10)$$

The refractive index (n) can be calculated using the following equation [83]:

$$n = \sqrt{4R - \frac{k2}{(R-1)2}} - \frac{(R+1)}{(R-1)} \quad \ldots\ldots (2.11)$$

2.3.7 The Extinction Coefficient (K)

The extinction coefficient (K) presents the amount of attenuation of the electro-magnetic wave that passes through a material. Its value is determined by the density of the free electrons within the material and its structure [84]. It is the imaginary part of the complex refractive index (n) [85]:

$$N = n - i\,K \quad \ldots\ldots (2.12)$$

Where (n) represents the real part of refractive index.

$$K = \alpha\,\lambda/4\pi \quad \ldots\ldots (2.13)$$

Where (k) is the extinction coefficient, and (λ) is the wavelength of incident light [86].

2.3.8.The Dielectric Constant (ε')

The real and imaginary portions for dielectric constant (ε_1) and (ε_2) are obtained as follows [87].

$$\varepsilon_1 = (n^2 - k^2) \quad \ldots\ldots (2.14)$$

$$\varepsilon_2 = (2nk) \quad \ldots\ldots (2.15)$$

2.3.9 The Optical Conductivity (σ_{op})

The optical conductivity (**σ_{op}**) relies directly on the absorption coefficient (α) and refractive index (n), using the following relation [88]:

$$\sigma_{op} = \frac{\alpha n c}{4\pi} \quad \ldots\ldots (2.16)$$

2.4 Electrical Properties

The electrical features of substances are determined by both its chemical composition and the atom structure in the solid. The presence of defects indicates that the electron states within the energy gap affects the electrical features of the substance. Such a may be minimized through several procedures, including the annealing procedure [89]. Polymers are not entirely free of conduction mechanisms, a limited amount of charge carriers may have low-level conduction, and basically insulating polymers may take a range of types. Conduction is very often caused by impurities which involve low concentrations of charge carriers that take form of electrons or ions [90].

The electrical properties heavily rely on both the deposition conditions and the preparation technique [91].Based on the ability of electrical conductivity, substances can be classified into insulators, conductors, semiconductors, and superconductors [92], whose conductivity ranges are 10^{-18}–10^{-8} $(\Omega\ .cm)^{-1}$, 10^{-8}–10^{3} $(\Omega.cm)^{-1}$, over 10^{3}–10^{8} $(\Omega\ .cm)^{-1}$, and 10^{8}–10^{20} $(\Omega\ .cm)^{-1}$, respectively. Figure (2.3) described the conductivity of materials [93].

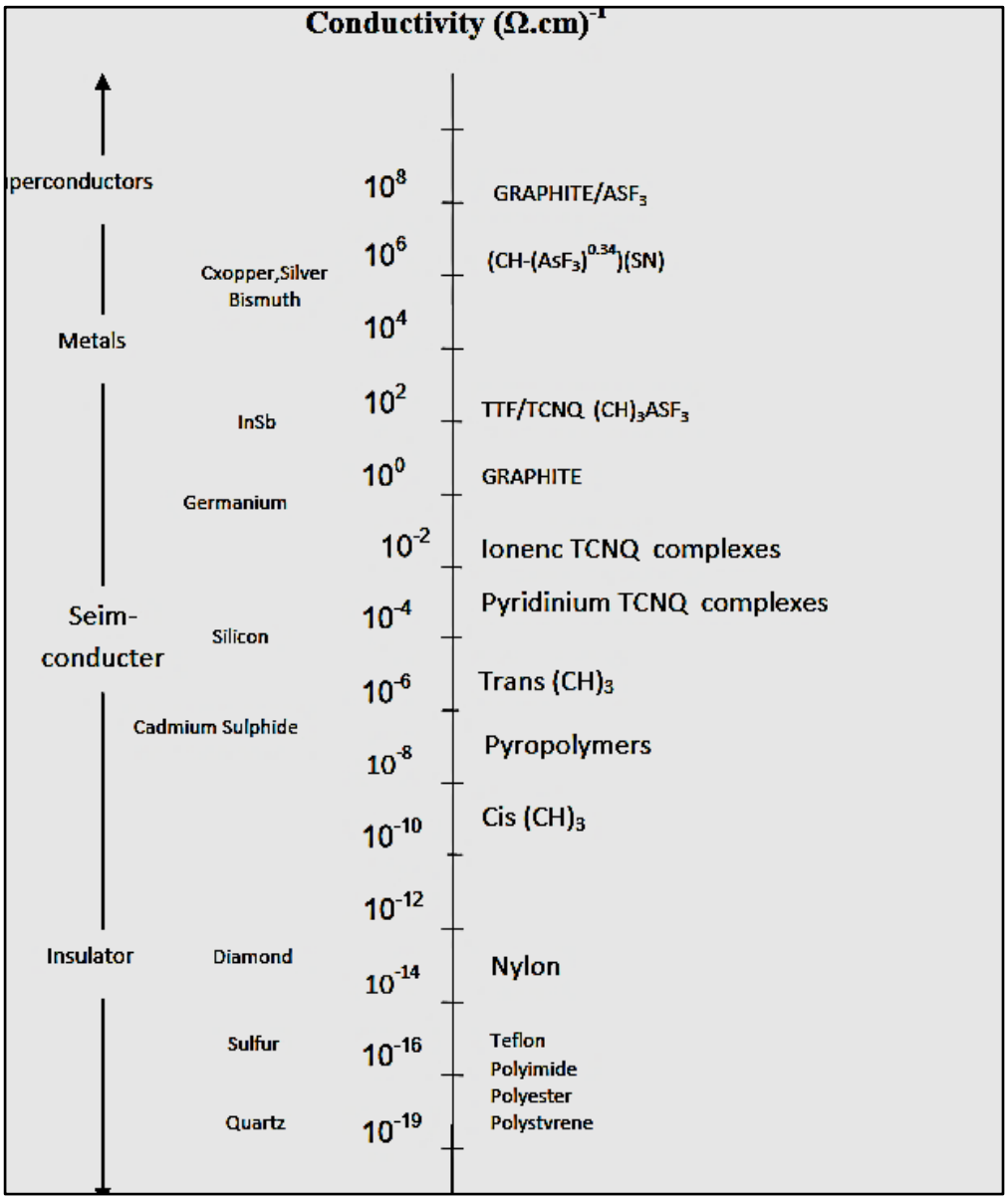

Figure (2.3): The Classification of Material Conductivity [93].

2.4.1 The A.C Electrical Conductivity

A.C conductivity affects the frequency of the electrical field [94]. Dielectric spectroscopy is based on the calculation of current and voltage phases and the amplitude A.C system. It is commonly used for the study of dielectric properties of polymers e.g. (ε' and tanδ) [95]. The electrical conductivity of isolation polymer materials can be improved through adding certain conductive fillers [96]. The dielectric constant represents the ratio of the capacitance of the condenser that contains an insulator material between its conductive plates, to the capacity of the same size but with

vacuum between its plates. Its value varies from material to material based on the amount of polarization that occurs in the material [97].

When an alternating potential $V = V_m e^{i\omega t}$ [97] is applied through a capacitor (C) loaded with an insulator, the current going through the capacitor will precede the potential by $\pi/2$ [98].

$$I = j\omega c v_m \quad \ldots\ldots. (2.17)$$

Where (**ω**) is the applied angular frequency of the filed **(ω=2πf)**, **(j)** refers to the number of imaginary and is equal to $\sqrt{-1}$, **(C)** is the capacitance of a capacitor, and **(V_m)** is the highest voltage. The angle between electric current and voltage is less than π/2, as seen in Figure (2.4). The sum of the conduction current (I_p) is assumed to be electric current. This is phase with voltage, whereas the capacitates current (I_q) is with the phase variation (π/2). The current can be obtained through the equation below[98]:

$$I = I_P + jI_q \quad \ldots\ldots. (2.18)$$

The capacitance of a condenser consisting of two parallel plates can be defined through the following equation [99]:

$$C = \frac{A_r}{d} \varepsilon \varepsilon_o \quad \ldots\ldots. (2.19)$$

where (A_r) is the area, and (d) is the thickness.

By substituting equation (2.24) in (2.22), the following relation is obtained:

$$I = i \omega \varepsilon \varepsilon_o V A_r/d \quad \ldots\ldots(2.20)$$

The dielectric constant is then viewed as a complex quantity (ε). The difference of the real and imaginary components of the complex dielectric constant is defined as follows [100]:

$$\varepsilon = \varepsilon' - i \varepsilon'' \quad \ldots\ldots(2.21)$$

where (ε") is the dielectric loss.

$$I = i\,\omega\varepsilon_o \frac{A_r}{d} (\varepsilon' - i\,\varepsilon'')\, V \quad \ldots\ldots(2.22)$$

By comparing equation (2.27) to (2.22), the following can be obtained:

$$I_p = \omega\varepsilon_o\,\varepsilon''\,\frac{A_r}{d}\,V \quad \ldots\ldots(2.23)$$

$$I_q = \omega\varepsilon_o\,\varepsilon'\,\frac{A_r}{d}\,V \quad \ldots\ldots(2.24)$$

Figure (2.4) shows that the loss factor (tanδ) is calculated by the following equation [98]:

$$\tan\delta = I_p / I_q = \varepsilon''/\varepsilon \quad \ldots\ldots(2.25)$$

The capacitor can be represented by an ideal capacitor connected in parallel with a resistance R_P at low frequencies, so:

$$I = I_p + iI_q = \frac{V}{R_P} + i\,\omega C_p\, V \quad \ldots\ldots(2.26)$$

Hence, the impedance **z** is then given by

$$\frac{1}{Z} = \frac{1}{R_P} + i\,\omega\,C_p \quad \ldots\ldots(2.27)$$

From equations (2.28), (2.29) and (2.31), one can write [97]:

$$R_P = d / \omega A_r \varepsilon_o\,\varepsilon'' \quad \ldots\ldots(2.28)$$

$$\varepsilon'' = 1 / \omega\, R_P\, C_o \quad \ldots\ldots(2.29)$$

$$C_P = \varepsilon_o\,\varepsilon'\,A_r / d \quad \ldots\ldots(2.30)$$

$$\varepsilon' = C_P / C_o \quad \ldots\ldots(2.31)$$

The dissipated power in the insulator is represented by the existence of alternating potential as a function of the alternating conductivity, as explained in the following equation:

$$\sigma_{A.C} = \omega\,\varepsilon_o\,\varepsilon'' \quad \ldots\ldots (2.32)$$

$\sigma_{A.C}$ represents the measurement of the temperature produced by the insulation material arising from the vibration of the charges or rotation of the dipoles in their positions. This is the result of the alternation of the field [101].

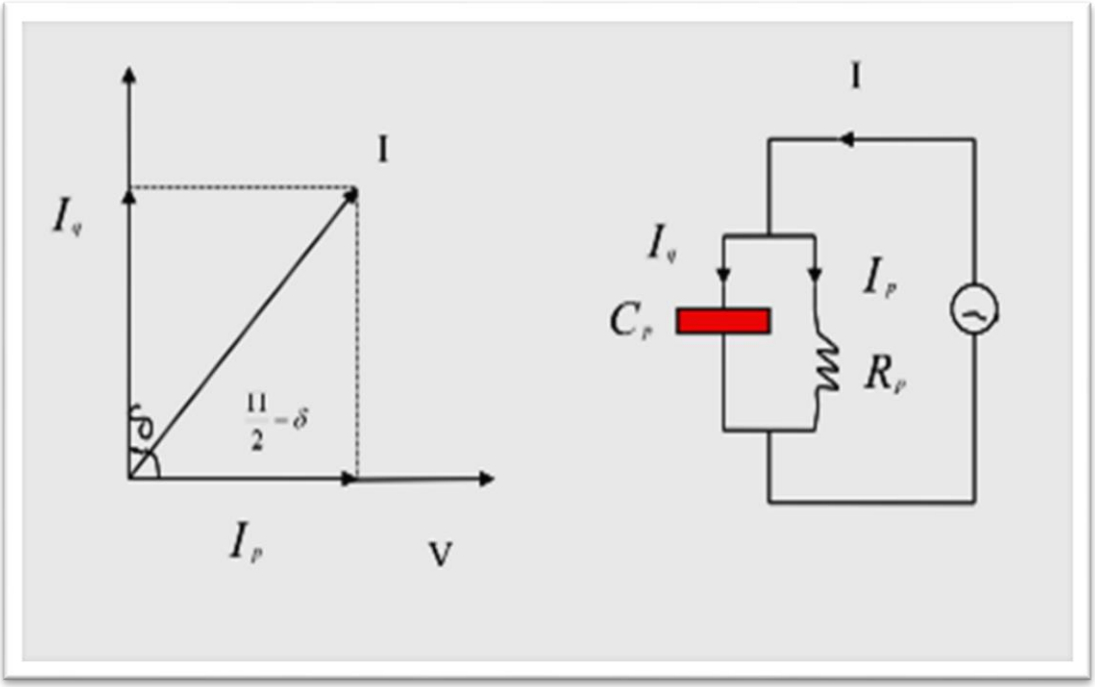

Figure (2.4) The circuit equivalent to non-ideal capacitor [98].

2.5 Gamma Ray Shielding Application

The contribution of nanocomposites has developing a novel generation of nanocomposite materials that has different approaches in engineering, military industrialization and medicine [102]. Industrial, science and technological instruments and communication techniques have been used on a comprehensive scale. However, electro-magnetic interference remains a big concern as it decreases the life and performance of the instruments [103]. A sufficient number of studies have been conducted on the effects rays of gamma radiation produced by gamma sources, nuclear reactors and even nuclear medicine on non-and living systems. High density materials composed of high-atom-number elements, such as lead or tungsten are the most effective shields for gamma-ray attenuation [104,105].

Electromagnetic interference shielding indicates the absorption or reflection of electromagnetic radiation by means of a substance serving as a barrier from radiation penetration through a shield [106].

With the use of active gamma ray isotopes in industry, agriculture and medicine, researching the attenuation index of different materials has become significant both biologically and technologically [107]. The following equation shows the properties of the radiation attenuation:

$$N = N_0 \exp(-\mu t) \quad \ldots\ldots \quad (2.33)$$

Where (N_0) represents the number of radiation particles counted at a given time. The period shall be without any absorber. (μ) is the attenuation coefficient of gamma radiation. (N) is the amount of counted radiation particles at the same time, with the thickness of the sampled [108].

Chapter Three

Experimental Work

3.1. Introduction

In any experimental work, there are a specific mechanism for manner of working, devices to examine the samples and an exact theorems to explain the results . In this chapter we will illustrate in details the materials used and the preparation process with devices that used in this work to find out the structural, optical, and electrical properties.

3.2. The Utilized Materials

3.2.1. Matrix material

3.2.1.1.Polyvinyl Alcohol (PVA)

PVA which is used with an average molecular weight of (12000-18000g /mol), its physical form: is pure, solid, white, odorless granules. CAS Number:9002-89-5, its melting point of PVA is 230^0C.

3.2.1.2. Polyvinyl Pyrrolidone (PVP)

(PVP) which is used with average molecular weight of (40.000), CAS No.:9003-39-8, by Chem Center 5580 la Jolla Blvd (La Jolla, CA92037)

3.2.1.3 Carboxymethyl Cellulose (CMC)

The material (CMC) used is a white powder, the molecular weight is 1.7×10^4 g/mol and could be obtained from local markets, and high purity (99.97 %).

3.2.1.4. Additive Material

Bismuth oxide(Bi_2O_3) nanoparticles were used in the study having purity : 99.8%, form: powder, yellow in colour, average particle size:20-30 nm, made in China by Honqwu international.

3.3. The Preparation of (PVA-CMC/Bi_2O_3) and (PVA-PVP/Bi_2O_3) Nanocomposites

The (PVA-PVP/Bi_2O_3) and (PVA-CMC/Bi_2O_3) nanocomposites are prepared by dissolving(1gm) from polymers in (50) ml of distilled water separated in two groups uneven concentrations which are 90wt.% PVA in temperature is (80^0C) and (10wt.% PVP , 10wt.% CMC) in temperature is (45^0C) by using magnetic stirrer to mix the polymers for (2 hour) to obtain more homogeneous solution. The Bi_2O_3 nanoparticles is added each one to polymers mixture with different weight ratios which are (0,1,3, and 5 wt.%) as shown in tables (3-1), (3-2). The casting method is used to prepare the samples of (PVA-PVP/Bi_2O_3) and (PVA-CMC/ Bi_2O_3) nanocomposites in the template (petri dish with diameter 10 cm). The stages of the experimental work and procedure are illustrated in Figure(3-1).

Table 3.1: Weight percentages for nanocomposites

PVA wt.%	PVP wt.% orCMC wt.%	Bi_2O_3wt.%
90	10	0
80	19	1
70	27	3
60	35	5

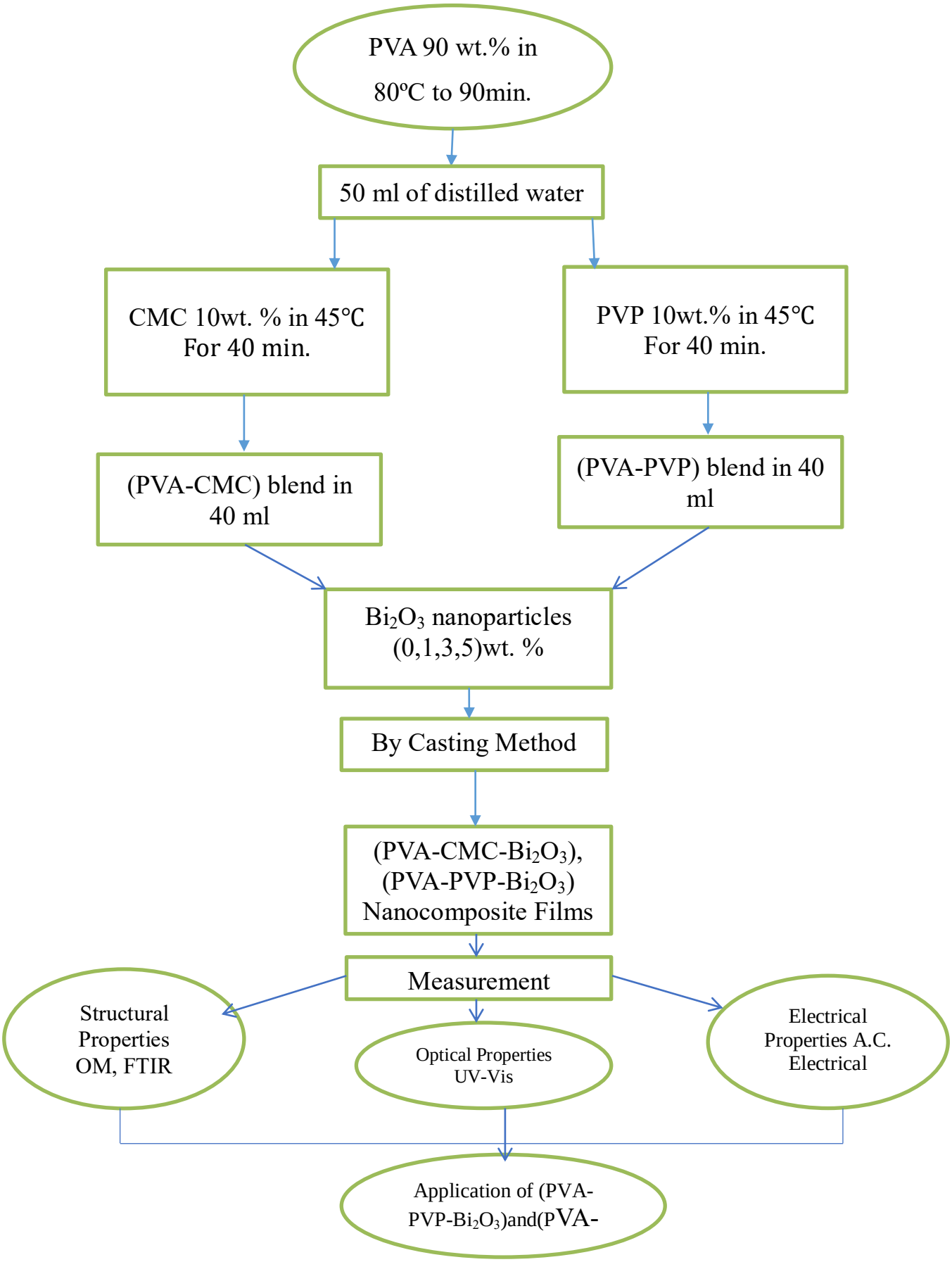

Figure (3.1):Scheme of Experimental work.

3.4 Measurement of Structural Properties for (PVA-PVP/Bi_2O_3) and (PVA-CMC/Bi_2O_3) Nanocomposites

3.4.1 Optical Microscope (OM)

Olympus (Top View) type Nikon-73346 optical microscope with automatic camera controlled by light intensity investigated the (PVA-PVP/Bi_2O_3) and (PVA-CMC/Bi_2O_3) nanocomposites specimens. The work on this device was carried out in University of Babylon College of Education , this measurement under magnfication (40x), as shown in Figure (3.2).

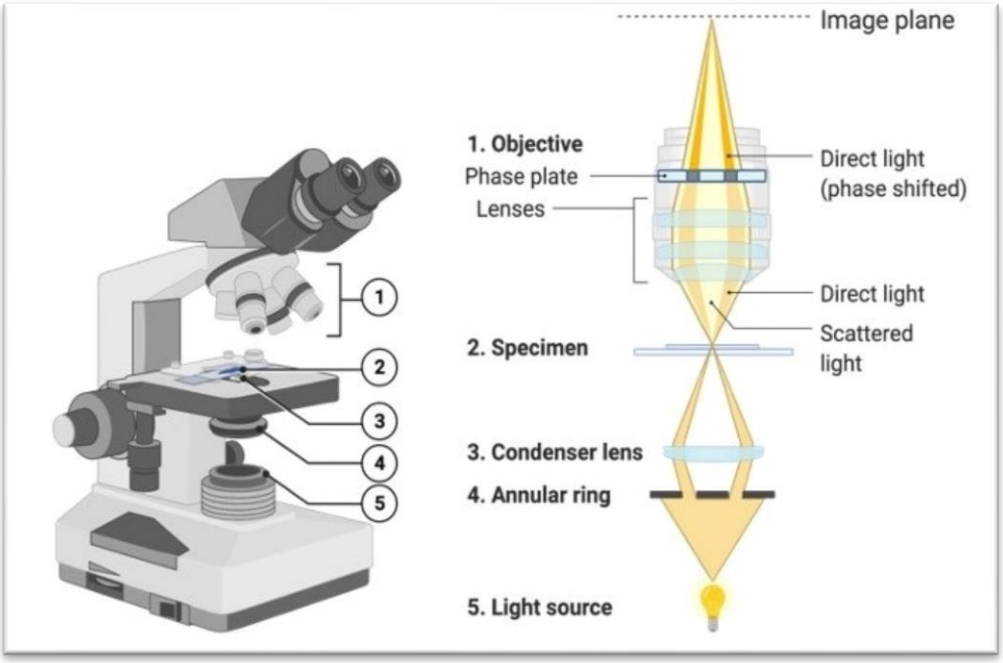

Figure (3.2):The optical Microscope.

3.4.2 FTIR Spectral Characterization

FTIR was used to capture FTIR spectra (Bruker company, German origin, type vertex -70),operated with wavenumber (4000-1000) cm^{-1}. In the University of Babylon College of Education for Pure Sciences-Department of Physics, FTIR was adopted, as shown in figure (3.3).

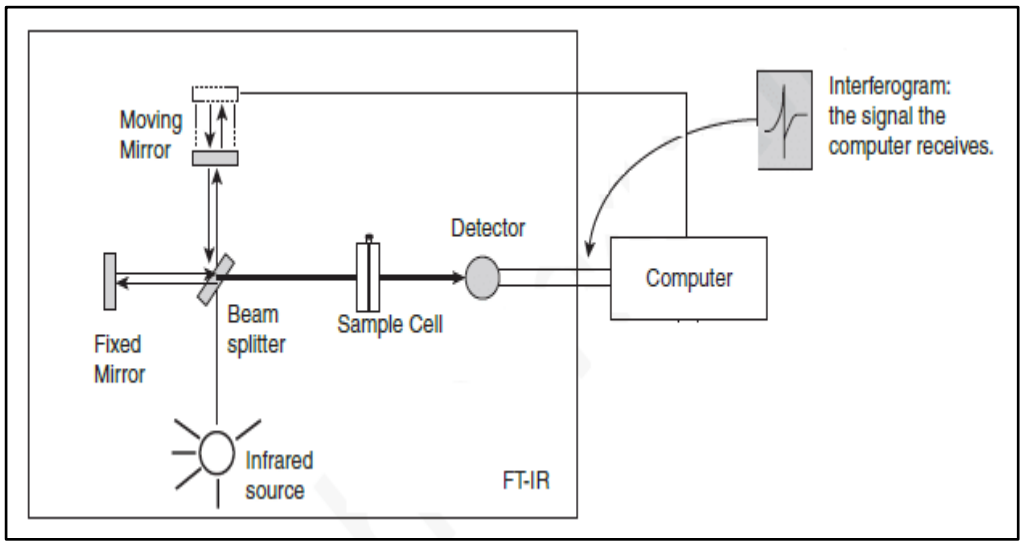

Figure (3.3): FTIR Spectroscopy.

3.5 Optical Properties Measurements

Measurements were made with a Shimadzu UV-18000A double beam spectrophotometer (190-1100nm) on films made of (PVA-PVP/Bi_2O_3) and (PVA-CMC/Bi_2O_3) nanocomposites. The University of Babylon College of Education for Pure Sciences implemented this measurement as indicated in Figure (3.4).

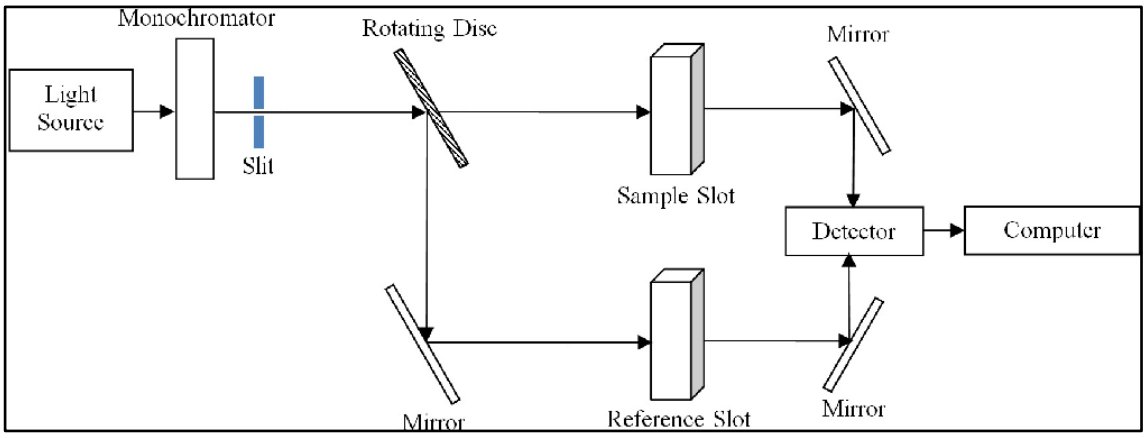

Figure (3.4): UV–Visible Spectrophotometer (Shimadzu-1800).

3.6. Measurement of A.C. Electrical Conductivity

A. C. Electrical Conductivity was calculated by (L.C.R) kind HIOKI 3532-50 LCR Hi TESTER (Japan) at labocatories of the University of Babylon /College of Education for Pure Sciences . Figure (3.5) displays a

picture the system of A .C electrical measurement dispersion factor and capacitance were reported for all samples at a frequency between (100-5×10^6) Hz at room temperature. Dielectric constant, dielectric loss ,and conductivity have been calculated from this data.

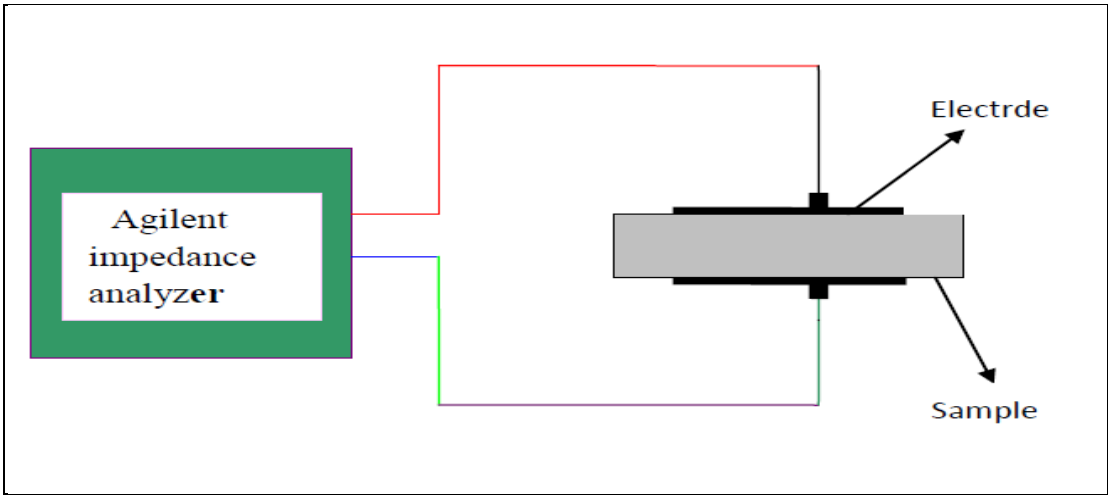

Figure (3.5): LCR Hi TESTER Devices.

3.7. Attenuation Gamma Ray

Gamma ray shielding measurements of (PVA-PVP/Bi_2O_3) and (PVA-PVP/Bi_2O_3) nanocomposites have been performed to examine attenuation properties of gamma rays for the specimens with various concentrations of (Bi_2O_3) nanoparticles. Test specimens with varying concentrations were order in front of the parallel beam emanating from the gamma ray exporter (Cs-137). The gamma ray exporter is situated at a distance of (2) cm from the detector. The nanocomposite (PVA-PVP/ Bi_2O_3) and (PVA-CMC /Bi_2O_3) sample is placed at a distance of 1 cm from the gamma ray exporter. The emitted gamma ray influxes through the specimens are determined by the Geiger counter which used for estimate the linear attenuation coefficients.

Chapter Four

Results and Discussions

4.1 Introduction

The structural, optical, and A.C electrical measurements for (PVA-PVP/Bi_2O_3) and (PVA-CMC/Bi_2O_3) nanocomposites were discussed in this chapter, as well as the effects of Gamma-Ray Shielding will also be examined for (PVA-PVP/Bi_2O_3) and (PVA-CMC/Bi_2O_3) nanocomposites.

4 .2 Structural Properties of (PVA-PVP/Bi_2O_3) and (PVA-CMC/Bi_2O_3) nanocomposites.

4..2.1 The Optical Microscope (OM)

Figures (4.1) and (4.2) show the pictures at (PVA-PVP/Bi_2O_3) and (PVA-CMC/Bi_2O_3) nanocomposites with different concentrations of Bi_2O_3 nanoparticles at magnification power (40x).

The optical microscope gives the change of surface morphology of nanocomposites.

Compared with pure sample images, there are many differences among this sample and both nanocomposites with adding different concentrations of Bi_2O_3 ,both figures show the addition of Bi_2O_3distributed through the polymeric blend with homogenous and ordered shape as well as the apparent of Bi_2O_3 network inside the polymer blend .

This constitutes paths inside the nanocomposites of charge carriers . This system can allow charge carriers to pass through the paths . In our opinion, these results agree with [109].

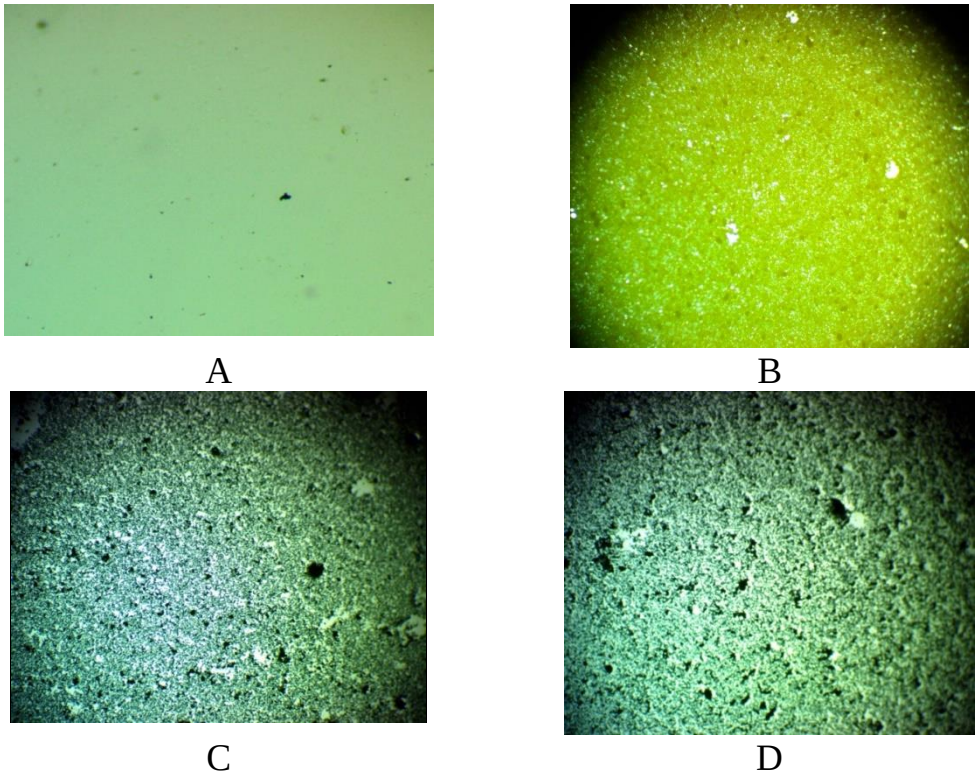

A B

C D

Figure (4.1): Photomicrographs (40x) for (PVA-PVP-Bi_2O_3) nanosheets A) , (PVA-PVP) blend, B) 1 wt% , C) 3 wt% , D) 5 wt% (Bi_2O_3)

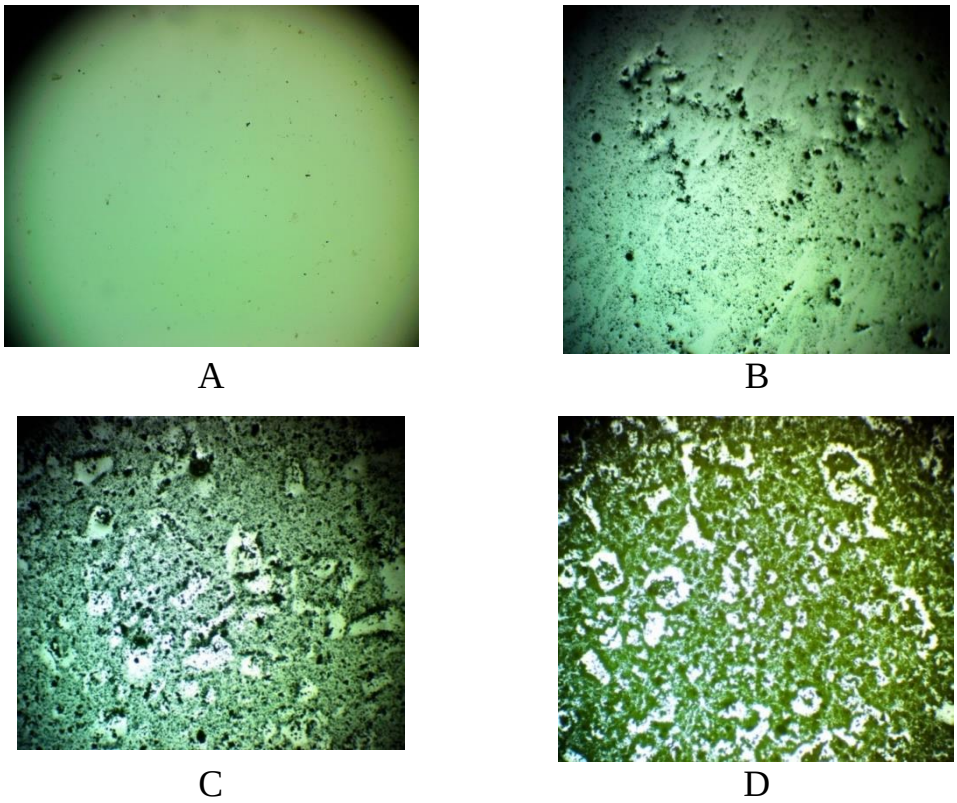

A B

C D

Figure (4.2): Photomicrographs (40x) for (PVA-CMC -Bi_2O_3) nanocomposites A. (PVA-CMC) blend B. 1 wt%, C. 3wt%, D. 5 wt%, Bi_2O_3 nanocomposites.

4.2.2 Fourier Transform Infrared Radiation (FTIR) of (PVA-PVP/ Bi_2O_3) and (PVA-CMC/Bi_2O_3) Nanocomposites.

The FTIR spectra of (PVA-PVP/Bi_2O_3) and (PVA-CMC/Bi_2O_3) nanocomposites with different concentrations of (Bi_2O_3) nanoparticles were recorded at room temperature in the region shown in Figures (4.3) and (4.4). (1000-4000) cm^{-1} . Pure blend (PVA-PVP), with wave number (cm^{-1}) in parentheses (3401-3480) O-H stretching, as well as (1607-1694) C=C will stretch you (2910-2996) CH2 stretching in an asymmetrical direction (1708-1760) Stretching out C=O (1607- 1694) Stretching the C=C chain, stretching the C-N chain (1469-1484) CH2 bending or bending O-H (1038-1078) Stretching of C=O, bending of C-H and OH (907-943) CO is an abbreviation for symmetric stretching [110,111]. The spectra characteristic bands of stretching and bending vibrations of the functional groups formed in nanocomposites were displayed in tables (4.1) and (4.2).

Fourier Transform Infrared Radiation FTIR spectrum appearances a shifting in peak location along with the change in form with intensity compared with pure (PVA -PVP) and (PVA-CMC) films and it can be noted that there is a reduction in the transmittance at a concentration increasing of Bi_2O_3 nanoparticles. So far, the density increment of the pictures revenue that there is increasing of atoms and ions in the light path.

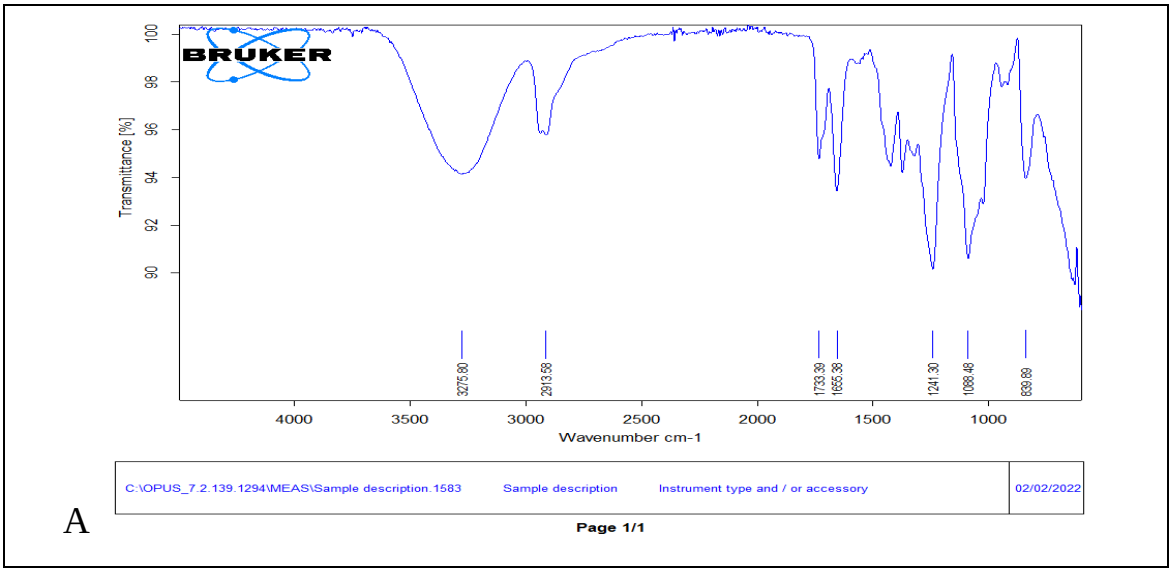
BRUKER
Transmittance [%]
100
98
96
94
92
90
3275.80
2913.68
1733.39
1655.38
1241.30
1088.48
839.89
4000
3500
3000
2500
2000
1500
1000
Wavenumber cm-1
C:\OPUS_7.2.139.1294\MEAS\Sample description.1583
Sample description
Instrument type and / or accessory
02/02/2022
Page 1/1

A

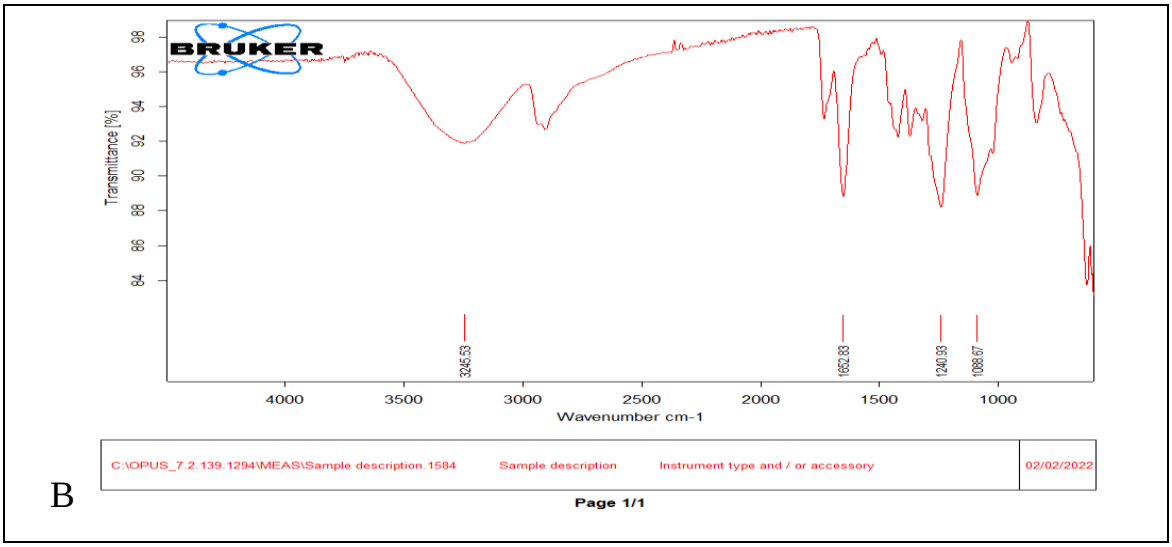
BRUKER
Transmittance [%]
98
96
94
92
90
88
86
84
3245.53
1652.83
1240.93
1088.67
4000
3500
3000
2500
2000
1500
1000
Wavenumber cm-1
C:\OPUS_7.2.139.1294\MEAS\Sample description.1584
Sample description
Instrument type and / or accessory
02/02/2022
Page 1/1

B

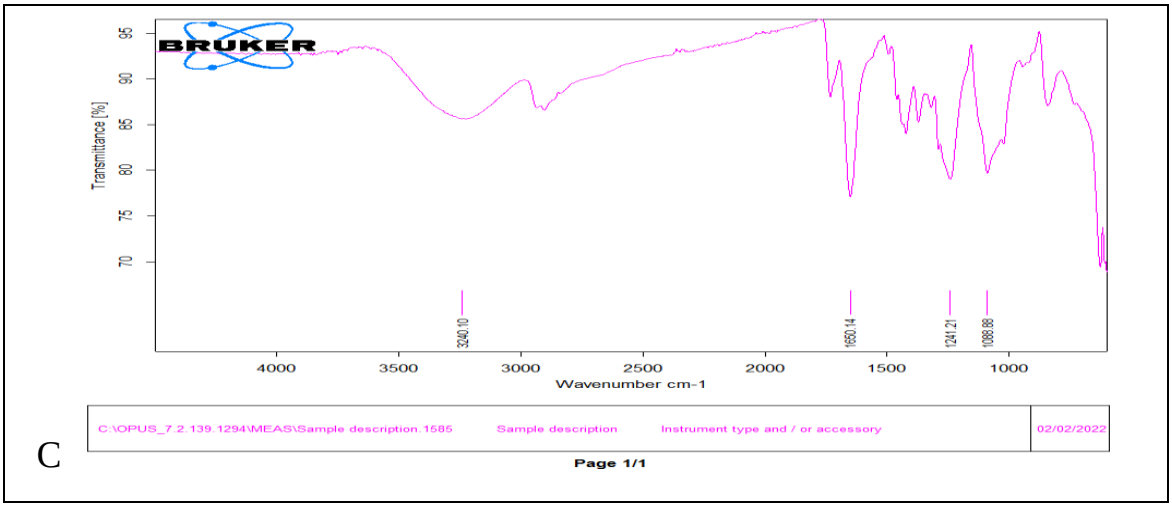
BRUKER
Transmittance [%]
95
90
85
80
75
70
3240.10
1650.14
1241.21
1088.88
4000
3500
3000
2500
2000
1500
1000
Wavenumber cm-1
C:\OPUS_7.2.139.1294\MEAS\Sample description.1585
Sample description
Instrument type and / or accessory
02/02/2022
Page 1/1

C

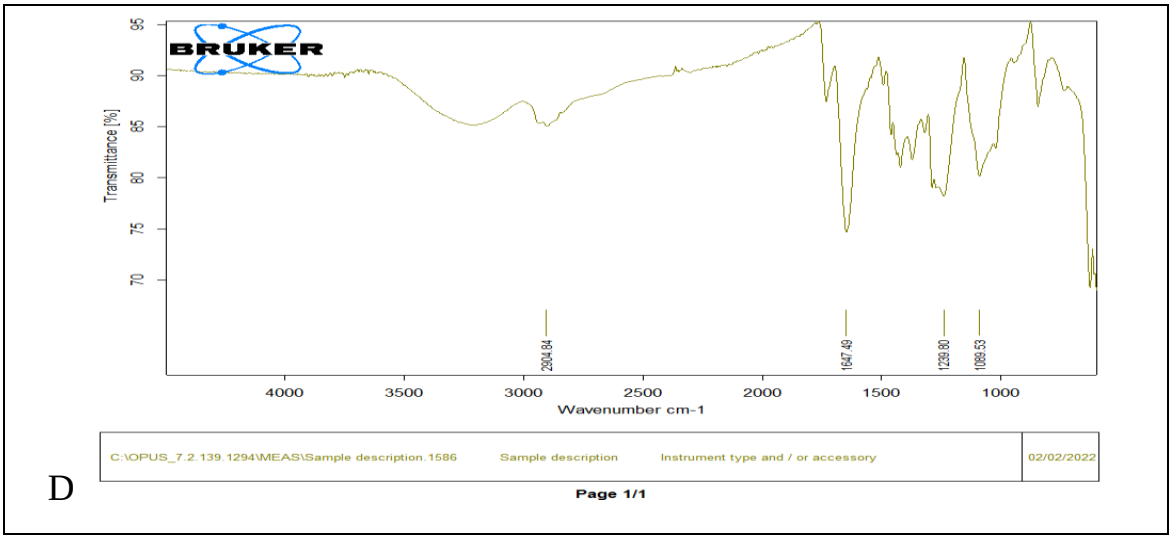

D

Figure (4.3): FTIR spectra for (PVA-PVP/Bi2O3) nanocomposite: (A) (PVA-PVP) blend, (B) 1wt% Bi_2O_3,(C) 3wt%Bi2O3, (D) 5wt%Bi_2O_3.

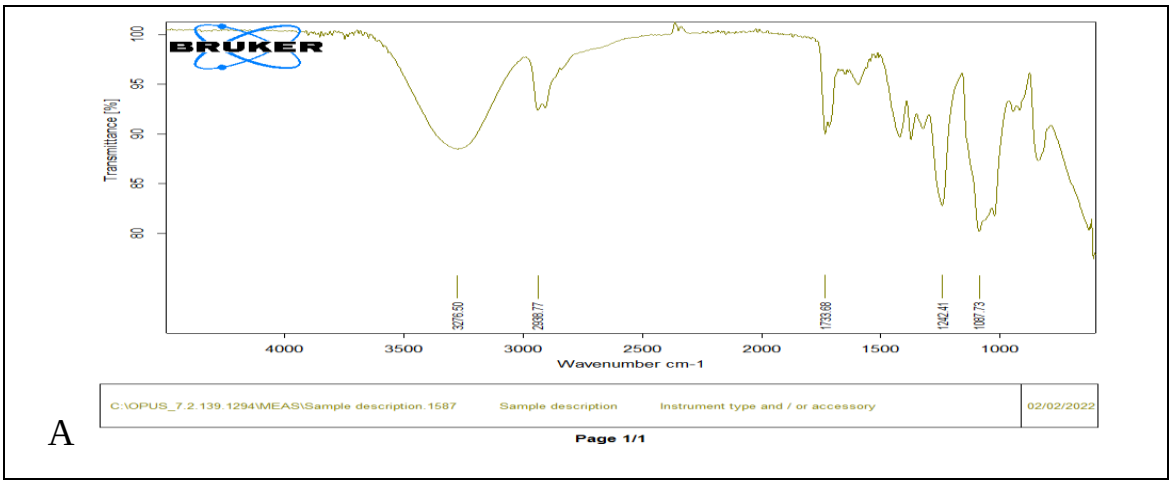

A

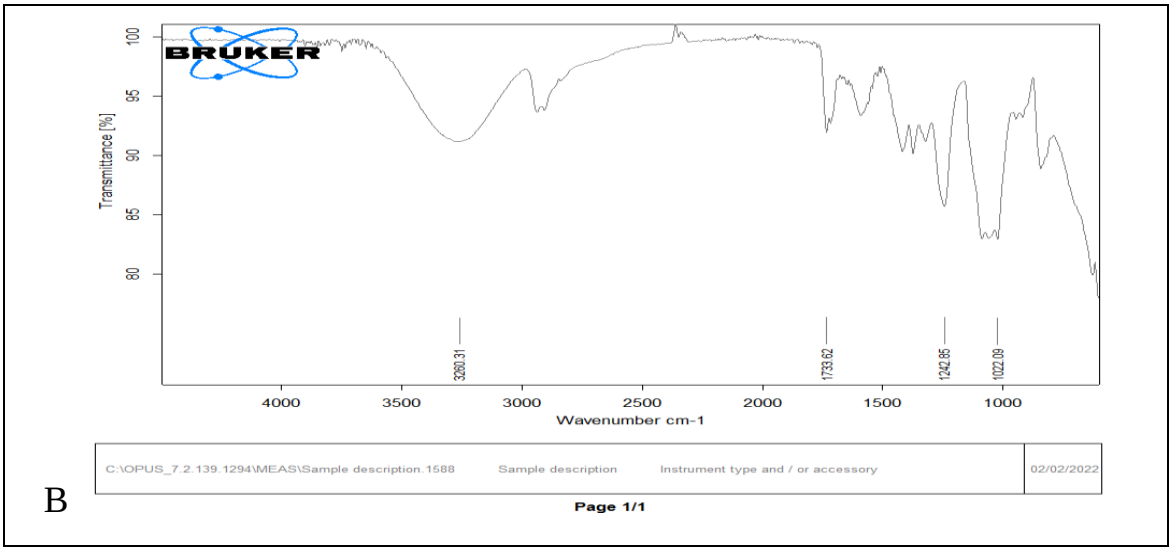

B

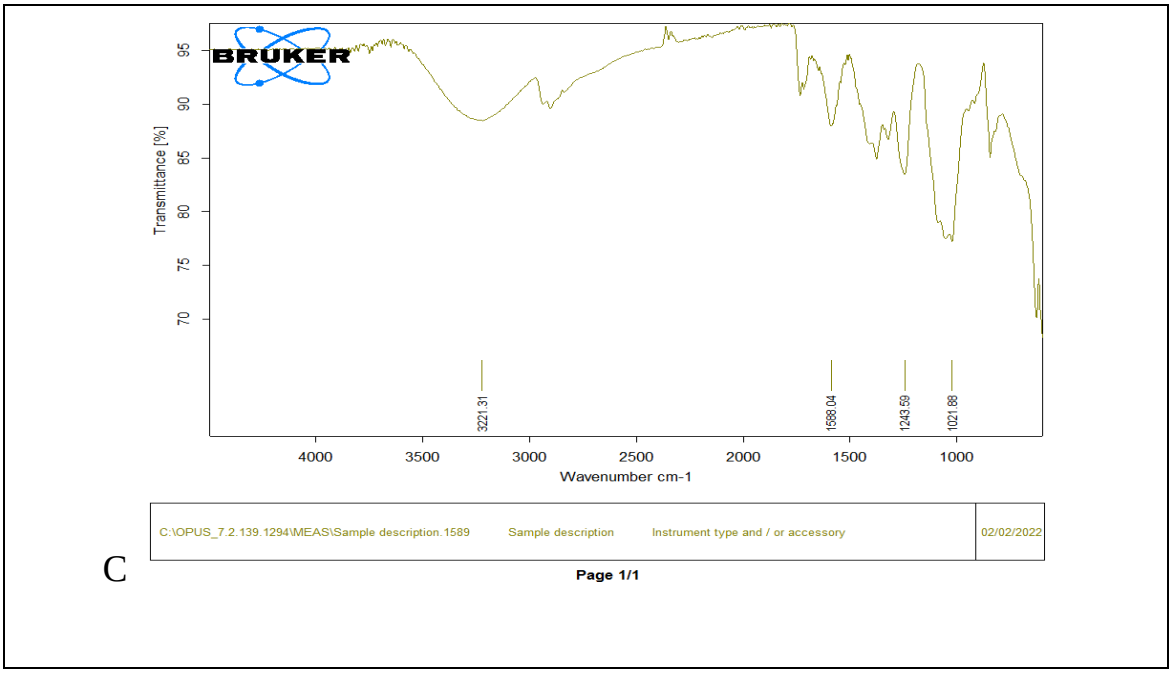

C

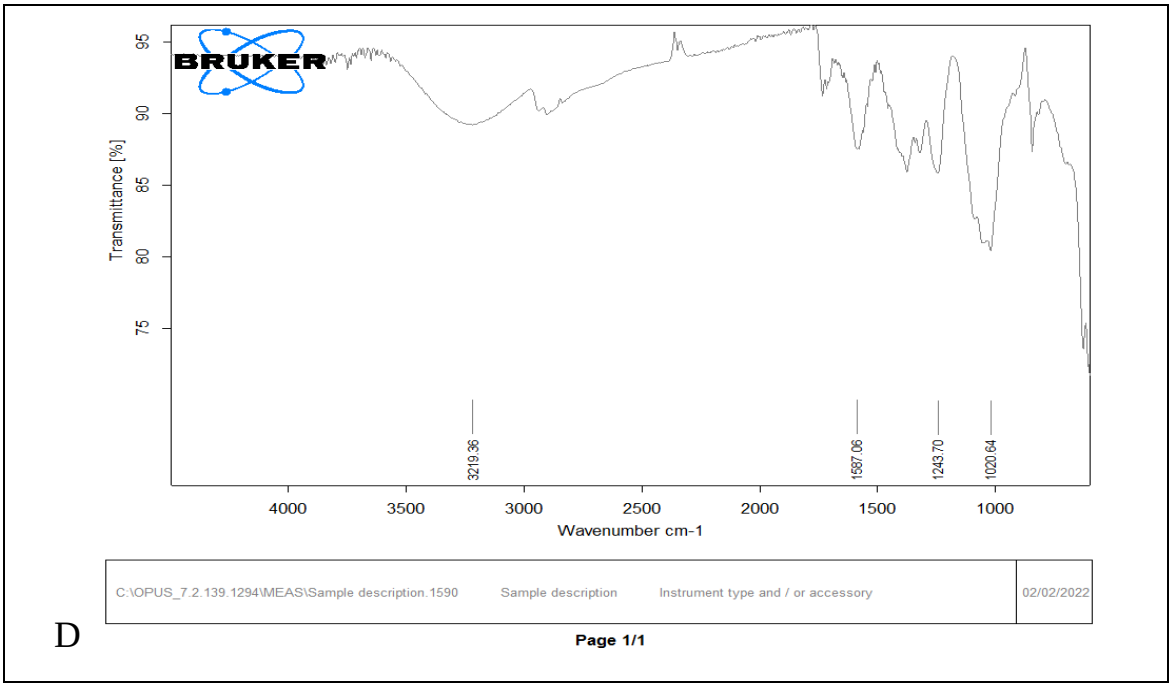

D

Figure (4.4): FTIR spectra for (PVA-CMC/Bi_2O_3) nanocomposite: (A) (PVA-CMC) blend, (B) 1wt% Bi_2O_3,(C) 3wt%Bi_2O_3, (D) 5wt%Bi_2O_3.

Table 4.1: FTIR-characteristic for (PVA-PVP/Bi_2O_3) Nanocomposites.

Active band	0wt%Bi_2O_3	1wt%Bi_2O_3	3wt%Bi_2O_3	5wt%Bi_2O_3
(C-H) StretchingVibration (3000-3300) cm^{-1} (≡C-H,SP-1S),(3300 cm^{-1})	3275	3245	3240	-----
(CH2) Asymmetric Stretching (2910-2996) cm^{-1}	2913	-------	------	2904
(C-O) Stretching Aldehyde (1720-1740) cm^{-1}	1733	------	-----	-----
(C=C) Stretching Aromatic (1607-1694) cm^{-1}	1655	1652	1650	1667
(CH2)wagging, Twisting(out of plane) Bending vibrations 1250 cm^{-1}	1241	1240	1241	1239
(C-O) Single band (1100 cm^{-1})	1188	1088	1088	1089

Table 4.2: FTIR-characteristic for (PVA-CMC/Bi_2O_3) Nanocomposites.

Active band	0wt%Bi_2O_3	1wt%Bi_2O_3	3wt%Bi_2O_3	5wt%Bi_2O_3
(C-H) StretchingVibration (3000-3300) cm^{-1} (≡C-H,SP-1S), (3300 cm^{-1})	3276	3260	3221	3219
(CH2) Asymmetric Stretching (2922-2942) cm^{-1}	2938	-----	-----	-----
(C=O) Carbonyl Groups (1850-1650) cm^{-1}	1733	1733	-----	-----
(CH2) Bending (1250 cm^{-1})	1242	1292	1243	1243
(C-O) Single Band (1100 cm^{-1})	1087	1022	1021	1020

4-1 The Optical Properties of (PVA-PVP/Bi_2O_3) and (PVA–CMC/Bi_2O_3) Nanocomposite

4.1.1 The Absorbance (A) of (PVA-PVP/Bi_2O_3) and (PVA-CMC/Bi_2O_3) Nanocomposites.

The absorption (PVA-PVP/Bi_2O_3) and (PVA-CMC/Bi_2O_3) nanocompsite with various content (Bi_2O_3) nanoparticles were recorded at wavelengths range (200-800) nm at room temperature. The absorbance for (PVA-PVP/Bi_2O_3) and (PVA-CMC/Bi_2O_3) nanosheets through wavelength at the occurrence light are shown in fig. (4.5) and (4.6) respectively. From this figures, the absorbance rise with rising content of Bi_2O_3, while it is reduce with rising wavelength, because of donor level electrons being excited to the conduction-band at high energy. Because photons have enough energy to make atoms to respond, it is possible for an electron to be stimulated from a lower to a higher energy level just by absorbing a photon that has already been established[112]. These results agree with other studies[113-115].

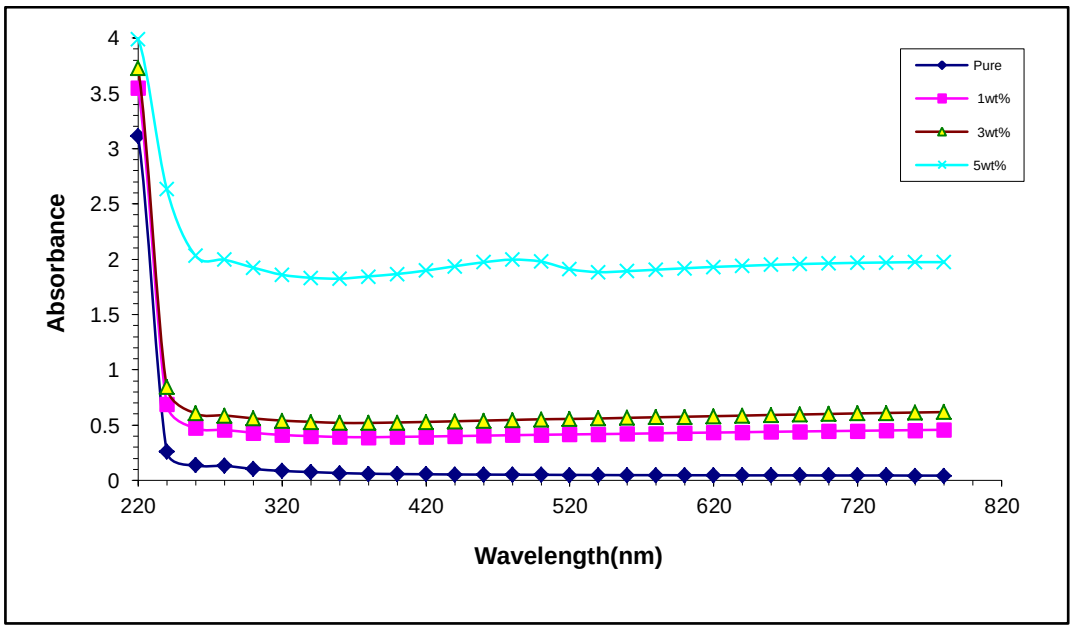

Figure(4.5): The absorbance as a function of wavelength of (PVA-PVP/Bi_2O_3) nanocomposite with different content.

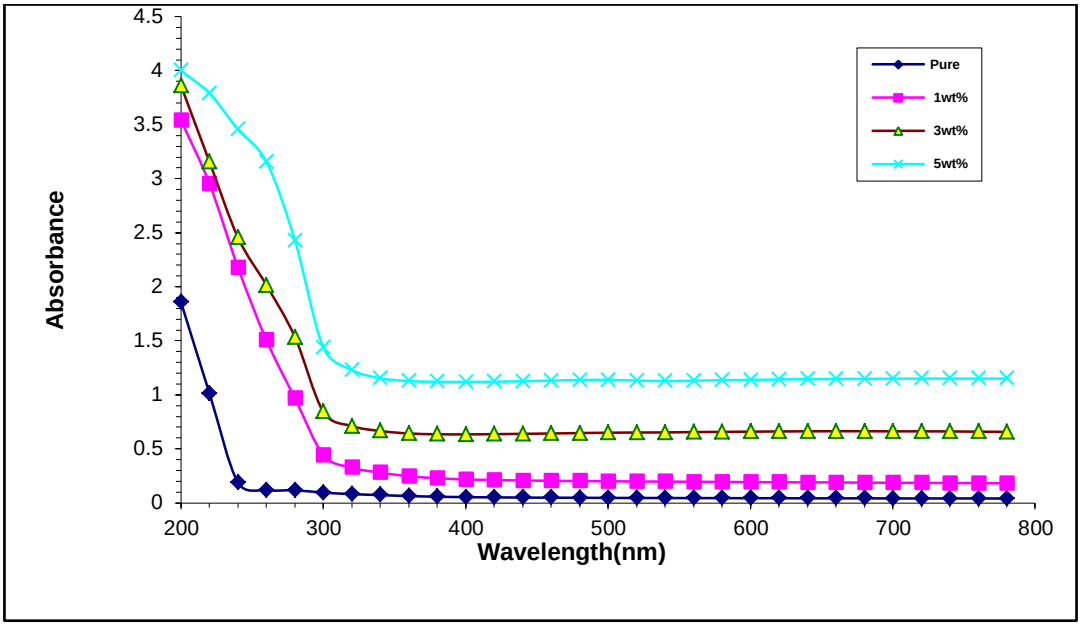

Figure(4.6): The absorbance as a function of wavelength of (PVA-CMC/Bi_2O_3) nanocomposite with different content.

4.1.2 The Transmittance (T) of (PVA-PVP/Bi_2O_3) and (PVA-CMC/Bi_2O_3) Nanocomposites.

Figures (4.7) and (4.8) demonstrate the transmittance of (PVA – PVP/Bi_2O_3) and (PVA-CMC/Bi_2O_3) nanocomposite with wavelength. The transmittance reduces as the concentration of Bi_2O_3 nanoparticles rise, also increased with increasing of wavelength , which is due to the agglomeration of nanoparticles with increasing content [116].

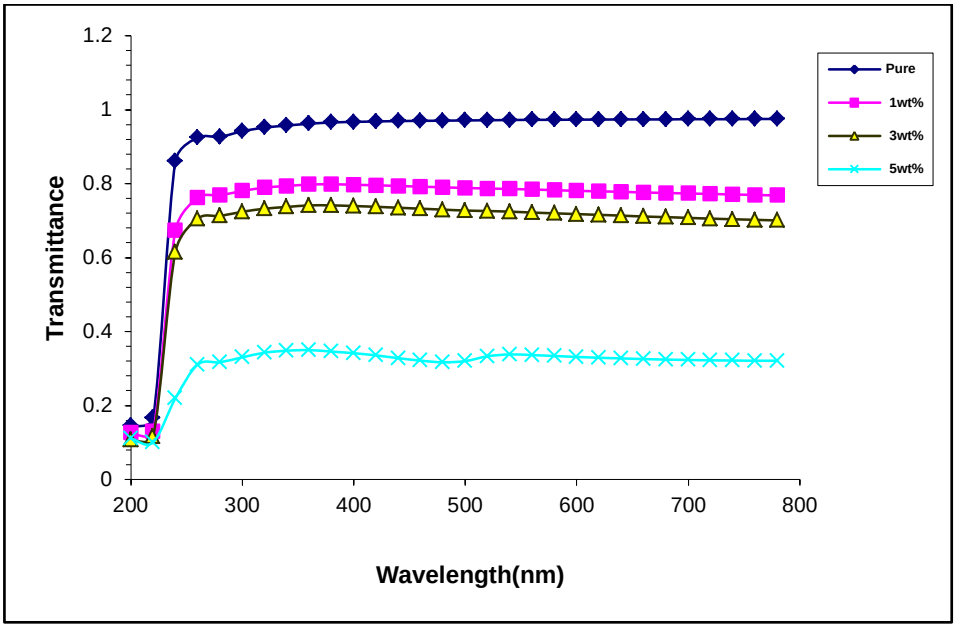

Figure (4.7): Variation transmittance of (PVA-PVP/Bi_2O_3) nanocomposite with the wavelengths.

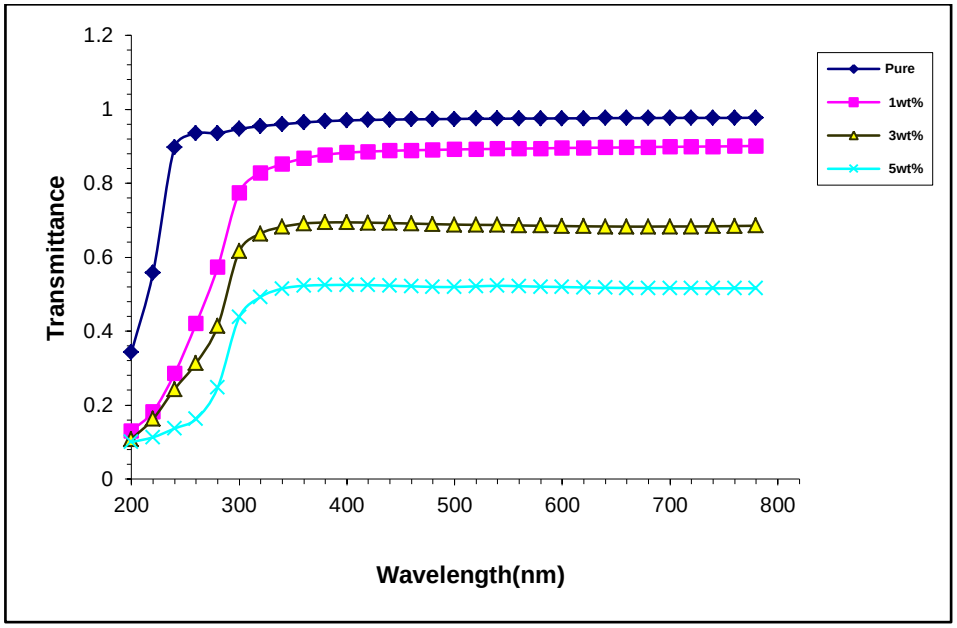

Figure(4.8): Variation transmittance of (PVA-CMC/Bi_2O_3) nanocomposite with wavelengths.

4.1.3 Absorption Coefficient (α)

Figures (4.9) and (4.10) illustrate, respectively, the relationship between the photon energy of the incoming light and the absorption coefficient of the (PVA-PVP/Bi_2O_3) and (PVA-CMC/Bi_2O_3)

nanocomposite. The absorption coefficient was calculated by equation (2-6).

The absorption coefficient might help to figure out what kind of electron transition dealing with [111,112]. It is assumed that direct electron transitions occur when the material's absorption coefficient is large ($>10^4$) cm^{-1}. When the material's absorption coefficient is low (10^4 cm^{-1}), an indirect transition of electrons is assumed. The values of α of (PVA-PVP/Bi_2O_3) and (PVA-CMC/Bi_2O_3) nanocomposite, the transition of the electron takes place in a round about way. Because of an increase in the total number of charge carriers, the absorbance and absorption coefficient of (PVA-PVP/Bi2O3) and (PVA-CMC/Bi2O3) nanocomposites both increased with increasing of Bi_2O_3 nanoparticles. The rise in the value of nanocomposites can be attributed to this phenomenon. [119].

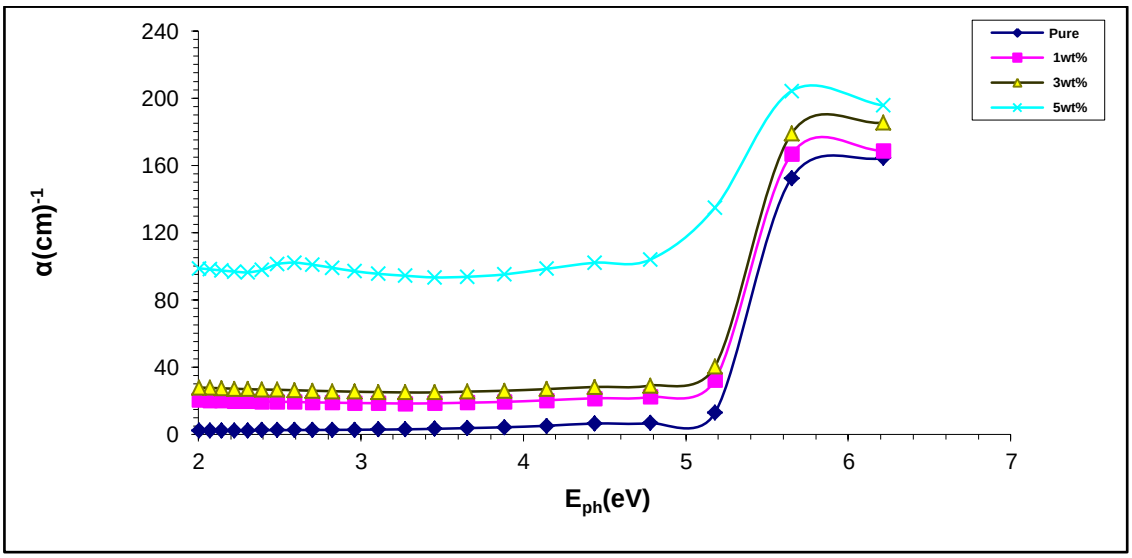

Figure(4.9): The variation absorption coefficient of (PVA-PVP/Bi_2O_3) nanocomposite with the photon energies.

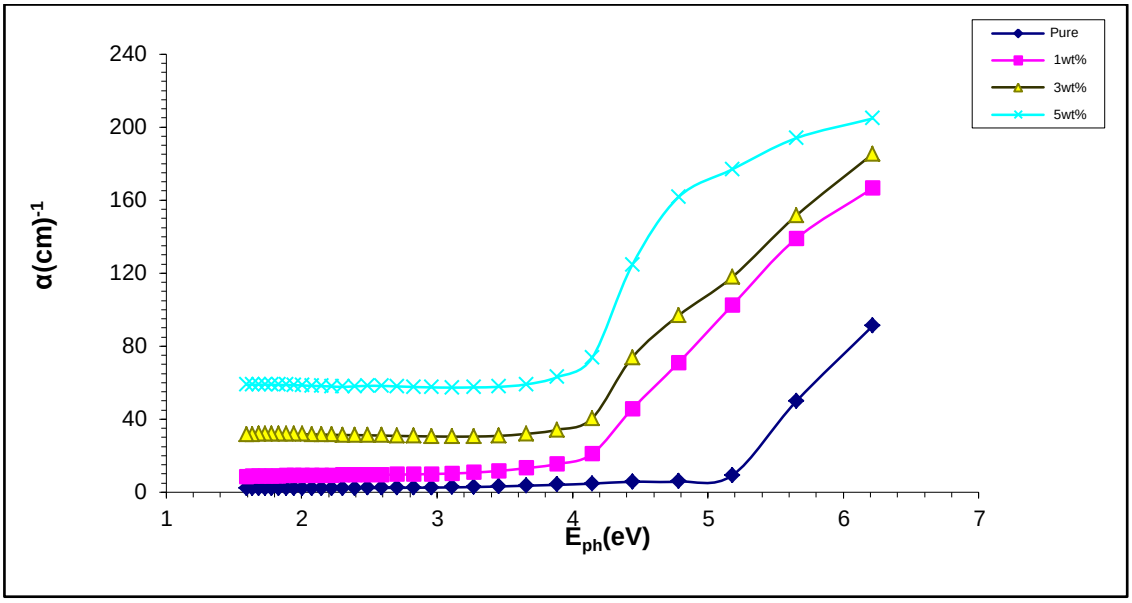

Figure(4.10): The variation absorption coefficient of (PVA-CMC/Bi_2O_3) nanocomposite with the photon energies.

4.1.4 Energy gaps of the (allowed and forbidden) indirect transition E_g

The energy band gap of nanocomposites were calculated by equation (2-7). The E_g for allowed indirect transitions of (PVA-PVP/Bi_2O_3) and (PVA-CMC/Bi_2O_3) nanocomposites are explain in figs.(4.11) and (4.12) and the forbidden indirect transitions of (PVA-PVP/Bi_2O_3) and (PVA-CMC/Bi_2O_3) nanocomposites are explain in figs.(4.13) and (4.14) respectively.

finding the energy gap for the indirect transition by plotting the data or tang cut from the top of the curve to the (x axis) at (hv) [120]. From this figures, the E_g for allowed and forbidden indirect transitions are reduce with the rises of the Bi_2O_3 nanoparticles content, this action is due to the formation of levels in the E_g and therefore, these local levels reduce the energy gap with rise of the Bi_2O_3 nanoparticles content [121]. The value of the E_g of nanocomposites are listed in Table (4-3) and (4-4).

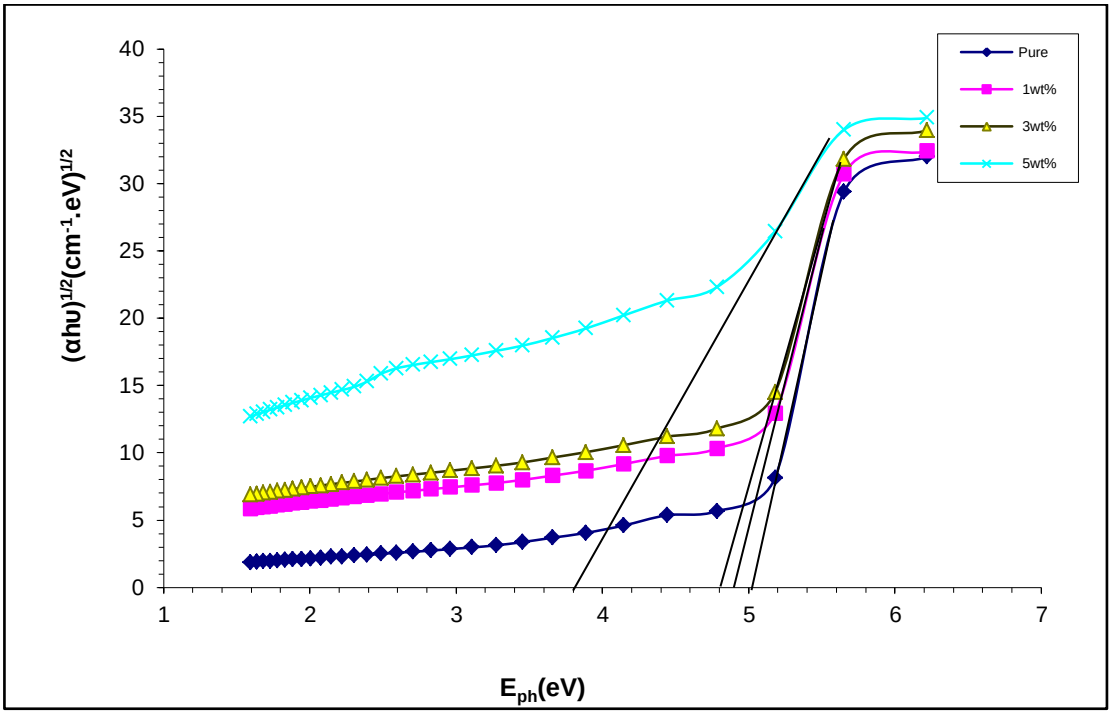

Figure (4.11): The E_g for the allowed indirect transition $(\alpha hv)^{1/2}$ $(cm^{-1}.eV)^{1/2}$ of ($PVA\text{-}PVP/Bi_2O_3$) nanocomposite.

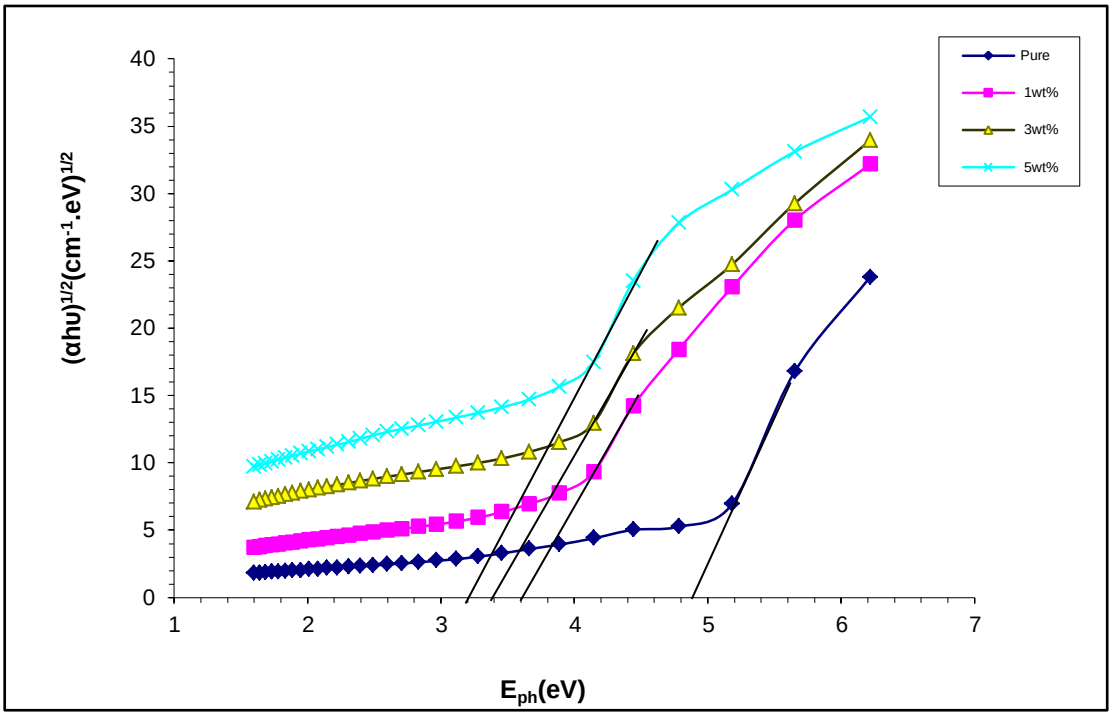

Figure (4.12): The E_g for the allowed indirect transition $(\alpha hv)^{1/2}$ $(cm^{-1}.eV)^{1/2}$ of ($PVA\text{-}CMC/Bi_2O_3$)nanocomposite.

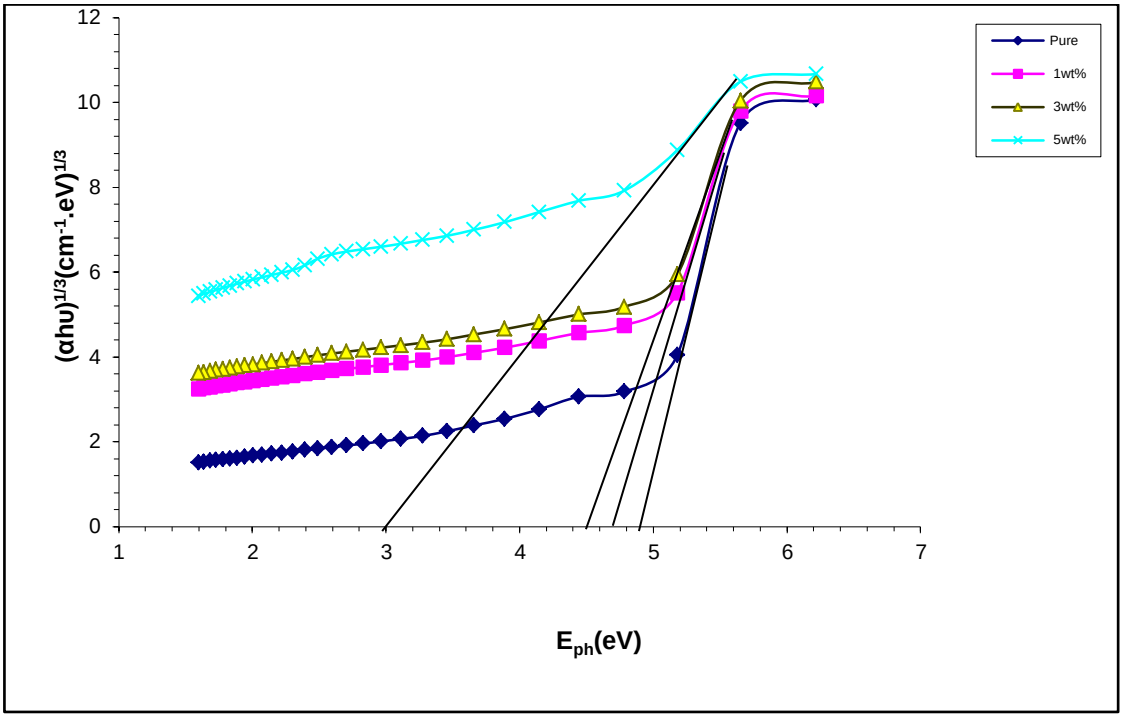

Figure(4.13): The E_g for the forbidden indirect transition $(\alpha hv)^{1/3}(cm^{-1}.eV)^{1/3}$ of ($PVA\text{-}PVP/Bi_2O_3$) nanocomposite.

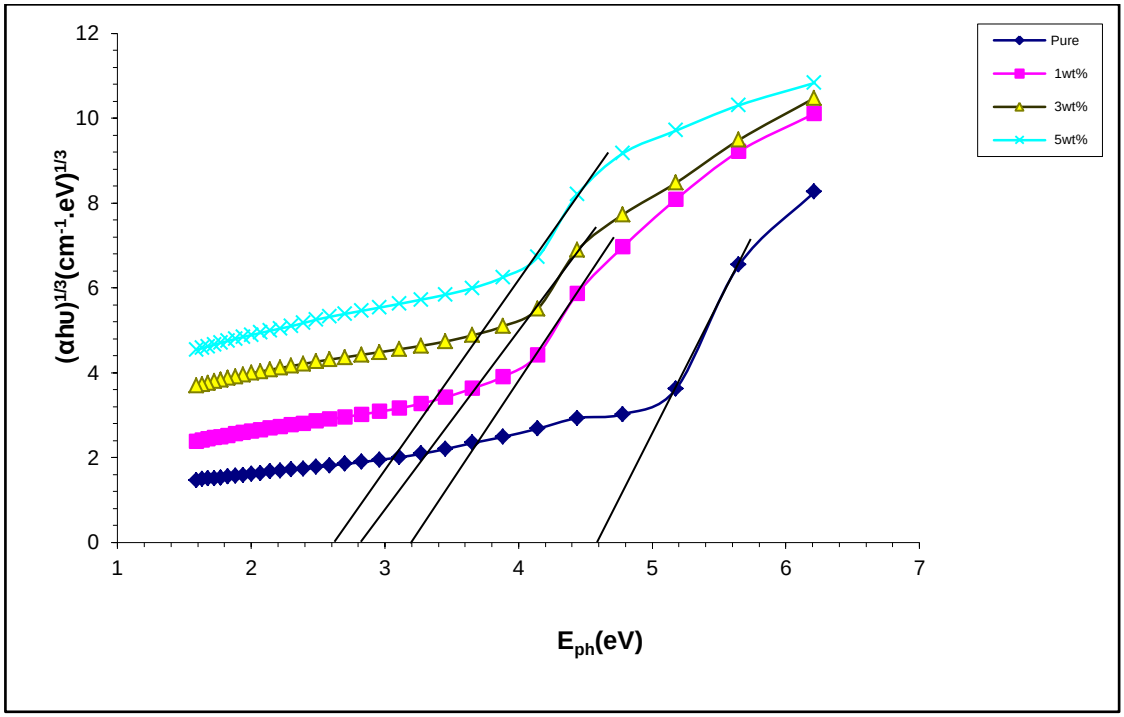

Figure(4.14): The E_g for the forbidden indirect transition $(\alpha hv)^{1/3}(cm^{-1}.eV)^{1/3}$ of ($PVA\text{-}CMC/Bi_2O_3$)nanocomposite.

Table 4.3: The values of optical energy gap for allowed Indirect transitions of ($PVA-PVP/Bi_2O_3$) and ($PVA-CMC/Bi_2O_3$)nanocomposite.

Bi_2O_3 wt% Nanoparticle's content	E_g allowed indirect for the ($PVA/PVP/Bi_2O_3$)(eV)	E_g allowed indirect for the ($PVA/CMC/Bi_2O_3$)(eV)
0	5	4.9
1	4.9	3.6
3	4.8	3.4
5	3.8	3.2

Table 4.4:): The values of optical energy gap for forbidden Indirect transitions of ($PVA-PVP/Bi_2O_3$) and ($PVA-CMC/Bi_2O_3$)nanocomposite.

Bi_2O_3 wt% Nanoparticle's concentration	E_g forbidden indirect for the ($PVA-PVP/Bi_2O_3$)(eV)	E_g forbidden indirect for the ($PVA-CMC/Bi_2O_3$)(eV)
0	4.9	4.6
1	4.7	3.2
3	4.5	2.8
5	3	2.6

4.1.5 The Extinction Coefficient (K) of ($PVA-PVP/Bi_2O_3$) and ($PVA CMC/ Bi_2O_3$) nanocomposite

The extinction coefficient were calculated by using the equation (2-13). Figures (4.15) and (4.16) explain the extinction coefficient of ($PVA-PVP/Bi_2O_3$) and ($PVA-CMC/Bi_2O_3$) nanocomposites versus of wavelength respectively. It is observe that the extinction coefficient of nanocomposites rise with the rises of the Bi_2O_3 nanoparticles content and reduce with rising wavelength, this is due to the rise in optical absorption and photons

distribution in the (PVA-PVP) and (PVA-CMC) polymer matrix respectively[122].

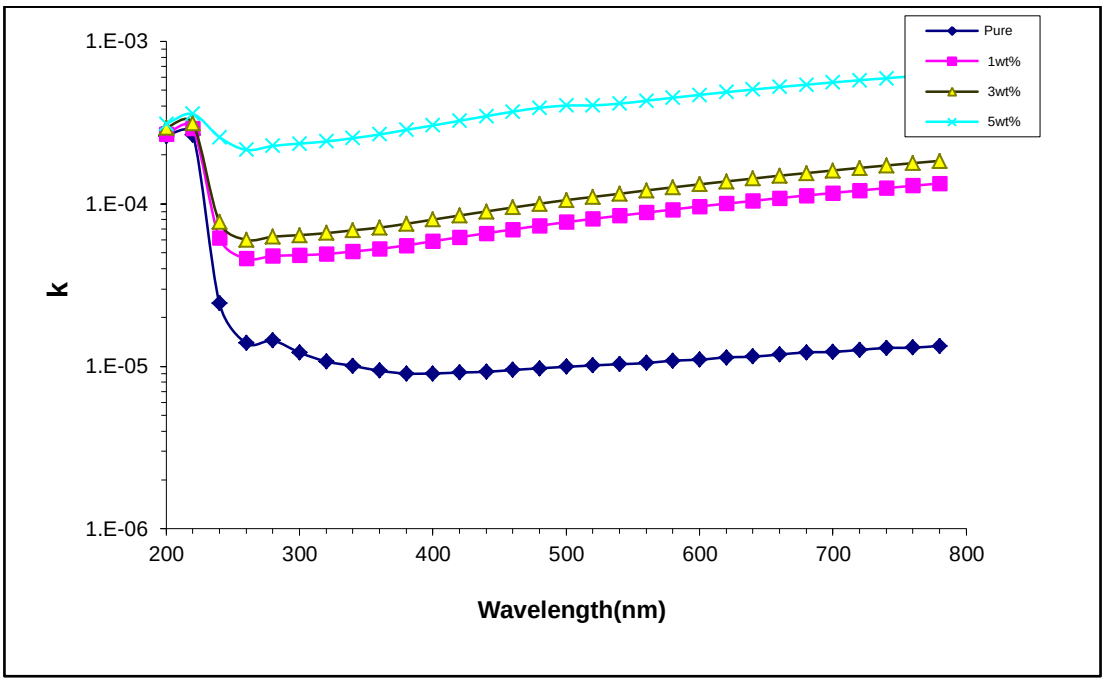

Figure(4.15): Variation of K for (PVA-PVP-Bi_2O_3) nanocomposite with wavelength.

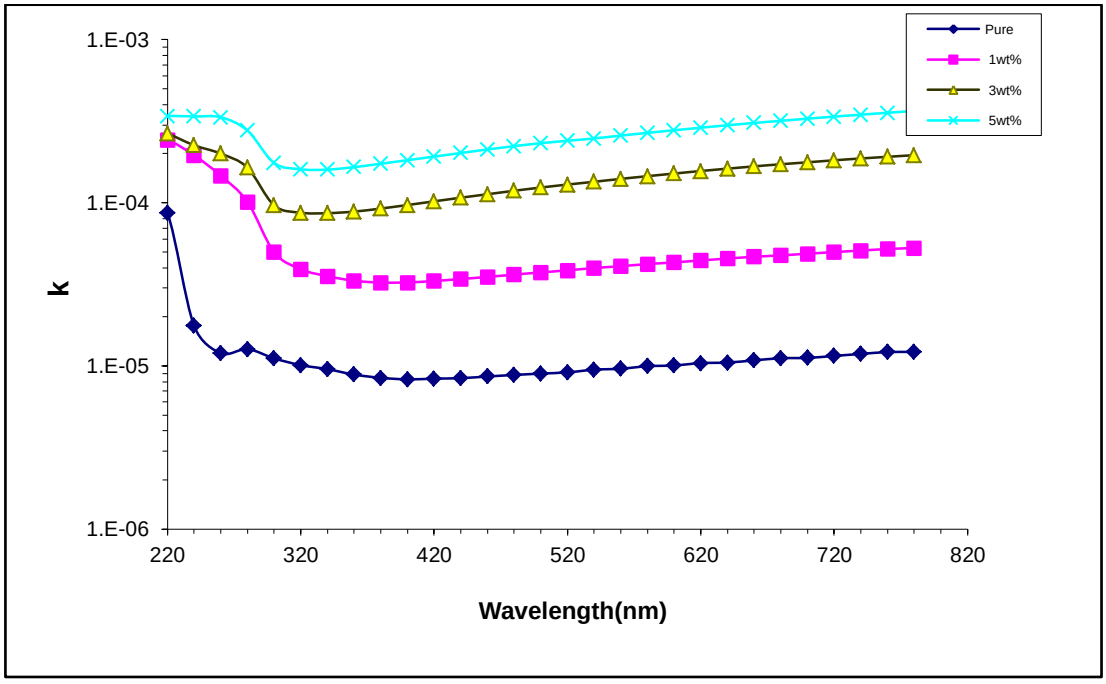

Figure (4.16): Variation of K for (PVA-CMC/Bi_2O_3) nanocomposite with wavelength.

4.1.6 Refractive Index (n)

The refractive index is calculated by using equation (2-11). The n of (PVA-PVP/Bi_2O_3) and (PVA-CMC/Bi_2O_3) nanocomposites versus with wavelength are shown in figures (4.17) and (4.18) respectively. It is obtain that the refractive index of increases with the increasing of the content of Bi_2O_3 nanoparticles and it is decreased with the increase of the wavelength. This action due to the increase of the density of nanocomposites.[123,124].

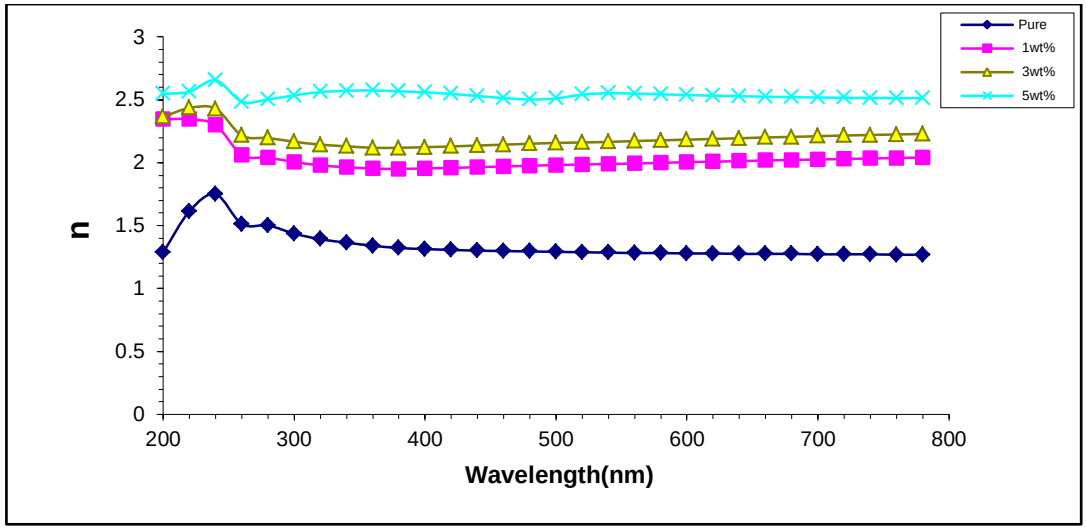

Figure (4.17): Variation of n for of (PVA-PVP/Bi_2O_3) nanocomposites with wavelength

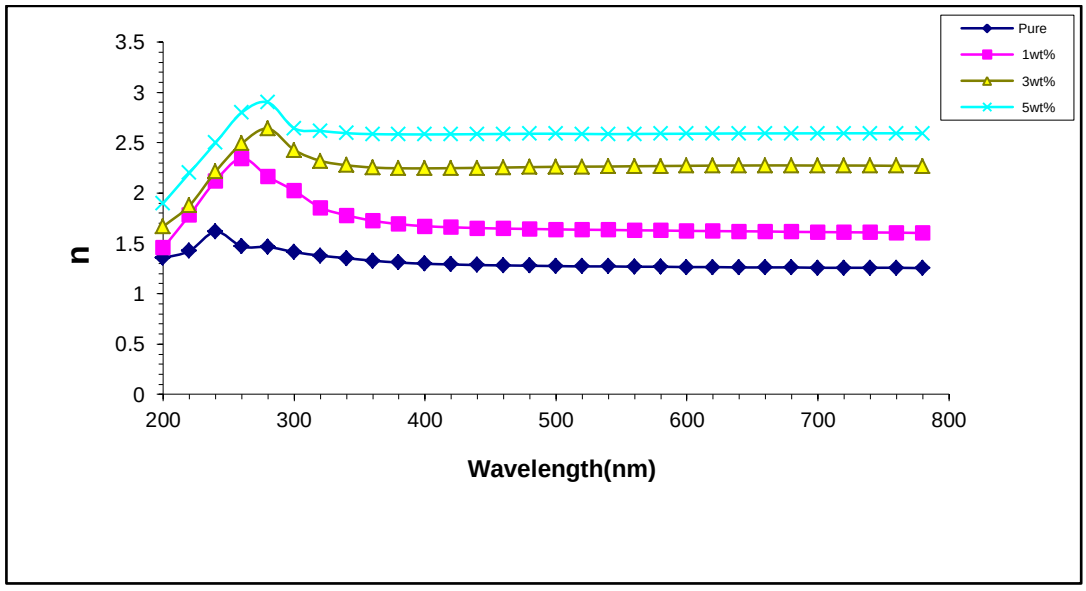

Fig. 4.18: Variation of n for (PVA-CMC/Bi_2O_3) nanocomposite with wavelength

4.1.7 The Real and Imaginary Parts of Dielectric Constant (ε_1, ε_2) of (PVA-PVP/Bi_2O_3) and (PVA-CMC/Bi_2O_3)Nanocomposites .

By using the equations (2-14) and (2-15), the real and imaginary parts of dielectric constant were calculated. The real part of dielectric constant with the wavelength for (PVA-PVP/Bi_2O_3) and (PVA-CMC/Bi_2O_3) nanocomposites are explain in figures (4.19) and (4.20) and imaginary part of dielectric constant with the wavelength for the (PVA-PVP/Bi_2O_3) and (PVA-CMC/Bi_2O_3) nanocomposites are explain in figures (4.21) and (4.22) respectively. From this figures, the real and imaginary parts of dielectric constant of the nanocomposite are rise with the rises of Bi_2O_3 nanoparticles content and reduce with rising wavelength, the increase in electrical polarization related to the contribution of nanoparticles content in the sample caused this finding [125]. The real and imaginary parts of dielectric constant of nanocomposite change with wavelength. This is due to the real part of dielectric constant depends on refractive index because the effect of extinction coefficient is small, whereas the imaginary part of dielectric constant depends on extinction coefficient [126].

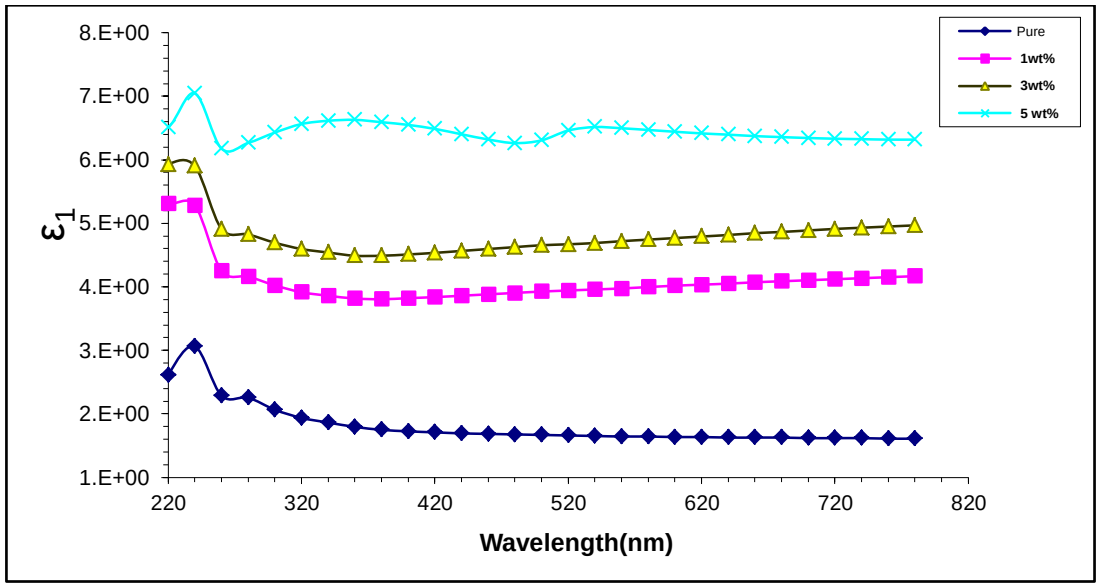

Figure (4.19): Variation of ε_1 of (PVA –PVP/Bi_2O_3) nanocomposites with wavelength.

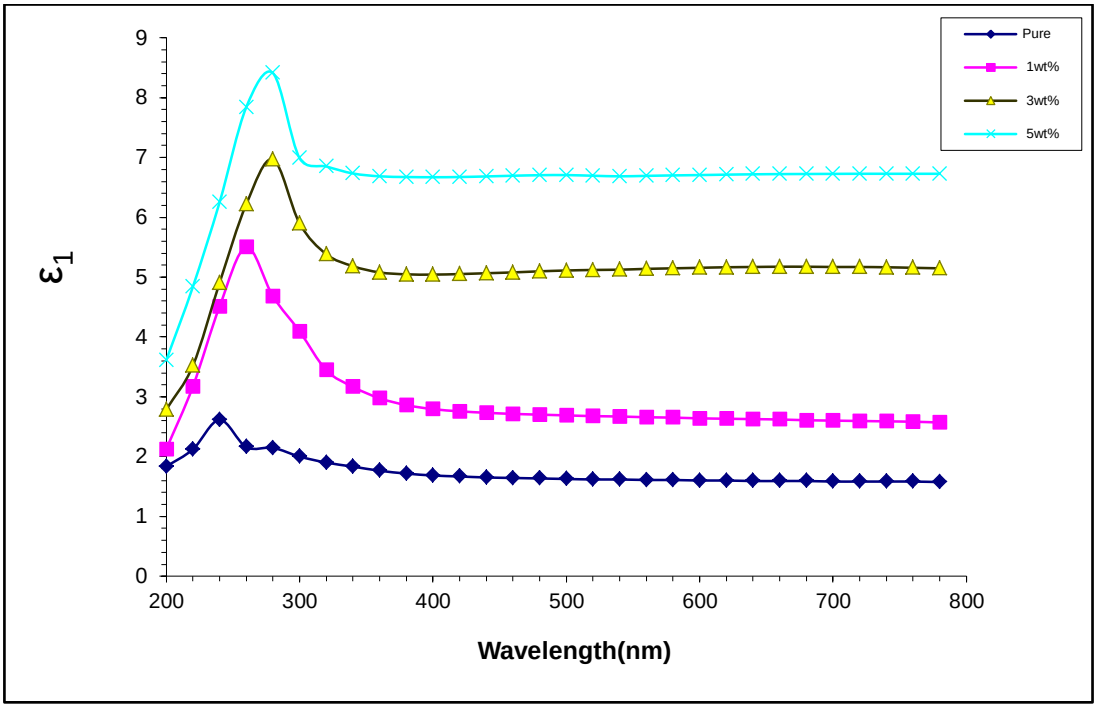

Figure (4.20): Variation ε_1 of (PVA-CMC/Bi_2O_3) nanocomposites with wavelength.

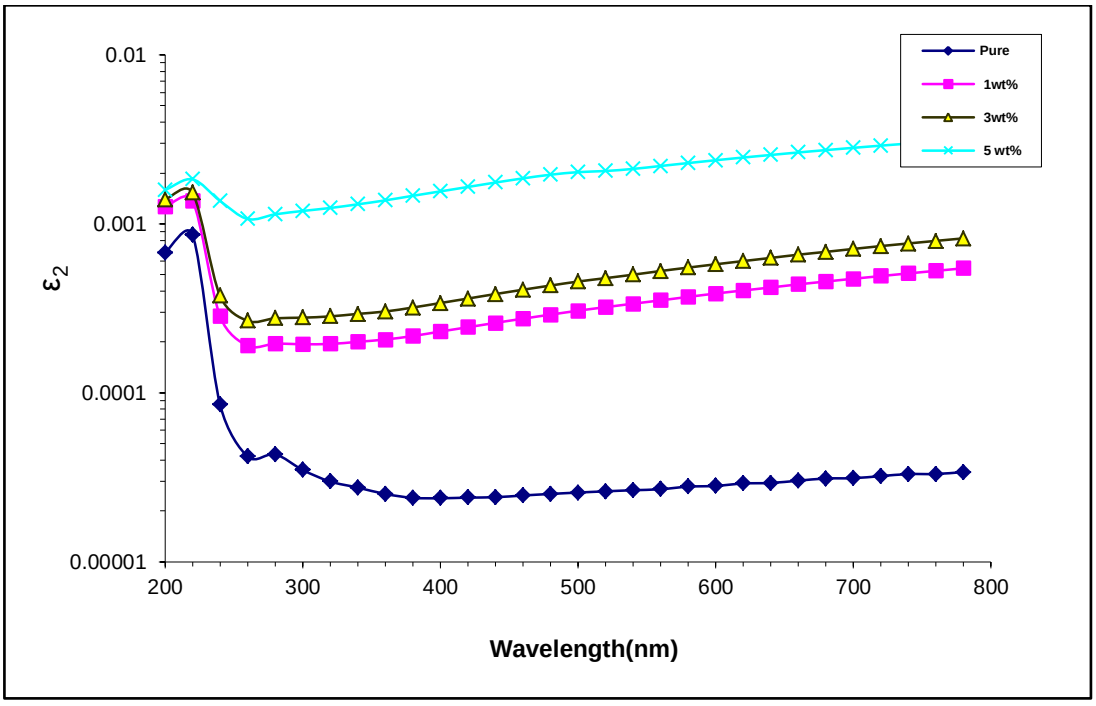

Figure (4.21): Variation ε_2 of (PVA-PVP/Bi_2O_3) nanocomposites with the wavelength.

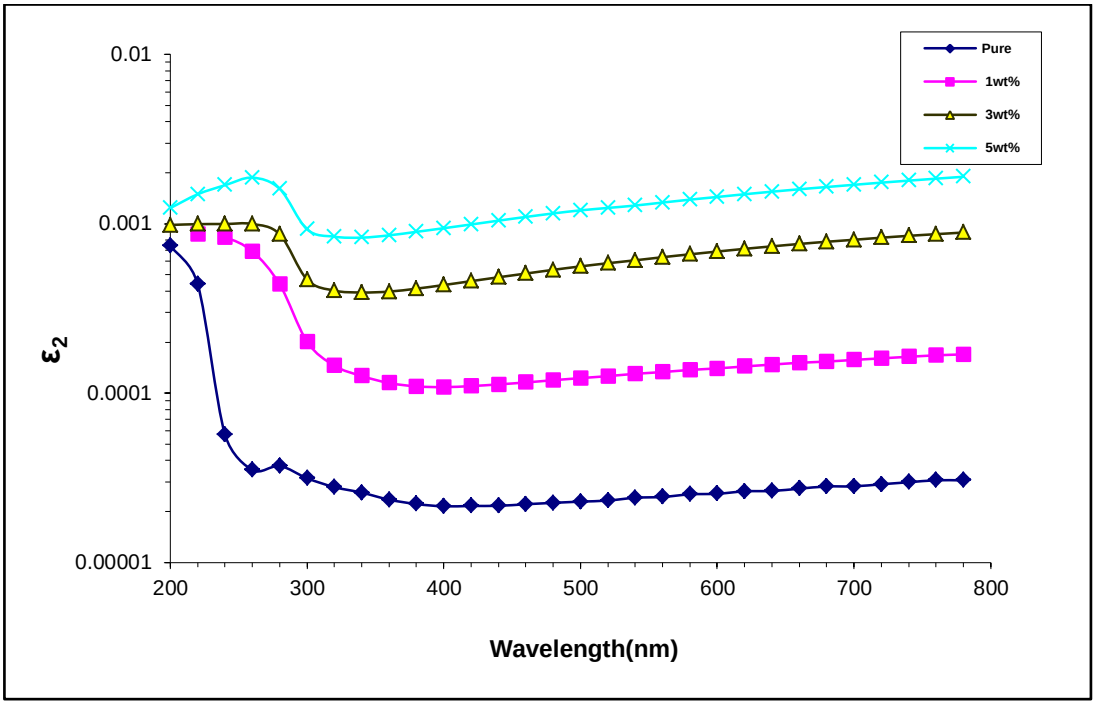

Figure(4.22): Variation ε_2 of (PVA-CMC/Bi_2O_3) nanocomposites with wavelength.

4.1.8 Optical Conductivity (σ_{op}) of (PVA-PVP-Bi_2O_3) and (PVA-CMC-Bi_2O_3) Nanocomposites .

The optical conductivity was calculated from the equation (2- 16). The optical conductivity of the of (PVA-PVP/Bi_2O_3) and (PVA-CMC/Bi_2O_3) nanocomposites with a wavelength are shown in Figs.(4.23) and (4. 24) respectively. It is note that the σ_{op} increased with an increasing of content of Bi_2O_3 nanoparticle which associated with the creation of localized concentrations in the energy gap, the increase in concentrations of nanoparticle induced an increase in the density of localized phases in the band structure; thus, an increase in the absorption coefficient suggests an increase in optical conductivity of the nanocomposites while the optical conductivity decreased with the increased in wavelength, this result due to that the optical conductivity depend on the wavelength of the radiation incident on the nanocomposite specimen. Because the high absorption at low photon wavelength, the optical conductivity is increase at this area, the

optical conductivity spectra indicated that the samples are transmittance within the infrared regions, the visible and near. This result is agree with researches [127].

.

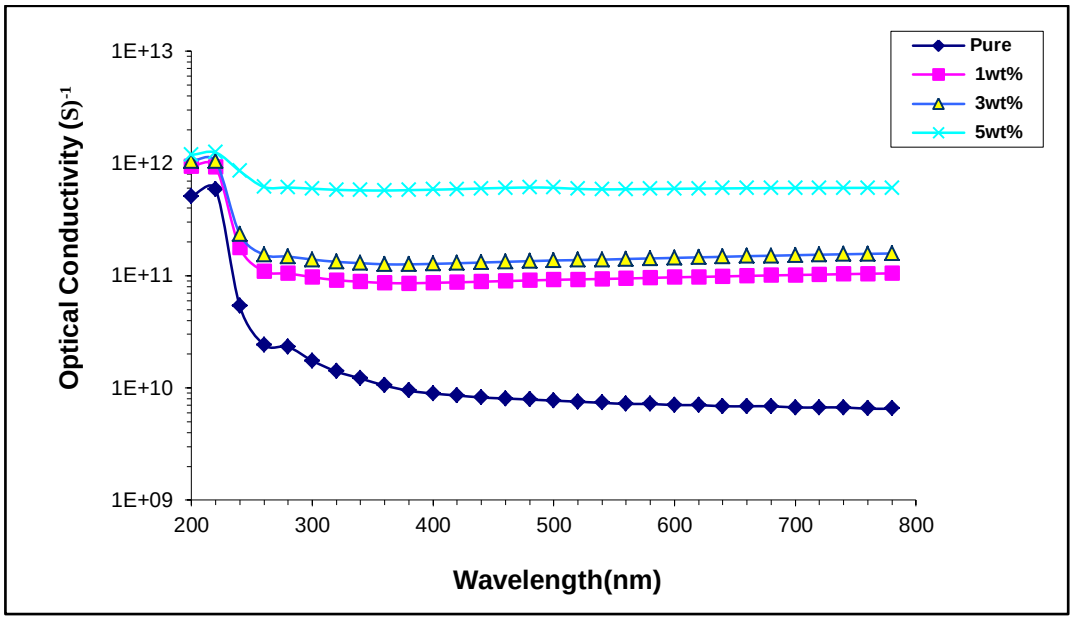

Figure (4.23): Variation σ_{op} of (PVA-PVP/Bi_2O_3) nanocomposites with wavelength.

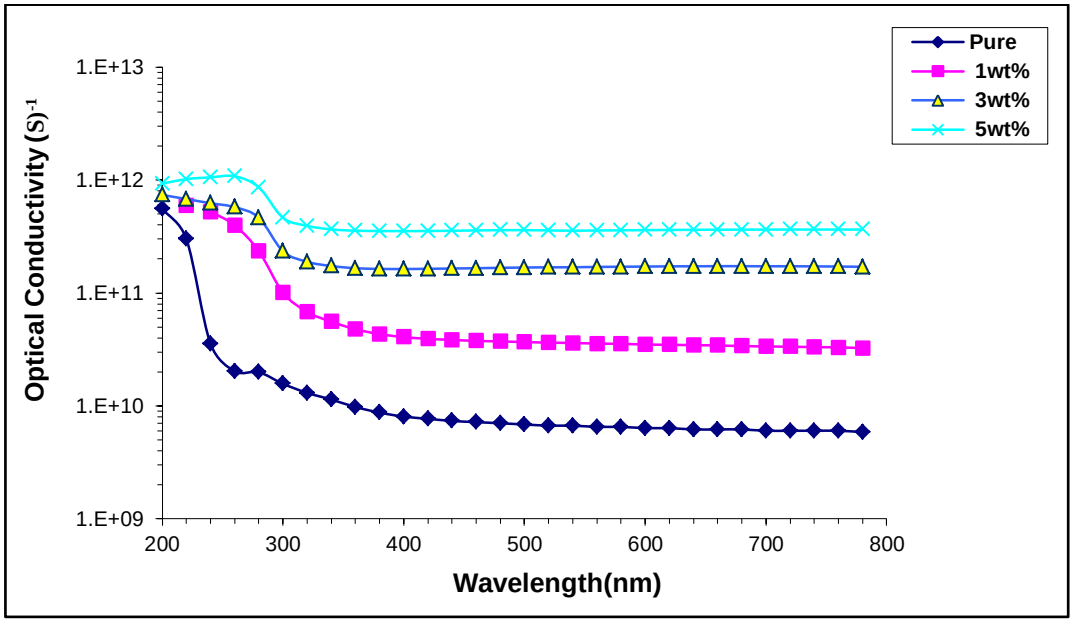

Figure (4.24): Variation of Optical conductivity for of (PVA-CMC/Bi_2O_3) nanocomposites with wavelength.

4.4 The A.C Electrical Properties.

The A.C electrical properties of the (PVA-PVP-Bi_2O_3) and (PVA-CMC-Bi_2O_3) nanocomposites at different frequencies were investigated (100 - $5*10^6$) Hz.

4.4.1 The Dielectric Constant.

The dielectric constant of (PVA-PVP/Bi_2O_3) and (PVA-CMC/Bi_2O_3) nanocomposites at frequency 100 Hz and at temperature of 25^0 C , figures (4.25) and(4.26) respectively. It is abundantly obvious that an increase in the concentration of Bi_2O_3 nanoparticles causes a corresponding rise in the dielectric constant. This can be due to the creation of a continuous network of Bi_2O_3 nanoparticles inside the nanocomposite itself. This was clearly seen in the microscopic photographs that were obtained of the nanocomposites made of (PVA-PVP/Bi_2O_3) and (PVA-CMC/Bi_2O_3) samples with varying concentrations.

Due to the formation of clusters and separated groups when the Bi_2O_3 nanoparticles are present at a low concentration (1wt%), the dielectric constant is reduced to an approximation of a lower value. On the other hand, Bi_2O_3 nanoparticles form a continuous network inside the nanocomposite when present in high concentrations (5wt%). This causes the value of the dielectric constant to grow in proportion to the volumetric rate of the Bi_2O_3 nanoparticles, results and agreed with other finding by [128,129].

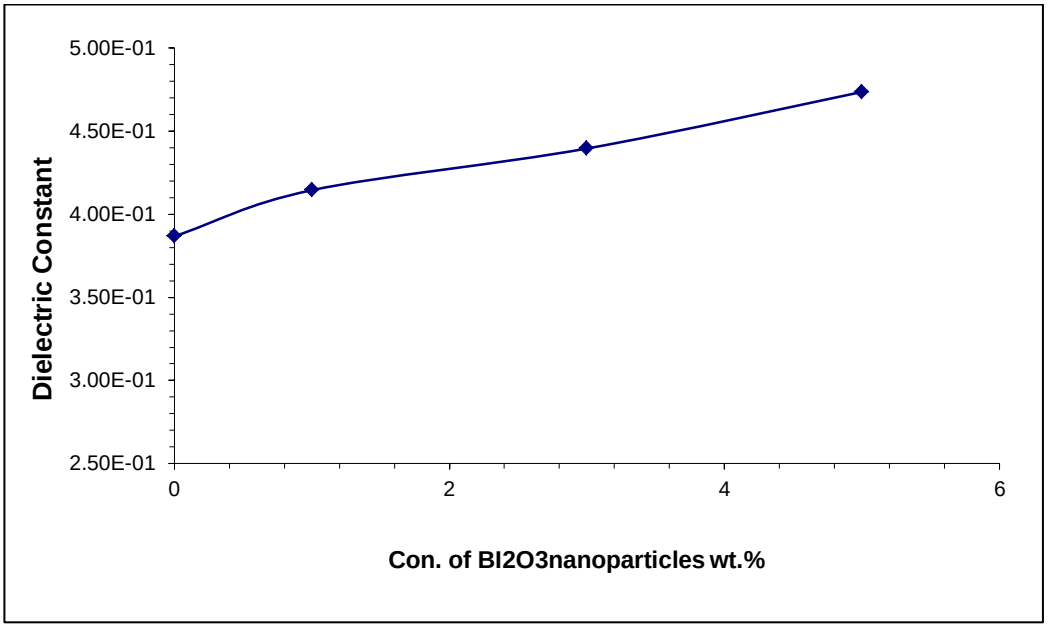

Figure (4.25): Variation of dielectric constant (ε') with concentration of (Bi_2O_3) nanoparticles at 100Hz of (PVA-PVP/Bi_2O_3) nanocomposites.

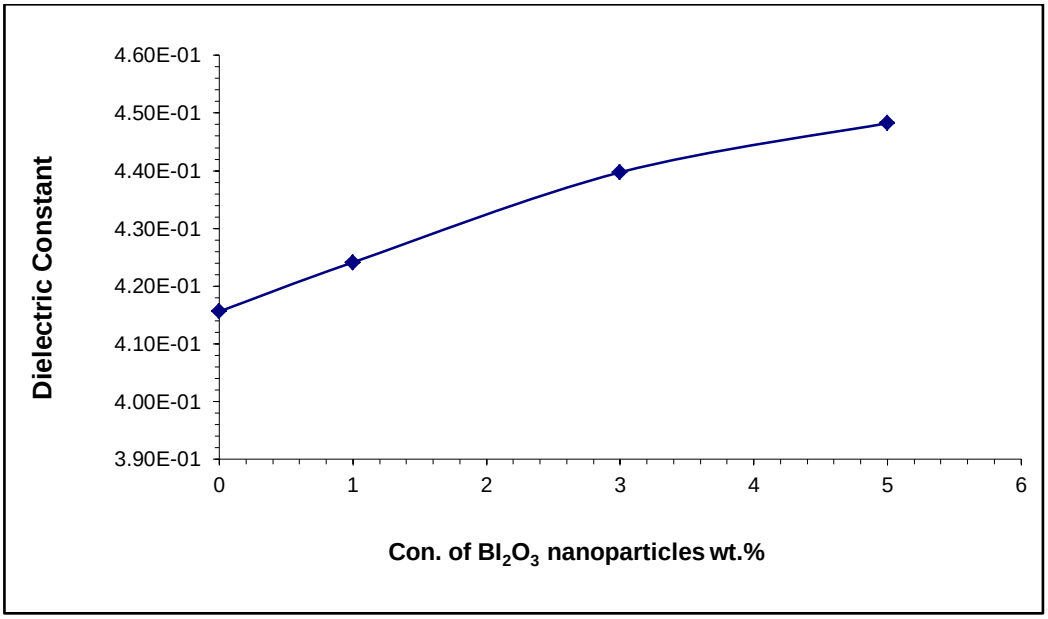

Figure(4.26): Variation of dielectric constant (ε') with concentration of(Bi_2O_3)nanoparticles at 100Hz of (PVA- CMC/Bi_2O_3) nanocomposites.

The dielectric constant variation for (PVA-PVP-/Bi_2O_3) and (PVA-CMC/Bi_2O_3) nanoparticles with frequency for all specimen are shown in Figures (4.27) and (4.28). Because of the different polarization states, it is clear from the figures that the dielectric constant will drop with an increase in the frequency that is being applied (ionic and electronic, dipolar, space

charge), at low frequencies, the polarization of the space charge plays a significant role in increasing the dielectric constant. Becomes less contributing to the rise in frequency and it more contributing of polarization, and this action induces the decrease in the dielectric constant values for all samples with an increase in the frequency of electrical field, the other types of polarizations occur at subsequent frequencies . This is due to the fact that the mass of an ion is greater than that of an electron. As a consequence of this difference in mass, electrons are able to respond to field vibrations at even the highest frequencies, making electronic polarization the only type of polarization that can occur at higher frequencies[49].

however; dipoles will barely be able to orient themselves in the direction of the applied field in the high frequency range, hence the value of the dielectric constant is almost constant, this is agreed with S. Mustafa [130].

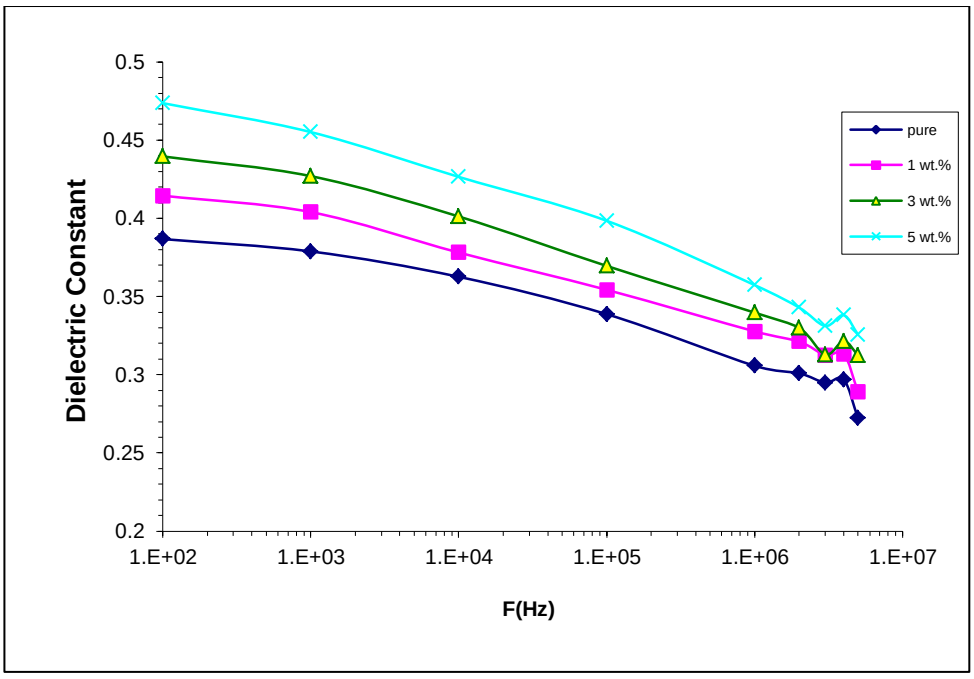

Figure (4.27): Variation of the dielectric constant(ε') of (PVA-PVP/Bi_2O_3) nanocomposites with frequency(Hz).

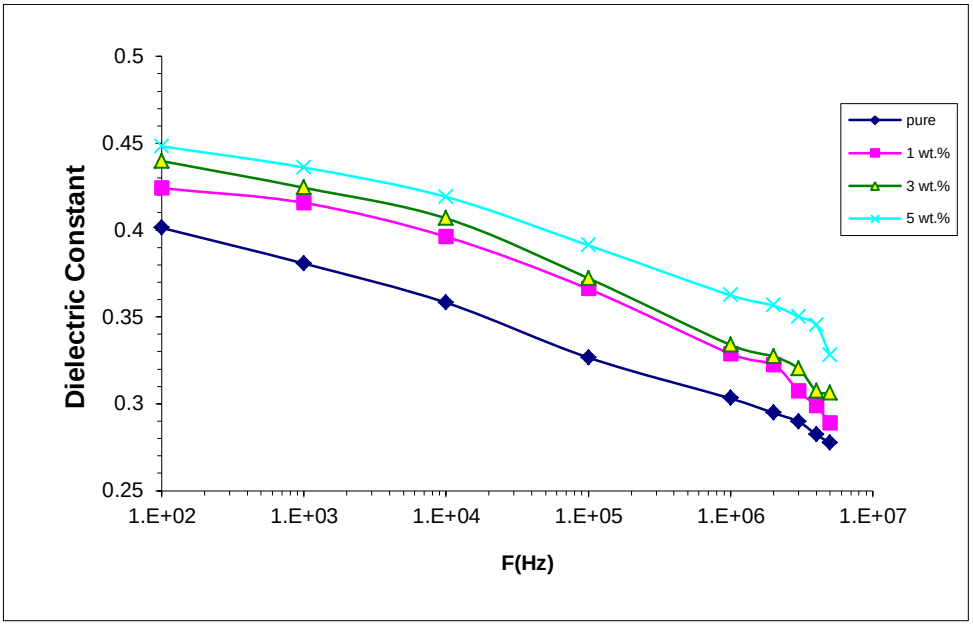

Figure(4.28): Variation of the dielectric constant(ε') of (PVA-CMC/Bi_2O_3) nanocomposites with frequency (Hz).

4.4.2 The Dielectric Loss

The dielectric loss of nanocomposites is depicted as a function of frequency in figures (4.29) and (4.30) respectively. This behavior is attributed to a decline in the contribution of space charge polarization as well as a high value of dielectric loss for (PVA-PVP/Bi_2O_3) and (PVA-CMC/Bi_2O_3) nanocomposites at low frequency. The figures demonstrates that the dielectric loss of (PVA-PVP/Bi_2O_3) and (PVA-CMC/Bi_2O_3) nanocomposites decreases with an increase in the applied electric field. When there is a higher concentration of Bi_2O_3 nanoparticles, there is also an increase in the dielectric loss. When the frequency increases, there is a relatively modest change in the amount of dielectric loss. This is because various types of polarization are able to take place at high frequencies, as demonstrated by the mechanisms described in reference [49]. As demonstrated in the figures(4.31) and (4.32) increase in the concentration of bismuth oxide leads to increase in the number of ionic charge carriers,

which in turn leads to increase in the value of dielectric loss. This phenomenon can be observed when the concentrations of nanoparticles is increased, this is agreed with the results of A. A. Abid et al.[52].

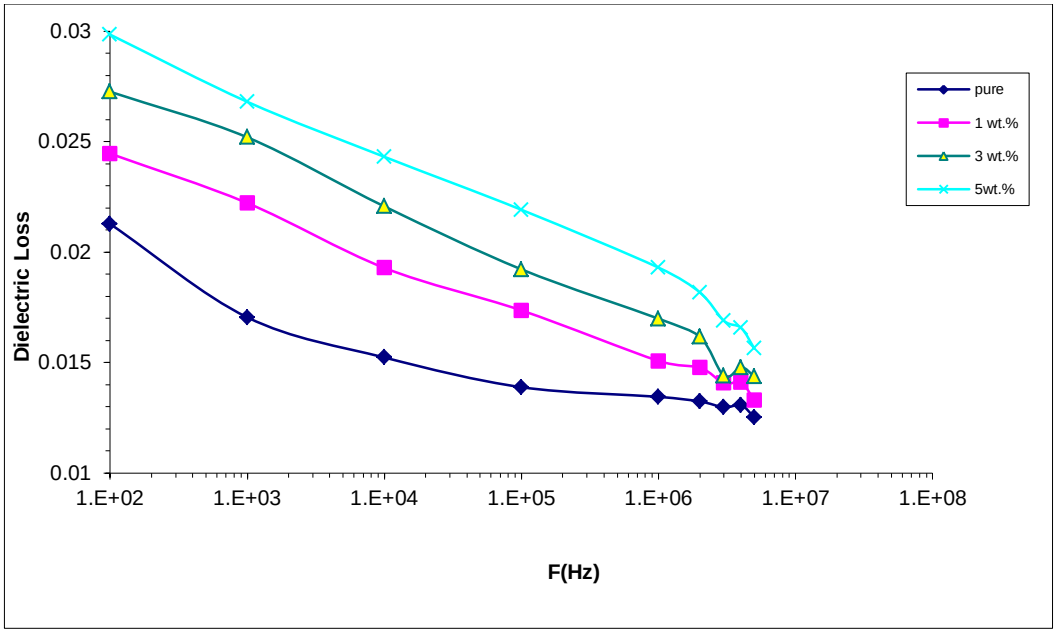

Figure(4.29): Variation of the dielectric loss (ε'') of (PVA-PVP/Bi_2O_3) nanocomposites with frequency(Hz).

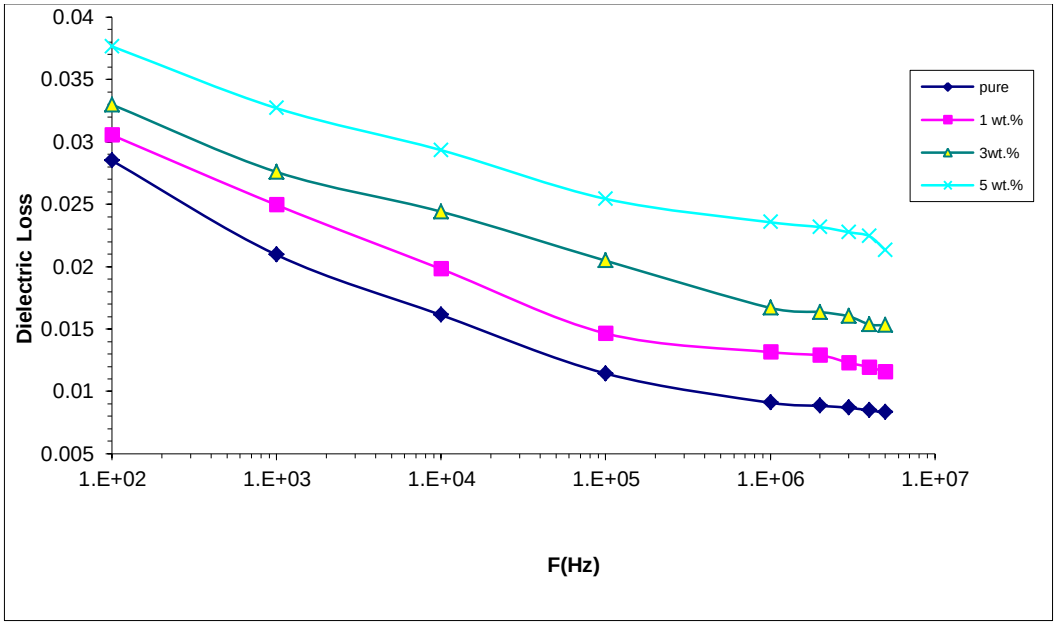

Figure(4.30): Variation of the dielectric loss (ε'') of (PVA-CMC/Bi_2O_3) nanocomposites with frequency (Hz).

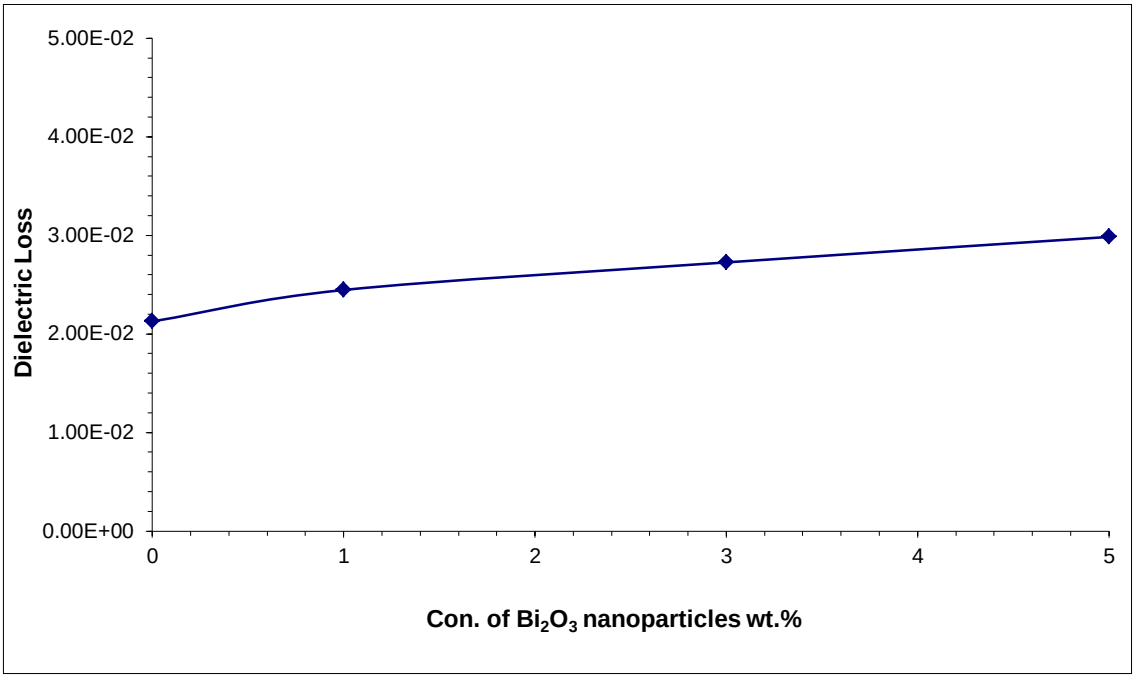

Figure(4.31): Variation of dielectric loss (ε'') with concentration of (Bi_2O_3) Nano-particles for (PVA-PVP/Bi_2O_3) nanocomposites.

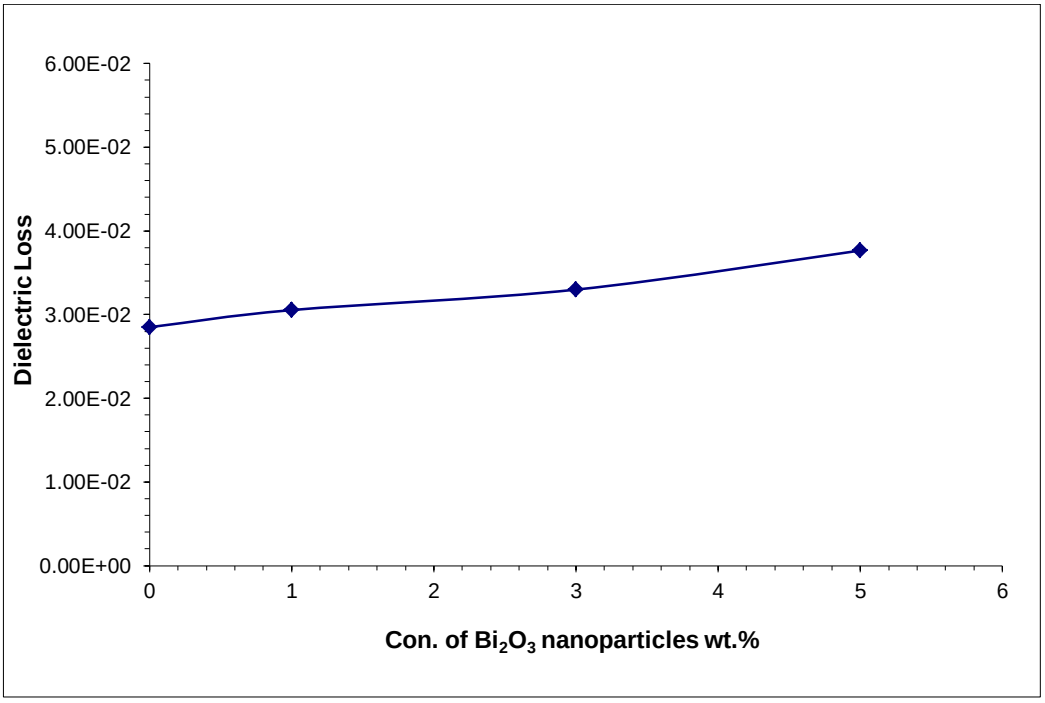

Figure(4.32): Variation of dielectric loss (ε'') with concentration of (Bi_2O_3) Nano-particles for (PVA-CMC/Bi_2O_3) nanocomposites.

4.4.3 The A.C Electrical Conductivity of (PVA-PVP/Bi_2O_3) and (PVA-CMC/Bi_2O_3) Nanocomposites.

The variation of A.C electrical conductivity as a function of frequency for (PVA-PVP/Bi_2O_3) and (PVA-CMC/Bi_2O_3) nanocomposites at 100Hz, is shown in figures (4.33) and (4.34) respectively. From figures the electrical conductivity of nanocomposites increases with increased frequency in (low, moderate and higher) frequency regions this is due to the hop-up of charge carriers in the localized state and also to the excitation of charge carriers in the conduction band in the upper regions. Two influences that affect A.C conductivity are main chain motion and ion motion, in other words, the increase in A.C electrical conductivity at low frequency area can be related to interfacial polarization while the increase in conductivity is due to the passage of electrons at frequencies, intermediate and the high [49]. Figures (4.35) and (4.36) show that an increase in the concentration of (Bi_2O_3) nanoparticles in nanocomposites results in the conductivity increasing of the nanocomposites. This occurs as a result of an increase in the number of ionic charge carriers as well as the formation of a continuous network of (Bi_2O_3) nanoparticles within the composites, these results agree with others [131]

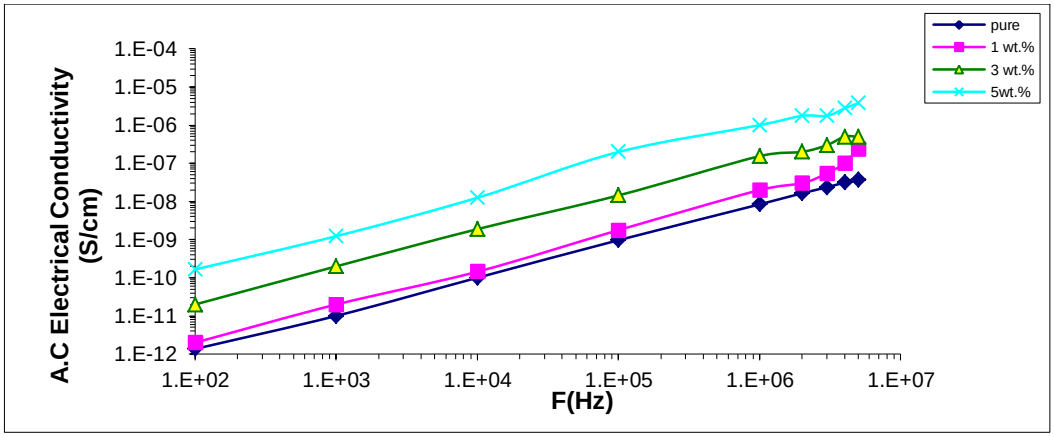

Figure (4.33): Variation of the A.C electrical conductivity (s/cm) with frequency (Hz) for(PVA-PVP/Bi_2O_3) nanocomposites.

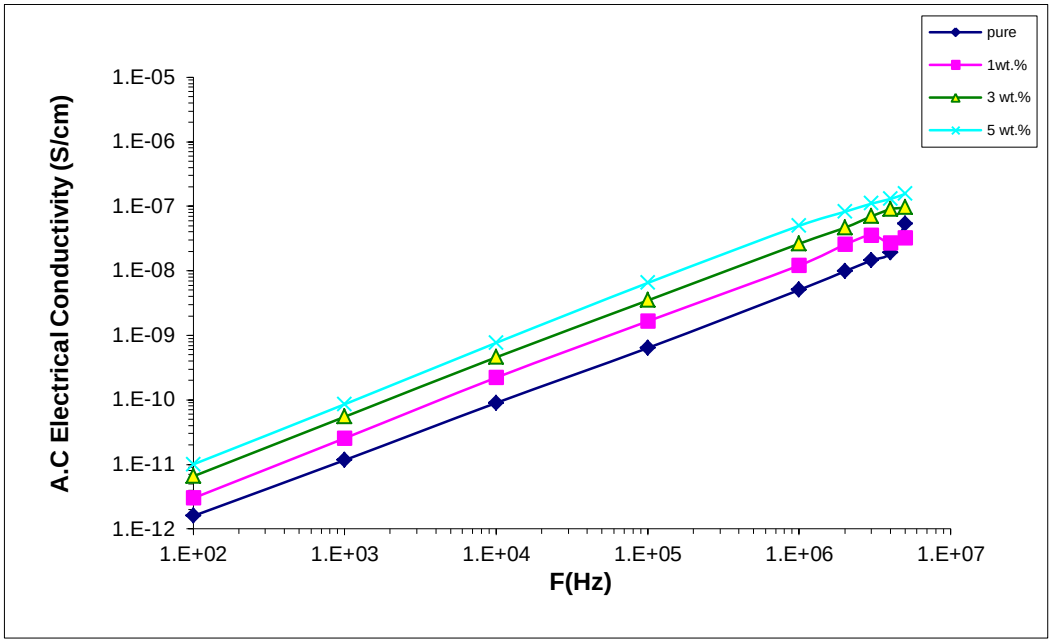

Figure(4.34): Variation of the A.C electrical conductivity (s/cm) with frequency (Hz) for (PVA-CMC /Bi_2O_3) nanocomposites.

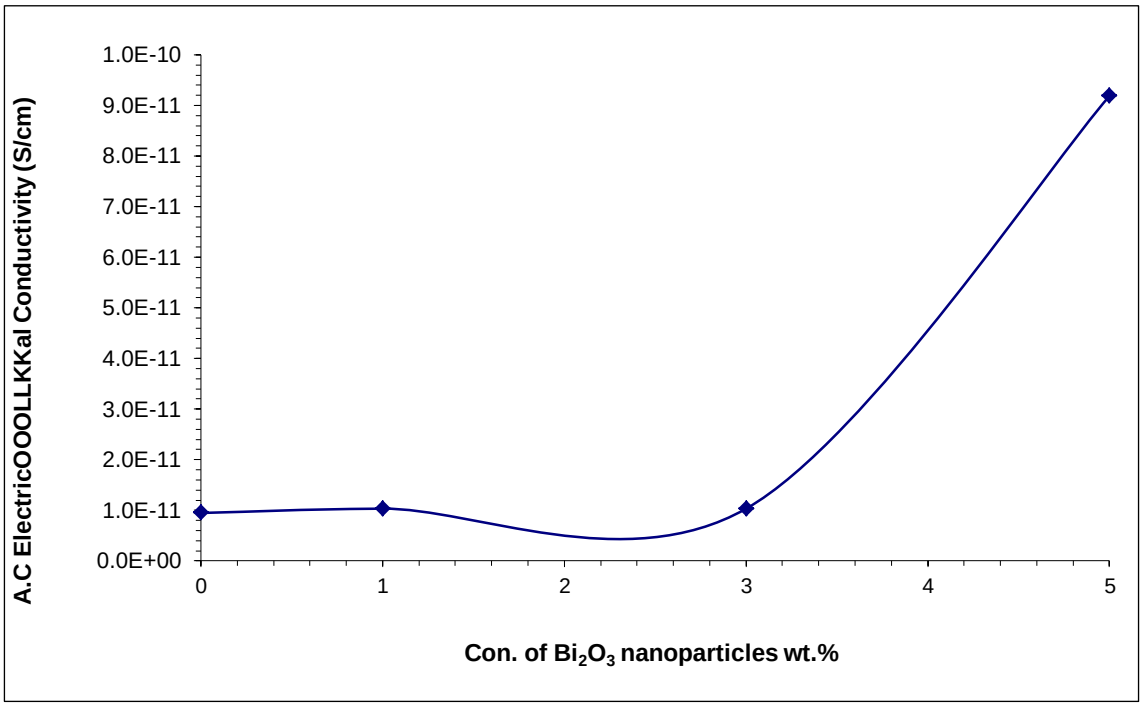

Figure (4.35): Variation of the A.C electrical conductivity (s/cm) with different concentration for (PVA- PVP/Bi_2O_3) nanocomposites.

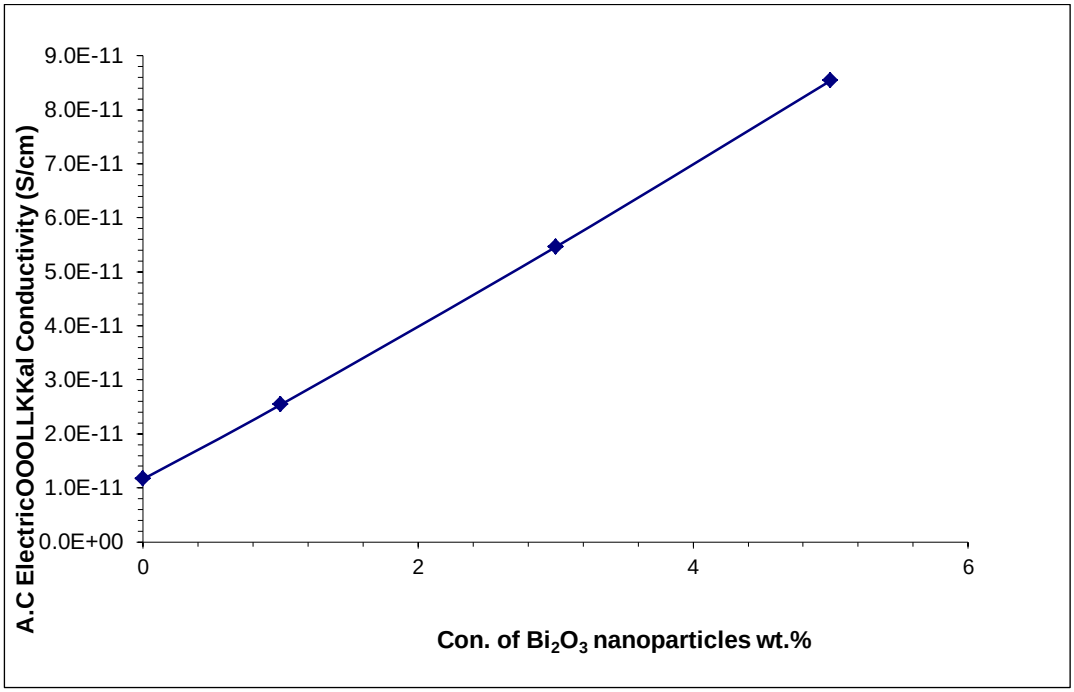

Figure (4.36): Variation of the A.C electrical conductivity (s/cm) with different concentration for (PVA-CMC/Bi_2O_3) nanocomposites.

4.5 Application of (PVA-PVP/Bi_2O_3) and (PVA-CMC/Bi_2O_3) Nanocomposites for Gamma Ray Shielding.

Figures (4.37) and (4.38) show the variation of ($N/N_\circ$) for (PVA-PVP)and (PVP-CMC) blend with different concentrations of Bi_2O_3 nanoparticles. The transmission radiation decreases with the increasing of the concentrations of Bi_2O_3 nanoparticles which is attributed to the increase of the attenuation radiation[132].

The variety of gamma radiation attenuation coefficients for the (PVA-PVP) and (PVA-CMC) blend as a function of Bi_2O_3 nanoparticle levels is shown in figures (4.39) and (4.40).

The coefficients of attenuation rise with increased levels of nanoparticles; this is due to the absorption or reflection of gamma radiation by nanocomposites shielding materials. From the figures, it showed very close results by comparing the attained results by polymer nanocomposite

with concrete, however, composite polymer because of its mobility and lower electrical properties, it has an advantage over concrete and the ability to avoid neutron emission [106].

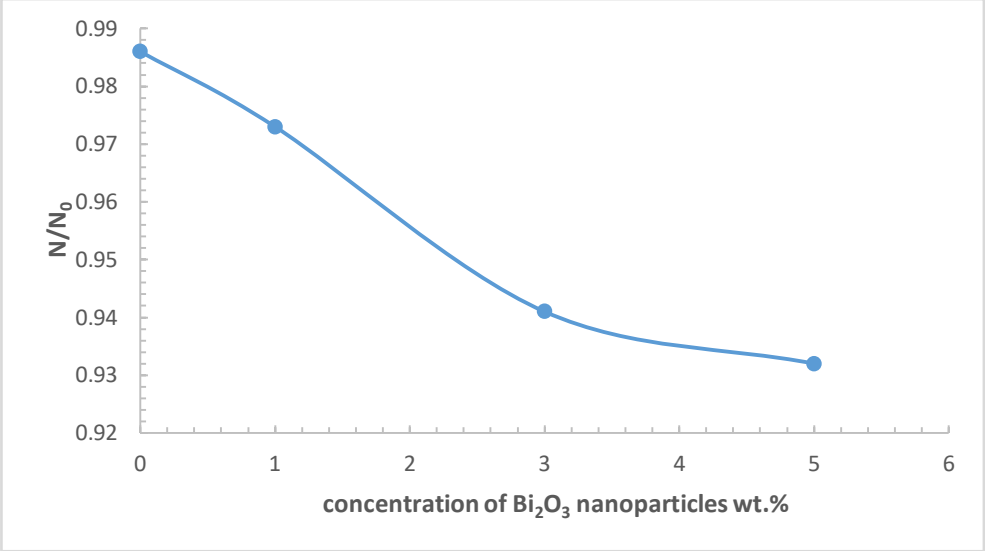

Figure (4.37): Variation of (N/N_0) for (PVA-PVP/Bi_2O_3) nanocomposites.

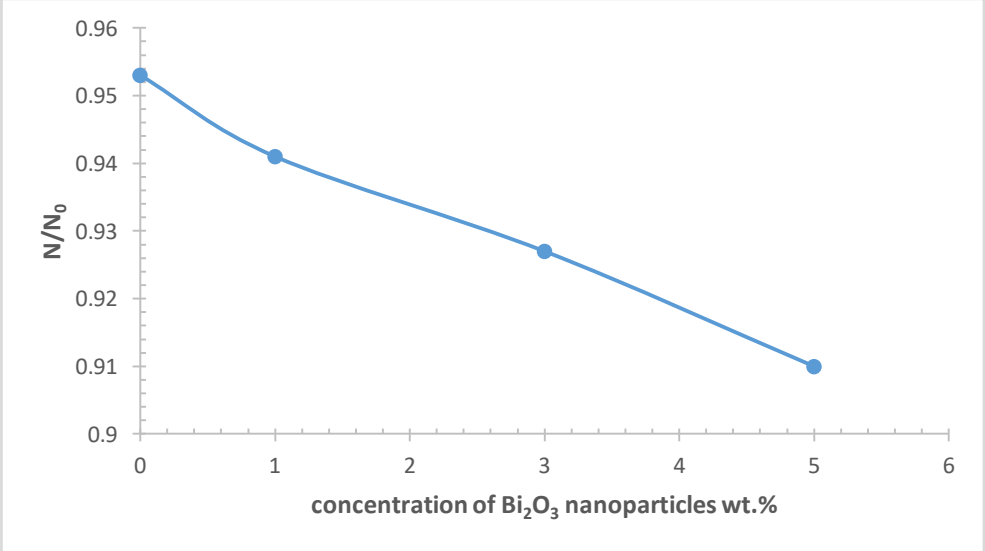

Figure(4.38): Variation of (N/N_0) for (PVA-CMC/Bi_2O_3) nanocomposites.

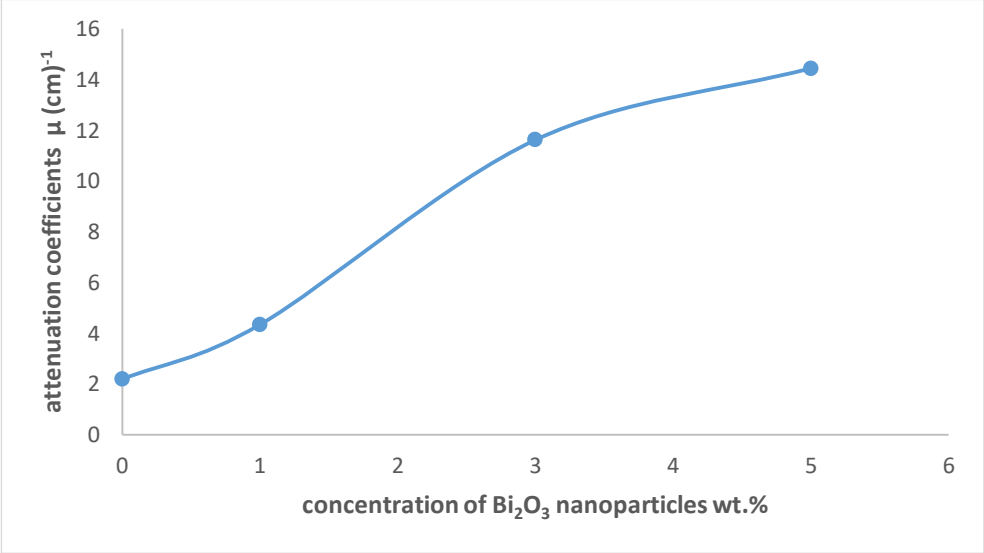

Figure(4.39): Variation of attenuation coefficients μ of gamma radiation for (PVA-PVP/Bi_2O_3) nanocomposites.

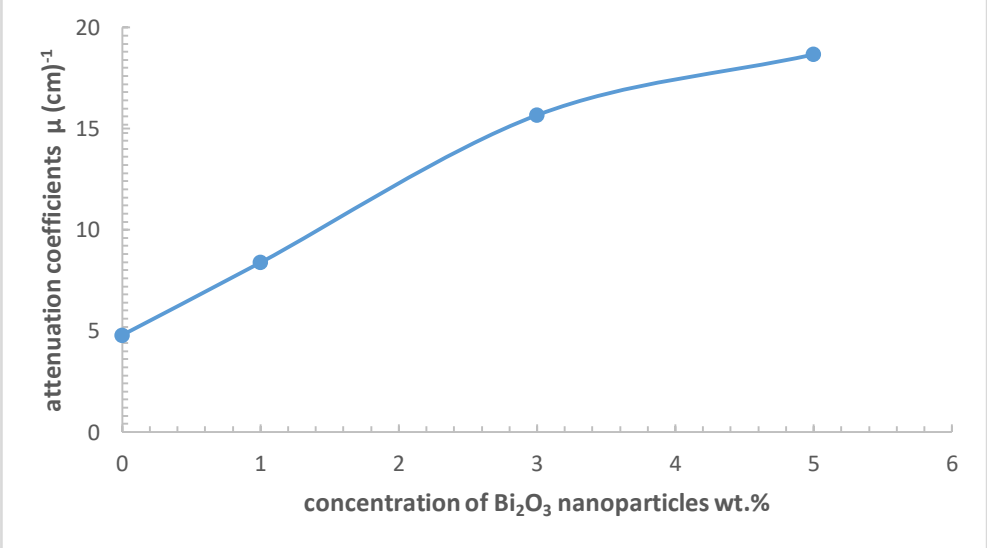

Figure(4.40): Variation of attenuation coefficientsμ of gamma radiation for (PVA-CMC/Bi_2O_3) nanocomposites.

Chapter Five

Conclusions and Future Works

5.1 Conclusions

The following points are concluded from the obtained results and discussions:

1- The optical microscope images showed that Bi_2O_3 nanoparticles made of continuous network inside the blend at concentration (0,1,3 and 5 wt%).

2- The FTIR measurements indicate vibration bands for polymer blend before and after addition Bismuth oxide nano composites, and it was concluded that the polymer after addition may have formed chains networks of polymer nanocomposites and their effects appeared in electrical and optical properties and decreased the intensity of peaks FTIR spectrum confirms that after additives the of (PVA-PVP) and (PVA-CMC) chains increased in the structure of the films.

3- The absorbance increased with the increasing of concentration of (bismuth oxide). This conclusion is useful in determining the industrial applications Such as the manufacture of food and drug preservation boxes and also increased absorbance and decrease transmittance with the increase in the percentage of Bismuth oxide, especially in an area UV Therefore, these compounds can be used in applications whose purpose is absorb ultraviolet rays. The absorption coefficient (PVA-PVP/Bi_2O_3) and (PVA-CMC/Bi_2O_3) nanocomposites is less than (10^4) $(cm)^{-1}$ at all concentrations and from these, the result is being indirect transition .

4- Comparison of the optical characteristics of (PVA-CMC/$Bi_2O_{3)}$ and (PVA-PVP/Bi_2O_3) nanocomposites increasing the concentration of Bi_2O_3 nanoparticles causes an increase in the refractive index (n), extinction coefficient (K), and the dielectric constant (real and imaginary part).The energy gap for indirect transitions, which can be either allowed or disallowed, narrows as the concentration of Bi_2O_3 nanoparticles in a material grows.

5- The dielectric constant and the dielectric loss of the (PVA-PVP/Bi_2O_3) and (PVA-CMC/Bi_2O_3) nanocomposites decrease with the rise in frequency of the applied electric field. On the other hand, the alternating current electrical conductivity increases with the increase in frequency. The dielectric constant and the dielectric loss of (PVA-PVP/Bi_2O_3) and (PVA-CMC/Bi_2O_3) nanocomposites for all concentrations increases with increasing concentrations of Bi_2O_3 nanoparticles. The conductivity increases with increasing Bi_2O_3 nanoparticles.

6- The attenuation coefficients for gamma radiation increase with increasingof the Bi_2O_3 nanoparticles concentrations**.**

5.2 Future works

1. A study of the thermal properties of the (PVA-PVP/Bi_2O_3) and (PVA-CMC/Bi_2O_3) nanocomposites.

2. A studying of the mechanical properties of the(PVA-PVP/Bi_2O_3) and (PVA-CMC/Bi_2O_3) nanocomposites.

References

References

[1] F. J. Davis, "Polymer Chemistry", Oxford,New York, 0 19 850309 1(Hbk), 2004 .

[2] W. Hu," Introductionin Polymer Physics A Molecular Approach" (Springer Wien Heidelberg, New York Dordrecht, London), 2012950781, 2013.

[3] L.H. Sperling,"Introduction to physical polymer science", 4th ed.,(Wiley), Printed in the United States of America, QD381.S635, 2006.

[4] A. K. Mikitaev, M.Kh. Ligidov and G.E. Zaikov, "Polymers, Polymer blends, Polymer Composites and Filled Polymers", published by Nova Science Publishers, Inc.New York, QD381.P6127 , 2006.

[5] L. W. Hamley, " Introduction to Soft Matter: Synthetic and Biological Self- Assembling Materials", Wiley, 2007.

[6] A. K. Haghi, , Eduardo A. Castro, PhD, Sabu Thomas, , P. M. Sivakumar, , and ndrew G. Mercader, "Material Science of Polymers", Taylor & Francis Group, 3: 978-1-4822-9913-7 (eBook – PDF), 2015.

[7] G. E. Wnek and G. L. Bowlin," Encyclopedia of Biomaterials and Biomedical engineering"2nd ed. 13: 978-1-4200-7802-2 (hb : alk. paper), 2008.

[8] C. E. Carraher Jr,"Introduction to Polymers", in (Introduction to polymer chemistry) 4th ed(Taylor & Francis Group), FL 33487-2742, 2017.

[9] M. Yousefi, E. Noori, D. Ghanbari, M. Salavati-Niasari, and T. Gholami, “A Facile Room Temperature Synthesis of Zinc Oxide Nanostructure and Its Influence on the Flame Retardancy of Poly Vinyl Alcohol,” J. Clust. Sci., vol. 25, no. 2, pp. 397–408, 2014.

[10] T. A. Osswald," Material Science of Polymers for Engineers", 3rd ed. Hanser Publishers, Munich, 978-1-56990-514-2, 2012.

[11] R. K. Goyal," Nanomaterials and Nanocomposites", by Taylor &Francis Group, LLC, 3: 978-1-4987-6166-6 (Hardback), 2018.

[12] J. P. Davim," Nanocomposites", Materials, Manufacturing and Engineering, DE GRUYTER, Germany, Berlin, 2013.

[13] P. M. Ajayan, L. S. Schadler and P. V. Braun," Nanocomposite Science and Technology", WILEY-VCH Verlag GmbH Co. KGaA, Weinheim,2003.

[14] J Jabir, "The optical properties of (PVA+ PVP) +PANI blends," *Iraqi Journal of Physics*,vol. 13, no. 28, pp. 162– 129,2015.

[15] S Bhadraiah, "Creation of Crosslinkable Interphases in Polymer Blends," *In Macromolecular Symposia*. Vol. 210 ,no. 1, pp. 165-174,2004.

[16] C Sarath, R Shanks, and S Thomas, "Nanostructured Polymer Blends " , *Chapter Polymer Blends*, pp. 1–14 ,2014.

[17] S Mayu, and T Harald, "Compatibilizing bulk polymer blends by using organoclays," Macromolecules, vol , no , pp.4793 –4801,2006.

[18] H. Samiha, "Optical properties of polymers and their applications" New Jersey Institute of Technology , 2019.

[19] J. A. Brydson," PLASTICS MATERIALS", 6th Ed. ISBN 0 7506 1864 7 (pbk.), Oxford [u.a.]. Butterworth-Heinemann. XXVII, 896 S ,1995.

[20] Y. S. Lipatov and A. E. Nesterov,"Thermodynamic of Polymer Blends", USA, ISBN 1-56676-624-9,(1997).

[21] K. Pal and I. Banerjee," Polymeric Gels", Elsevier Ltd, ISBN 978-0-08- 102179-8, (2018). References.

[22] M. S. Ågren," Wound Healing Biomaterials", volume 2, Elsevier Ltd. ISBN978-1- 78242-456-7, (2016).

[23] J. Hu, "Fabric Testing", Woodhead Publishing Limited, ISBN 978-1-84569-297- 1,(2008).

[24] Abdul-K. Al-Bermany and Rusul Abdul-Amir Ghazi," Study the effect of increasing Gamma ray doses on some physical properties of Carboxy methyl cellulose", Advances in Physics Theories and Applications, Vol.6,pp. 1-14, 2012 .

[25] H.H. J.Al Janabi,"Addition Effect of Polyacrylamide on the Physical Properties of Carboxymethylcellulose", M. Sc Thesis, Babylon University, College of Education for Pure Sciences , 2014.

[26] A. Bono, P.H. Ying, F.Y. Yan, C.L. Muei, R. Sarbatly, and D. Krishnaiah,"Synthesis and Characterization of Carboxymethyl Cellulose from Palm Kernel Cake", *Advances in Natural and Applied Sciences*, Vol.3,pp.5-11, 2009.

[27] H. D. Heydarzadeh, G.D. Najafpour and A.A. Nazari Moghaddam," Catalyst-Free Conversion of Alkali Cellulose to Fine Carboxymethyl Cellulose at Mild Conditions", World Applied Sciences Journal, Vol.6 ,pp. 564-569, 2009 .

[28] K. Boruvkova and Jakub Wiener," Water Absorption In Carboxymethyl Cellulose ", *AUTEX Research Journal*, Vol.11,no.4, pp.110- 113, 2011.

[29] J. Davis, A. McLister, J. Cundell and D. Finlay," Smart Bandage Technologies", Design and Application, Elsevier Inc. ISBN 978-0-12-803762-1, 2016.

[30] Z. Ping, Q.T.Nguyen, A.Essamri,and J.Ne el, Polym. Adv.Technol." Macromol. Chem. Phys.,No. 195,pp.21, 1994.

[31] K. Sreekanth, T. Siddaiah, N.O. Gopal, Y. Madhava Kumar, Ch. Ramu*" Optical and electrical conductivity studies of VO2+doped Polyvinyl pyrrolidone (PVP) polymer electrolytes" journal of Science: Advanced Materials and Devices ISBN 4. 230- 236,2019.

[32] H.D. Wu, I.D.Wu, and F. C. change," The Interaction Behavior of Polymer Electrolytes Composed of Poly(vinyl pyrrolidone) and Lithium Perchlorate ($LiClO_4$)",*J. Polymer*, Vol.42, No.2, pp.555- 562, 2001.

[33] N. Karak," Nanomaterials and Polymer Nanocomposites",Elsevier Inc. ISBN 978-0-12-814615-6, 2019.

[34] J. Bonilla, E. Fortunati, L. Atarés, A. Chiralt, J.M. Kenny, "Physical, structural and antimicrobial properties of poly vinyl alcohol–chitosan biodegradable films", *Food Hydrocolloids*, Vol. 35 ,pp. 463-470,2014.

[35] B. He, W. Wang, Y. Song, Y. Ou, J. Zhu ,"Structural and physical properties of carboxymethyl cellulose/gelatin films functionalized with antioxidant of bamboo leaves", *International Journal of Biological Macromolecules*, Vol.164,No, 1,pp. 1649-1656,2020.

[36] Y .Ma, T.Bai, F. Wang, "The physical and chemical properties of the polyvinylalcohol/polyvinylpyrrolidone/hydroxyapatitecomposite hydrogel,"*Materials Science and Engineering*,Vol. 59,No. 1;59,pp.948-957, 2016.

[37]P.Patnaik, "Handbook of Inorganic Chemical Compounds," McGraw-Hill. p. 243. ISBN 0-07-049439-8, (2003).

[38] M. Anilkumar, R. Pasricha, V. Ravi," Synthesis of bismuth oxide nanoparticles by citrate gel method", *Ceramics international*, Vol.31 No. 6 PP.889-891,2005.

[39] C. Fontainha, N. Baptista, T. Annibal, LO. Faria," Radiation shielding with Bi_2O_3 and ZrO_2: Y composites: preparation and characterization" International Nuclear Atlantic Conference,2015.

[40] H. A. Harwig, "On the Structure of Bismuthsesquioxide: The α, β, γ, and δ-phase". *Zeitschrift für anorganische und allgemeine Chemie*,Vol.444 No.1,pp.151-166,1978.

[41] M. Ali Habeeb,"Effect of Nanosilver Particles on Thermal and Dielectric Properties of (PVA-PVP) Films",*International J. of Applied and Natural Sciences (IJANS),* Vol. 2,No. 4, pp. 103-108,(2013).

[42] S. Asath Bahadur, R. Natarajan, S. Subramanian, S. Chinnappandar and J. Kuwamura," A study on polymer blend electrolyte based on PVA/PVP with proton salt," *Polymer Bulletin* ,Vol.71,No.22 ,pp.1061-1080 , 2014.

[43] K. Hemalatha, H. Somashekarappa and S. Rudrappa," Micro-Structure," Micro-Structure, Ac Conductivity and Spectroscopic Studies of Cupric Sulphate Doped PVA/PVP Polymer Composites ", *Advances in Materials Physics and Chemistry*,Vol.5,No.10,pp.408-418,2015.

[44] A. M. El Sayed,S. El-Gama, W. M. Morsi, Gh. Mohammed," Effect of PVA and copper oxide nanoparticles on the structural, optical, and electrical properties of carboxymethyl cellulose films", *Journal of Materials Science* ,Vol.50,No.21,pp.4717-4728, 2015 .

[45] Z. A. Al-Ramadhan, J. Abdulsattar , H. Abdul and K. Hmud," Optical and Morphological Properties of (PVA-PVP-Ag) Nanocomposites, International *Journal of Science and Research (IJSR),*Vol. 5,No.3 pp. 1828-1836, 2016.

[46] Sk. Shahenoor Bash, M. Gnanakiran, B. R. Kumar and K. V. B. Reddy," Synthesis and spectral characterization on PVA/PVP: Go based

blend polymer electrolytes", *Rasayan Journal of Chemistry* , Vol.10,No.4,pp. 1159- 1166, 2017.

[47] A. M. Ismail, M. I. Mohammed and E. G. El-Metwally," Influence of Gamma irradiation on the structural and optical characteristics of Li ion-doped PVA/PVP solid polymer electrolytes",*Indian Journal of Physics,*Vol.93, No.15 ,pp.175-183,2018.

[48] S. Choudhary, R.J. Sengwa," ZnO nanoparticles dispersed PVA–PVP blend matrix based high performance flexible nanodielectrics for multifunctional microelectronic devices", *Current Applied Physics* , Vol.18,No.9, pp.1041-1058, 2018.

[49] K. Rajesh, V. Crasta, N. Rithin Kumar, G. Shetty, and P. Rekha, "Structural, optical, mechanical and dielectric properties of titanium dioxide doped PVA/PVP nanocomposite," *J. Polym. Res.*, vol. 26, No. 4,pp1-10, 2019.

[50] F.M. Ali, "Structural and optical characterization of [(PVA:PVP)-Cu^{2+}] composite films for promising semiconducting polymer devices," *Journal of Molecular Structure*, Vol. 1189, pp.352-359, 2019.

[51] H. S. Rasheed," The effect of Adding (ZrC) Nanoparticles to (PVP-PVA) Blend on their Optical properties for Humidity Sensor Application," *Journal of Physics: Conference Series*, Vol.1660, 2020.

[52] A. Abid,S. Al-Nesrawy and A. Abdulridha "New Fabrication (PVA-PVP-C.B) Nanocomposites: Structural and Electrical Properties" *Journal of Physics*),vol. 1804, no. 15, pp. 2524–2532, 2020.

[53] A. Hashim, "Enhanced Structural, Optical, and Electronic Properties of In2O3 and Cr_2O_3 Nanoparticles Doped Polymer Blend for Flexible Electronics and Potential Applications" *Journal of Inorganic and Organometallic Polymers and Materials*, Vol.30, pp.3894-3406, 2020.

[54] M.Irfan, A. Manjunath, S.S. Mahesh, R. Somashekar, T.Demappa, "Influence of NaF salt doping on electrical and optical properties of PVA/PVP polymer blend electrolyte films for battery application," *Journal of Materials Science*: *Materials in Electronics*, Vol. 32,no.5,pp.5520-37,2021.

[55] V. Siva, D. Vanitha, A. Murugan, A. Shameem, S. Asath Bahadur, "Studies on structural and dielectric behaviour of PVA/PVP/SnO nanocomposites", *Composites Communications*,Vol. 23, no.100597, pp. 2452-2139,2021.

[56] D. E. Al-Kateb, Ali R. Abdulridha,"Structural and Optical Properties of (PVA/PVP:Sr_2NO_3) Nanocomposites", *journal of NeuroQuantology*, Vol. 19,no. 4, pp. 27-37, 2021.

[57] H. A. H. Alzahrani, "CuO and MWCNTs nanoparticles Filled PVA–PVP nanocomposites: morphological, optical, thermal, dielectric, and electrical characteristics," J. Inorg. Organomet. Polym. Mater., vol. 32, No. 5, pp. 1913–1923, 2022.

[58] A. Di Gianfrancesco," Materials for Ultra-Supercritical and Advanced Ultra- Supercritical Power Plants", Elsevier Ltd., 978-0- 08-100552- 1,(2017).

[59] S. Ebnesajjad," Surface Treatment of Materials for Adhesive Bonding", Elsevier Inc. ISBN 978-0-323-26435-8,(2014).

[60] R. Timothy, Corle and Gordon S. Kino" Confocal Scanning Optical Microscopy and Related Imaging Systems', ISBN 978-0-12-408750-7, Elsevier Inc.(1996).

[61] A. Ramírez-hernández, C. Aguilar-flores, and A. Aparicio-saguilán, "Fingerprint analysis of FTIR spectra of polymers containing vinyl análisis en la huella dactilar de espectros FTIR de polímeros que contienen etileno," *Rev DYNA*, vol.86 , no 209, pp . 198-205,2019.

[62] O, Faix "4.1 Fourier Transform Infrared Spectroscopy," In *Methods in lignin chemistry* pp.83-109,1992.

[63] N. Jaggi and D. Vij, "Chapter 9 Fourier Transform Infrared," *Handb. Appl. Solid State Spectrosc.*, pp. 411–450, 2006.

[64] M. Zaid, K. Matori, S. Abdul , A. Zakaria, and M. Ghazali, "Effect of ZnO on the physical properties and optical band gap of soda lime silicate glass," *Int. J. Mol. Sci.*, vol. 13, no. 6, pp. 7550–7558, 2012.

[65] M. Habeeb and H. Mohssen, "Effect of (CoO) Nanoparticles on Someoptical Properties of (PVA- Paam) Composite," *International Journal* of *Engineering Research & Technology (IJERT)*, vol. 3, no. 5, pp. 2050–2053, 2014.

[66] A. Hashim, M. Habeeb, and B. Rabee, "Optical Properties of (PVA-CaO) Composites," Journal of Scientific Research ISSN 2301-2005 Issue, vol.69 ,No. October 2019 ,pp. 5-9, 2012.

[67] N. Wilkinson, A .Metaxas, E. Ruud, E. Raethke, "Internal structure visualization of polymer - clay flocculants using fluorescence," Colloids Interface Sci. Commun., vol. 10–11, No. 17 March pp. 1–5, 2016.

[68] C.Devi, A. Sharma, and V. Rao, "Electrical and optical properties of pure and silver nitrate-doped polyvinyl alcohol films," *Mater. Lett.*, vol. 56, No. 3, pp. 167–174, 2002.

[69] P. Allen, "Solid State Physics by H. E. Hall ," *Am. J. Phys.*, vol. 43, No. 10, pp. 929–933, 1975.

[70] F. Yakuphanoglu and H. Erten, "Refractive index dispersion and analysis of the optical constants of an ionomer thin film," *Opt. Appl.*, vol. 35, No. 4, pp. 969–976, 2005.

[71] S.Hassan,"OpticalProperties of Prepared Polyaniline and polymethylmethacrylate blends," *Int. J. Appl. or Innov. Eng. Manag.*, vol. 2, No. 9, pp. 19–22, 2013.

[72] M. Sauer, J. Hofkens, and J. Enderlein, "Handbook of Fluorescence Spectroscopy and Imaging from Ensemble to Single Molecules. Wiley-VCH Verlag GmbH & Co. KGaA, Weinheim, Germany, ISBN 978-3-527-31669-4 , pp 1-69, 2011.

[73] M. Al-Alousi, "The Effect of substrate temperature and the annealing time on the optical properties of the AgInS2 thin films prepared by chemical spray pyrolysis Technique," *J. Univ. Anbar Pure Sci.* , vol. 4, No. 2, pp. 50-56 , 2010.

[74] F. Hachim, "Effect of Thickness and Thermal Annealing on Optical Properties of Sb Thin films properties of Sb films, effect of thickness on optical properties of Sb films, effect of annealing on optical properties of Sb films," *Hachim Iraqi J. Sci.*, vol. 54, No. 3, pp. 612–616, 2013.

[75] F. El-kader, "Structural, optical and thermal characterization of ZnO nanoparticles doped in PEO/PVA blend films," *Nano Sci. Nano Technol. An Indian J.*, vol. 7, No. 5, , pp 608-619, 2013.

[76] A. Andriesh, M. Iovu, and S. Shutov, "Chalcogenide non-crystalline semiconductors in optoelectronics," *J. Optoelectron. Adv. Mater*, vol. 4, No. 3, pp. 631–647, 2002.

[77] T. Numai, "Fundamentals of semiconductor lasers: Second edition," *Springer Ser. Opt. Sci.*, vol. 93, No.28 Augst, pp.55147, 2015.

[78] J. Pankove and D. Kiewit, "Optical Processes in Semiconductors," *J. Electrochem. Soc.*, vol. 119, No. 5, pp. 156C, 1972.

[79] N. Ahmed, Z. Sauli, U. Hashim, and Y. Al-douri, "Investigation of the absorption coefficient , refractive index , energy band gap, and film

thickness for Al0.11Ga0.89N by optical transmission method," *Int. J. Nanoelectron. Mater.*, vol. 2, No. January, pp. 189–195, 2009.

[80] D. Narang, "Optical transitions in wse2 single crystals," *J. Ovnic Res.*, vol. 4, No 6,pp. 141, Oct. 2008.

[81] J. George and C. Kumari, "Growth and characterization of tin disulphide crystals grown by physical vapour transport method," *J. Cryst. Growth*, vol. 63, No. 2, pp. 233–238, 1983.

[82] J. Nahida, "Spectrophotometric Analysis for the UV-Irradiated (PMMA)," *Int. J. Basic Appl. Sci. IJBAS-IJENS*, vol. 12, No. April, pp. 58–67, 2012.

[83] P. Pmma, A. Ahmad, , and A. Awatif , "Dopping Effect On Optical Constants of," *Engineering and Technology Journal*, vol. 25, No. 4, pp 558-568 ,2007.

[84] A. Al-Khayatt, M. Jaafer, and A.Al-Khayatt, "Annealing Effect on The Structural and Optical Properties of CuS Thin Film Prepared By Chemical Bath Deposition (CBD) Introduction," *J. Kufa-Physics*, vol. 5, No. 1,pp79-90, 2013.

[85] R. Kadhim, "Study of Some Optical Properties of Polystyrene - Copper Nanocomposite Films," *World Sci. News*, vol. 30, No 17 November2015, pp. 14–25, 2016.

[86] A. Essahlaoui, H. Essaoudi, A. Hallaoui, M. Bouhadda, A. Labzour, and A. Housni, "Calculation of the thickness and optical constants of lead titanate thin films grown on MgO from their transmission spectra," *J. Mater. Environ. Sci.*, vol. 9, No. 1, pp. 228–234, 2018.

[87] S. Salman, M. Abdu-allah, and N. Bakr, "Optical Characterization of Red Methyl Doped Poly (Vinyl Alcohol) Films Sabah," *International*

Journal of Engineering and Technical Research (IJETR), vol 2, No. 4, pp. 126–128, 2014.

[88] S. Chiad, S. Oboudi, K. Abass, and N. Habubi, “Characterization of Silver / Poly (Vinyl Alcohol) (Ag / PVA) Filmsprepared by Casting Technique,” *Iraqi J. of polymers*, vol. 16, No. 2, pp. 10–18, 2012.

[89] S. Sze, "Physics of Semiconductor Devices", 2nd edition., John Wiley and Sons, New York, 1981.

[90] D. Bigg, “Mechanical, thermal, and electrical properties of metal fiber-filled polymer composites,” *Polym. Eng. Sci.*, vol. 19, No. 16, pp. 1188–1192, 1979.

[91] M. Iwama, N. Tagawa, and T. Homma, “On Determination of Molecular Weight Distribution,” *J. Soc. Chem. Ind. Japan*, vol. 72, No. 4, pp. 926–929, 1969.

[92] A. Szabo, “Theory of fluorescence depolarization in macromolecules and membranes,” *J. Chem. Phys.*, vol. 81, No. 1, pp. 150–167, 1984.

[93] N. Abbas, M. Habeeb, and A.Algidsawi, “Preparation of chloro penta amine cobalt(III) chloride and study of its influence on the structural and some optical properties of polyvinyl acetate,” *Int. J. Polym. Sci.*, vol. 2015, No. 15 Feb ,pp.1-15 , 2015.

[94] H. Jafar, N. Ali, and A. Shawky, “Study of A . C Electrical Properties of Aluminum – Epoxy Composites,” *Al-Nahrain Journal of Science*, vol. 14, No. 3, pp. 77–82, 2011.

[95] T. Seghier and F. Benabed, “Dielectric Proprieties Determination of High Density Polyethylene (HDPE) by Dielectric Spectroscopy,” *Int. J. Mater. Mech. Manuf.*, vol. 3, No. 2, pp. 121–124, 2015.

[96] S. Shekhar, V. Prasad, and S. Subramanyam, “Structural and electrical properties of composites of polymer-iron carbide nanoparticles embedded in carbon,” *Mater. Sci. Eng. B Solid-State Mater. Adv. Technol.*, vol. 133, No. 1–3, pp. 108–112, 2006.

[97] T. Furukawa, “Electrical properties of polymers,” *Reports Prog. Polym. Phys. Japan*, vol. 43, pp. 369–390, 2000.

[98] R. Dorf, The Electrical Engineering Hand Book, CRC Press LLC, 2nd Edition, Piscataway, New Jersey, USA, pp.1-2976 (2000).

[99] R. AL-Morshdy, M. Habeeb, and H. AL-Asadi, “Effect of Nanosilver Particles on the Optical and Structural Properties of (PVA-PVP) Films", *Advances in Physics Theories and Applications*, Vol. 34, No. January,PP.30-39, 2014.

[100] N. Azahari, N. Othman, and H. Ismail, “Biodegradation studies of polyvinyl alcohol/corn starch blend films in solid and solution media,” *J. Phys. Sci.*, vol. 22, No. 2, pp 15–31, 2011.

[101] I. Yüceda\ug, A. Kaya, \cSemsettin Alt\indal, and I. Uslu, “Frequency and voltage-dependent electrical and dielectric properties of Al/Co-doped {PVA}/p-Si structures at room temperature,” *Chinese Phys. B*, vol. 23, No. 4, pp. 47304, Apr. 2014.

[102] S. Zhang, Q. Tao, Z. Wang, and Z. Zhang, “Controlled heat release of new thermal storage materials: The case of polyethylene glycol intercalated into graphene oxide paper,” *J. Mater. Chem.*, vol. 22, No. 22 elo, pp. 20166–20169, 2012.

[103] S. Harikrishnan and S. Kalaiselvam, “Experimental investigation of solidification and melting characteristics of nanofluid as PCM for solar water heating systems,” *Int J Emerg Technol Adv Eng*, vol. 3,No. 15, pp. 628–635, 2013.

[104] N. Singh, R. Kaundal, and K. Singh, “Gamma-ray shielding and structural properties of PbO-SiO2 glasses,” *Nucl. Instruments Methods Phys. Res. Sect. B Beam Interact. with Mater. Atoms*, vol. 266, No. 6, pp. 944–948, 2008.

[105] M. Kiani, S. Ahmadi, M. Outokesh, R. Adeli, and H. Kiani, “Study on physico-mechanical and gamma-ray shielding characteristics of new ternary nanocomposites,” *Appl. Radiat. Isot.*, vol. 143, No. 1, pp. 141–148, 2019.

[106] M. Roy, R. Mahloniya, J. Bajpai, and A. Bajpai, “Spectroscopic and morphological evaluation of gamma radiation irradiated polypyrole based nanocomposites,” *Adv. Mater. Lett.*, vol. 3, No. 5, pp. 426–432, 2012.

[107] G. Eid, A. Kany, M. El-Toony, A. Madbouly, I. Bashter, and F. Gaber, “Application of Epoxy/ Pb_3O_4 Composite for Gamma Ray Shielding,” *Arab J. Nucl. Sci. Appl.*, vol. 46, No. 2, pp. 226–233, 2013.

[108] L. Chaudhari and R. Nathuram, “Absorption Coefficient of Polymers (Polyvinyl Alcohol) by Using Gamma Energy of 0.39 MeV,” *Bulg. J. Phys*, vol. 37, No. 1, pp. 232–240, 2010.

[109] R.A.Abed Jassim," Effect of Chloride Groups ($Cocl_2$,$Crcl_2$ and Mncl2) on the Electrical and Optical Properties for (PVA-PVP) Films", *M.Sc. Thesis,University of Babylon, College of Education for Pure Sciences*, (2013).

[110] N.Rajeswari ,S. Selvasekarapandian , S. Karythikeyan, M. Prabu, G. Hirankumar ,H. Nithya, C. Sanjeeviraja, "Conductivity and dielectric Properties of (PVA-PVP) poly blend film using non-aqueous medium". *Journal of Non- Crystalline Solids*, vol.357 ,Issues 22-23, 2011, page 3751-3756, (2011).

[111] M.A. Morsi , A.H. Oraby , A.G.Elshahawy, R.M. Abd El- Hady, "Preparation, structural analysis, morphological investigation and electrical properties of gold nanoparticales filled (PVA-CMC) blend",*Journal of Materials Research and Technology*, vol.8, No. 6 ,PP. 5996-6010, 2019.

[112] L. Chaudhari and R. Nathuram, " Absorption Coefficient of Polymers (Polyvinyl Alcohol) by Using Gamma Energy of 0.39MeV", *Bulg. Journal of Physics*, Vol. 37, PP. 232–240,2010.

[113] S. Kolpakov, N. Gordon, C. Mou, and K. Zhou, " Toward a New Generation of Photonic Humidity Sensors", *Journal of Sensors*, Vol.14, PP. 3986-4013; doi:10.3390/s140303986, 2014.

[114] N. D. Md Sin, M. F. Tahar, M. H. Mamat and M. Rusop, "Enhancement of Nanocomposite for Humidity Sensor Application", *Journal of Recent Trends in Nanotechnology and Materials Science, Engineering Materials*, DOI: 10.1007/978-3-319- 04516-0_2, P. 15-31, PP. 15-30, 2014.

[115] O. Abdullah1 , D. R. Saber and L. O. Hamasalih, "Complexion Formation in PVA/PEO/$CuCl_2$ Solid Polymer Electrolyte", *Universal Journal of Materials Science*, Vol. 3, No. 1, PP.1-5, 2015.

[116] N. B. Rithin Kumar, V. Crasta, R. F. Bhajantri and B.M. Praveen, "Microstructural and Mechanical Studies of PVA Doped with ZnO and WO_3 Composites Films", *Journal of Polymers*, Vol. 2014, Article ID 846140, 7 pages, 2014.

[117] J. Ramesh Babu and K.Vijaya Kumar, "Studies on Structural and Electrical Properties of $NaHCO_3$ Doped PVA Films for Electrochemical Cell Applications", *International Journal of Chem. Tech. Research*, Vol.7, No. 1, PP.171-180, 2014.

[118] S.H. Borova, O.M. Shevchuk, N.M. Bukartyk, E.Yu. Nikitishyn and V. Tokarev, "Nanocomposite Films Based on Functional Copolymers with Embedded Carbon Nanotubes", *proceedings of the International Conference Nanomaterials: Applications and Properties*, Vol. 3, No. 2, 2014.

[119] S. Salman, N. Bakr and M. H. Mahmood, "Preparation and study of some optical properties of (PVA- $Ni(CH_3COO)_2$) composites", International Journal of Current Research, Vol. 6, No.11, PP.9638-9643, 2014.

[120] A. Mohammad, K. Hooshyari, M. Javanbakht, and M. Enhessari, "Fabrication and Characterization of Poly Vinyl Alcohol/ Poly Vinyl Pyrrolidone/MnTiO Nanocomposite Membranes for PEM Fuel Cells", *Iranica Journal of Energy & Environment*, Vol. 4, No. 2, PP. 86-90, 2013.

[121] K. Karthikeyan, N. Poornaprakash, N. Selvakumar and Jeyasubrmanian, "Thermal Properties and Morphology of MgO-PVA Nanocomposite Film", *Journal of Nanostructured Polymers and Nanocomposites*, Vol. 5, No. 4, PP. 83-88, 2009.

[122] N. Elmarzugi1, T. Adali, A. Bentaleb, E. I. Keleb, A. T. Mohamed and A. M. Hamza, " Spectroscopic Characterization of PEG- DNA Biocomplexes by FTIR", *Journal of Applied Pharmaceutica*l *Science*, Vol. 4, No. 8, PP. 6-10, 2014.

[123] N. Arsalani, H. Fattahi and M. Nazarpoor, " Synthesis and characterization of PVP-functionalized superparamagnetic Fe_3O_4 nanoparticles as an MRI contrast agent", *Journal of EXPRESS Polymer Letters* Vol.4, No.6, PP. 329–338, 2010.

[124] D. Kumar, S. Karan Jat, P. K. Khanna, N. Vijayan, S. Banerjee, "Synthesis, Characterization, and Studies of PVA/Co-Doped ZnO Nanocomposite Films", *International Journal of Green Nanotechnology*, Vol. 4, PP.408–416, 2012.

[125] C. Srikanth, C. Sridhar, B. M. Nagabhushana and R.D.Mathad, " Characterization and DC Conductivity of Novel CuO doped Polyvinyl Alcohol (PVA) Nano-composite Films ", *Journal of Engineering Research and Applications*, Vol. 4, Issue 10, PP.38-46, 2014.

[126] S. D. Meshram, R. Rupnarayan, S. V. Jagtap, V. G. Mete and V. S. Sangawar, "Synthesis and Characterization of Lead Oxide Nanoparticles", International Journal of Chemical and Physical Sciences, Vol. 4, Special Issue, PP. 83-88, 2015.

[127] G. H. Murhekar and A.R. Raut, " Electrical properties of modified polyvinyl alcohol conjugates and doped modified polyvinyl alcohol conjugates", *International Journal of Chemical Studies*, Vol. 2, No. 2, PP. 77-82,2014.

[128] M. Harun, E. Saion, and A. Kassim, "Dielectric properties of poly (vinyl alcohol) /polypyrrole composite polymer films," *J. Adv. Sci. Arts*, vol. 1, No. January 2014, pp. 9–16, 2009.

[129] N. Habubi, Z. Al-ramadhan, and R. Khaleel, "(vinyl chloride) modified by nickel ethyl," *Proceeding of 3rd scientific conference*, No. 24 to 26 March, pp. 2080–2087, 2009.

[130] S. Mustafa ,"Engineering Chemistry", Library of Arab society for publication and distribution , Jordan, 2008.

[131] Q. Feng, Z. Dang, N. Li, and X. Cao, " Preparation and Dielectric Property of Ag -/PVA Nano-composite ",Mater. Sci. Eng. Vol.99 ,pp.325-328,2003.

[132] E. Sheha, H. Khoder, T.S. Shanap,M.G. El-Shaarawy and M.K. El Mansy," Structure, dielectric and optical properties of p-type (PVA/CuI) nanocomposite polymer electrolyte for photovoltaic cells" University of Benha, Egypt ,Vol.123, No. 13, PP.1161-1166, 2012.

الخلاصة

في هذا العمل تم تحضير المتراكبات النانوية ($PVP-PVA-Bi_2O_3$)و ($PVA-CMC-Bi_2O_3$)، بطريقة صب المحلول بتراكيز وزنية مختلفة من اوكسيد البزموث (0و1و3و5)wt% مع متوسط قطر الجسيمات النانويه (20-30) نانومتر. وتمت دراسة تأثير تراكيز الجسيمات النانوية Bi_2O_3 على الخصائص التركيبية والبصرية والتوصيلية الكهربائية للخليط البوليمري (PVA-PVP) و (PVA-CMC).

أظهرت نتائج فحص صور المجهر الضوئي ان الجسيمات النانويه (أوكسيد البزموث) يتوزع بشكل منتظم ومتجانس في داخل الخليط البوليمري (PVA-PVP) و (PVA-CMC) ويظهر طيف امتصاص FTIR تغيرا في الشدة والشكل وأزاحه في مواقع القمم مقارنة مع الاغشيه النقية للمتراكبات النانوية ($PVA-PVP/ Bi_2O_3$) و ($PVA-CMC/Bi_2O_3$) التي تشير الي الاهتزازات المقابلة للبوليمرات الاثنين والجسيمات النانوية لأوكسيد البزموث.

أظهرت نتائج فحوصات الخصائص البصرية للمتراكبات النانوية ($PVA-PVP/ Bi_2O_3$) و ($PVA-CMC/Bi_2O_3$) ان قيم كل من معامل الخمود والامتصاصية ومعامل الامتصاص ومعامل الانكسار والموصلية البصرية وثابت العزل الحقيقي والخيالي تزداد مع زيادة تراكيز مادة اوكسيد البزموث النانوية Bi_2O_3 بينما ان قيم النفاذية وفجوات الطاقة تتناقص مع زيادة تركيز اوكسيد البزموث النانوي (Bi_2O_3).

أظهرت نتائج فحوصات الخواص الكهربائية A.C للمتراكبات النانوي ($PVA-PVP/Bi_2O_3$) و($PVA-CMC/Bi_2O_3$) ان فقدان العزل وثابت العزل الكهربائي للتمراكبات النانوية يتناقصان مع زيادة كل من تردد المجال الكهربائي وتراكيز الجسيمات النانوية لأوكسيد البزموث النانوي فأن الموصلية الكهربائية A.C تزداد مع زيادة كل من التردد وتراكيز الجسيمات النانوية (اوكسيد البزموث).

أظهرت نتائج تطبيقات المتراكبات النانوية ($PVA-PVP/Bi_2O_3$) و($PVA-CMC/Bi_2O_3$) ان معاملات التوهين لأشعة كاما تزداد بزيادة تراكيز الجسيمات النانوية لأوكسيد البزموث(Bi_2O_3) .

جمهورية العراق

وزارة التعليم العالي والبحث العلمي

جامعة بابل

كلية التربية للعلوم الصرفة

قســـم الفـيزياء

تحضير ودراسه خصائص لخليط بوليمري :اوكسيد البزموث النانوي

رسالة مقدمة

إلى مجلس كلية التربية للعلوم الصرفة في جامعة بابل كجزء من

متطلبات نيل درجة الماجستير في التربية / الفيزياء

من قبل

هبه احمد مكي بدر

بكالـوريوس تربية فـيزياء

جامعة الكوفة 2010م

بأشراف

د. علي رزاق عبد الرضا

2022م **1444هـ**